



Title	Proteomics of <i>Physcomitrella patens</i> to elucidate the functions of 12-oxo-phytodienoic acid
Author(s)	Luo, WeiFeng
Degree Grantor	北海道大学
Degree Name	博士(農学)
Dissertation Number	甲第13321号
Issue Date	2018-09-25
DOI	https://doi.org/10.14943/doctoral.k13321
Doc URL	https://hdl.handle.net/2115/90534
Type	doctoral thesis
File Information	Luo_Weifeng.pdf



Proteomics of *Physcomitrella patens* to elucidate
the functions of 12-oxo-phytodienoic acid
(プロテオミクスを用いたヒメツリガネゴケにおける
12-オキソファイトジエン酸の機能解析)

Doctor Thesis Special English Program

英語特別コース 博士課程



A dissertation presented

By

Luo Weifeng

Laboratory of Natural Products Chemistry

Division of Bio-systems Sustainability

Graduate School of Agriculture

Hokkaido University

Proteomics of *Physcomitrella patens* to elucidate
the functions of 12-oxo-phytodienoic acid

(プロテオミクスを用いたヒメツリガネゴケにおける
12-オキソファイトジエン酸の機能解析)

By

Luo Weifeng

A dissertation submitted to the Special Postgraduate English Program in
biosphere sustainability science, graduate school of agriculture, Hokkaido
university, Japan.

Contents

Chapter 1 Introduction	1
1.1 Plant hormones	5
1.2 The octadecanoid pathway	7
1.3 Jasmonic Acid	10
1.4 12-oxo-Phytodienoic acid (OPDA)	11
1.6 Objectives of this study	12
Chapter 2 Comparative proteomic analysis of wild-type <i>P. patens</i> protonema treated with OPDA	13
2.1 Introduction	13
2.2 Results	14
2.2.1 Protein identification and functional categories of differentially expressed proteins	14
2.2.2 Proteins with increased abundance due to OPDA treatment of protonemata	18
2.2.3 Decreased proteins involved in carbohydrate metabolism and energy production	18
2.2.4 Proteins with decreased abundance involved in protein metabolism	19
2.2.5 Six histones were suppressed by OPDA	20
2.2.6 Comparison of proteomic data of gametophores and protonemata	21
Chapter 3 Comparative proteomic analysis of wild-type <i>P. patens</i> and OPDA-deficient <i>P. patens</i> mutant after wounding	25
3.1 Introduction	25
3.2 Results	27
3.2.1 <i>P. patens</i> mutants with disrupted <i>PpAOS1</i> and <i>PpAOS2</i> genes	27
3.2.2 Identification of proteins that are differentially accumulated in response to wounding	29
3.2.3 Functional categories and subcellular localization of identified wounding-responsive proteins	50
3.2.4 Proteins involved in protein synthesis	66
3.2.5 Proteins involved in protein degradation	66
3.2.6 Proteins involved in amino acid metabolism	67
3.2.7 Proteins involved in protein folding	67
3.2.8 Proteins involved in photosystems	68

3.2.9 Proteins involved in glycolysis, the TCA cycle, and energy synthesis.....	70
3.2.10 Proteins for reactive oxygen scavenging.....	72
3.2.11 Real -time quantitative PCR analysis of chaperonin genes in <i>P. patens</i>	72
3.3 Discussion	74
3.3.1 Phenotype of <i>P. patens</i> mutants with disrupted <i>PpAOS1</i> and <i>PpAOS2</i> genes.....	74
3.3.2 Proteins involved in protein metabolism	74
3.3.3 Proteins involved in protein folding.....	76
3.3.4 Photosystem proteins and proteins involved in energy synthesis.....	77
3.3.5 Comparison of proteomic data in this study with those in <i>P. patens</i> protonema treated with OPDA	78
3.3.6 Comparison of proteomic data in this study	78
Chapter 4 General conclusions	81
Chapter 5 General method	83
5.1 Plant growth and treatment	83
5.2 Prepare the BCDATG medium.....	83
5.3 Synthesis of OPDA	84
5.4 Analysis of OPDA concentration in <i>P. patens</i>	85
5.5 Generation of a <i>P. patens</i> mutant with disrupted <i>PpAOS1</i> and <i>PpAOS2</i>	85
5.6 Protein extraction	87
5.7 Digestion of proteins.....	87
5.8 Nano-liquid chromatography-tandem MS analysis	88
5.9 Protein identification using Mascot	88
5.10 Analysis of differentially accumulated proteins using the acquired MS data.....	89
5.11 Classification of proteins and bioinformatic analysis	89
5.12 Extraction of RNA and qRT-PCR analysis.....	90
5.13 Statistical analysis.....	91
Chapter 6 Acknowledgments	93
Chapter 7 Lists of abbreviations	94
Chapter 8 References	96

Chapter 1 Introduction

Bryophytes, including mosses, liverworts and hornworts, represent three out of four ancient lineages of land plants (Prigge & Bezanilla, 2010). The embryophytes (land plants) began to diverge about 450 million years ago. Bryophytes, comprising hornworts, mosses and liverworts, are remnants of early diverging lineages of embryophytes and thus occupy an ideal phylogenetic position for reconstructing ancient evolutionary changes and illuminating one of the most important events in earth history—the conquest of land by plants. About 400 million years ago, mosses and vascular plants were diverged from each other and they developed their own characteristics in the time line of evolution thereafter (Rensing et al., 2008). Similar to vascular plants, mosses show alternative haploid gametophyte and diploid sporophyte generations. The gametophyte of mosses is a free-living organism, whereas the gametophyte of the gymnosperms and angiosperms is dependent on the sporophyte (Cove, 2005).

Physcomitrella patens is a moss used as a model organism for studies on plant evolution, development and physiology. Like all mosses, the life cycle of *P. patens* is characterized by an alternation of two generations (Fig. 1.1): a haploid gametophyte that produce gametes and a diploid sporophyte where haploid spores are produced. A spore develops into a filamentous structure called protonema, composed of two types of cells: chloronema with large and numerous chloroplasts and caulonema with very fast growth (Marion-Poll, 2005).

Mosses share fundamental genetic and physiological processes with vascular plants, although the two lineages diverged early in land plant evolution, as showed in Fig. 1.2 and Fig. 1.3 (Rensing et al., 2008). Comparative genomic study between *P. patens* and flowering plants can give an insight into the evolution of the mechanisms behind the complexity of the modern plants (Rensing et al., 2008). For this reason, *P. patens* is used as a model organism. Additionally, *P. patens* is one of few known multicellular organisms with highly efficient homologous recombination (Schaefer

& Zryd, 1997, Schaefer & Zryd, 2001). This means that an exogenous DNA sequence can be inserted to a specific genomic position (a technique called gene targeting) to create knockout mosses. This method is called reverse genetics. It is a powerful and sensitive tool to study the function of genes and can be used to study molecular plant evolution, when combined with studies in higher plant such as *Arabidopsis thaliana*.

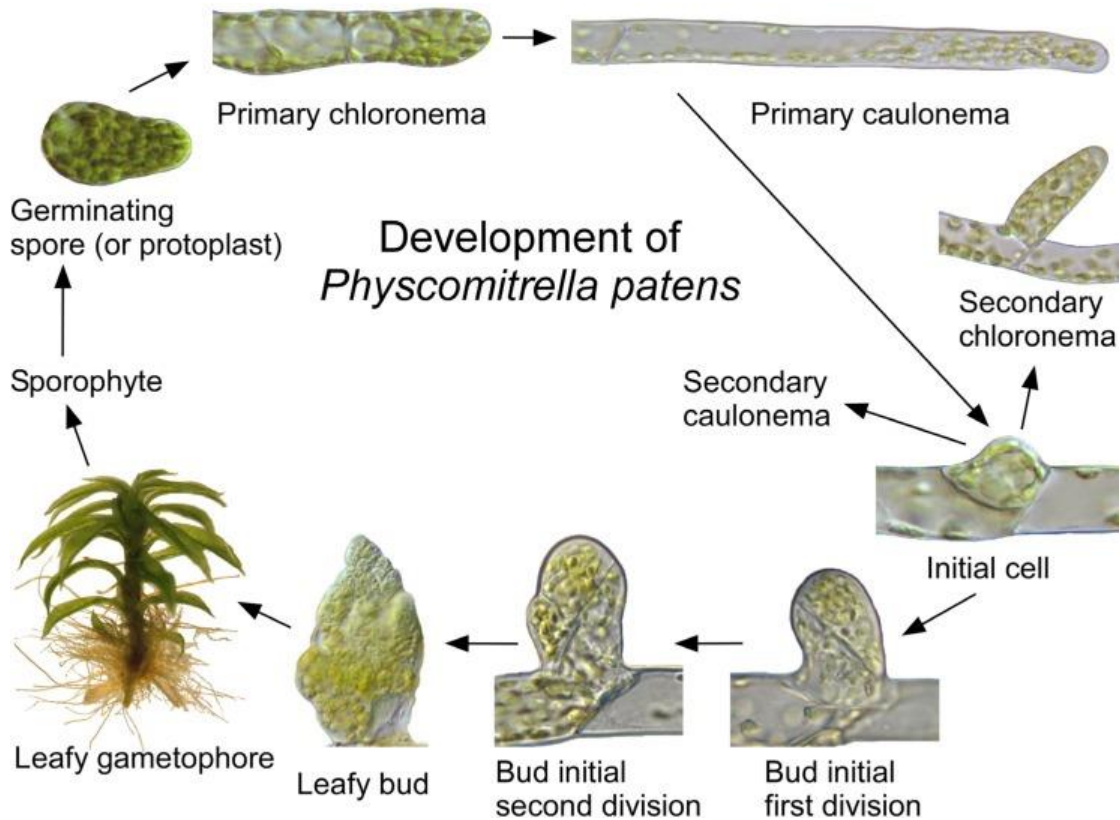


Fig. 1.1. Development of *P. patens* (Roberts et al., 2012).

Note: The protonema stage means the time from primary caulonema to secondary chloronema in the life cycle of *P. patens*.

As Fig. 1.1 shows, a haploid spore or protoplast germinates to form a primary chloronema with numerous chloroplasts and transverse cross walls, which subsequently differentiates into a more rapidly growing primary caulonema with fewer chloroplasts and oblique cross walls. The caulonemal subapical cells divide to produce initials cells, which develop into lateral secondary

chloronemata, secondary caulonemata, or buds. Buds develop into leafy gametophores, which produce apical gametangia. Fertilization of an egg by swimming sperm at the gametophore apex produces a zygote, which develops into a diploid sporophyte consisting of a stalk and sporangium. Meiotic divisions within the sporangium generate haploid spores (Cove, 2005, Schaefer & Zryd, 2001, Knight, 1993, Eckermann, 2002).

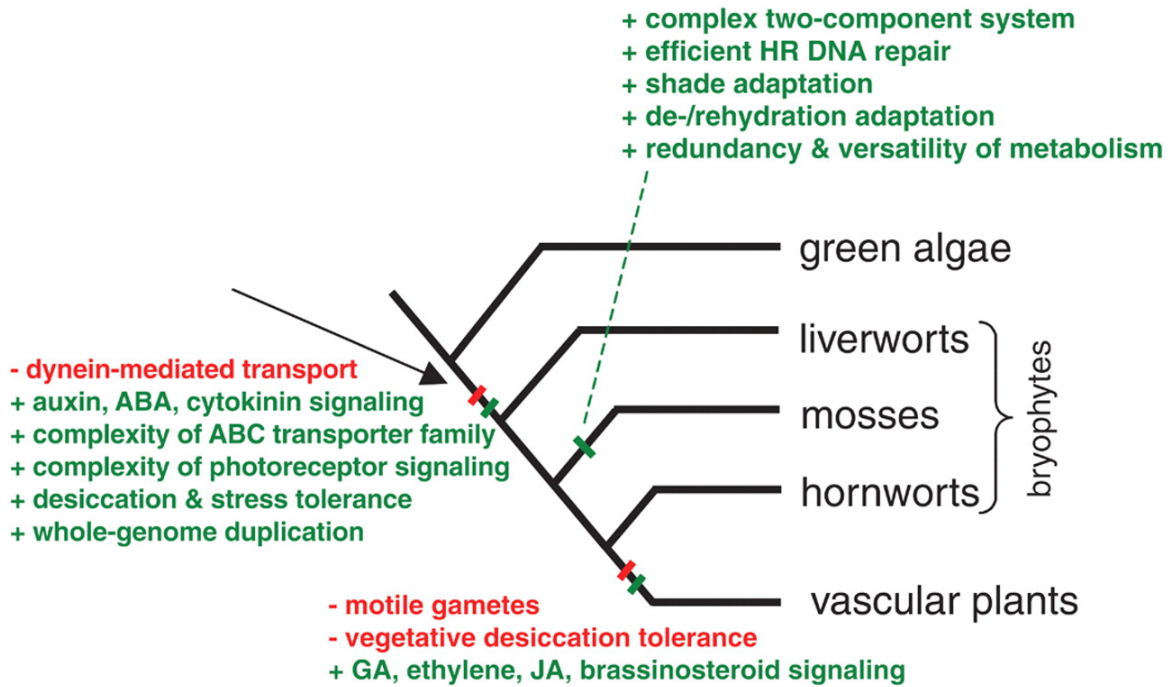


Fig. 1.2. Land plant evolution (Rensing et al., 2008).

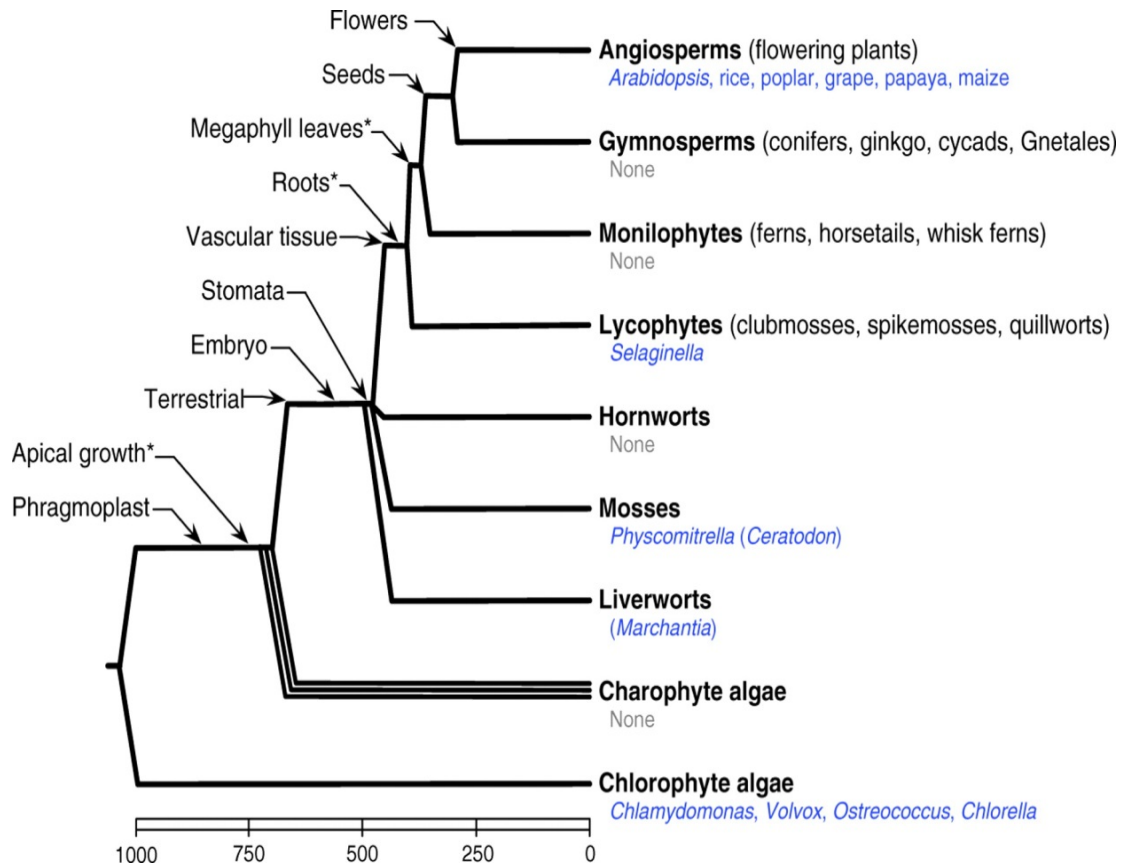


Fig. 1.3. Phylogenetic relationships among green plants

(Prigge & Bezanilla, 2010).

Previous findings report that *P. patens* has recently recognized as a powerful genetically tractable model plant system (Prigge & Bezanilla, 2010). Therefore *P. patens* was provided to be a unique and valuable opportunity to study the evolution of myriad of plant traits, such as polarized cell growth, gametophyte-to-sporophyte transitions. The complete genome sequence and the ability to conduct efficient gene targeting in *P. patens* can make a difference to answer the essential questions in plant developmental biology (Prigge & Bezanilla, 2010).

1.1 Plant hormones

Plant hormones are signal molecules produced within the plant, which can regulate a wide variety of physiological processes such as plant growth, senescence, adaptations against abiotic and biotic stresses, and occur in extremely low concentrations. Plant hormones regulate cellular processes in targeted cells locally. And when moved to other locations of plant, they can also have functions on other tissues of the plant. Each cell in the plant is capable of producing hormones and also its biological activities are affected by plant hormones in return.

Generally, there are five major classes of plant hormones, some of which are made up of many different chemicals that can vary in structures from one plant to the next. The chemicals are each grouped together into one of these classes based on their structural similarities and on their effects on plant physiology. Each class of the plant hormones has positive and inhibitory functions that can affect the growth regulation of plant. These five major classes are abscisic acid, auxins, cytokinins, ethylene and gibberellins (Fig. 1.4).

Abscisic acid (ABA) has functions in many development processes of plant. ABA-mediated signaling also plays an important part in plant responses to stand for environment stress and plant pathogens (Zhu, 2002, Seo & Koshiba, 2002). In addition, ABA also plays a role in seed germination and early embryo development.

Auxin is a kind of plant hormones with some morphogen-like characteristics. Auxins have a cardinal role in coordination of many growth and behavioral processes in the plant's life cycle and are essential for plant body development. Auxin participates in phototropism, geotropism, hydrotropism and other development changes. The uneven distribution of auxin, due to environmental cues, such as unidirectional light or gravity force, results in uneven plant tissue growth. Auxin generally governs the form and shape of plant body, direction and strength of growth of all organs, and their mutual interaction (Benkova et al., 2003).

Cytokinins are plant hormones that promote cell division and cytokinesis in plant roots and

shoots. They are primarily involved in cell growth and differentiation, and also affect apical dominance, axillary bud growth, and leaf senescence. The ratio of auxin to cytokinin plays an important role in plant growth. Cytokinin alone has no effect on parenchyma cells. When cultured with auxin but no cytokinin, plants grow large but do not divide. High concentration of cytokinin induces growth of shoot buds, while high concentration of auxin induces root formation (Campbell, 2008).

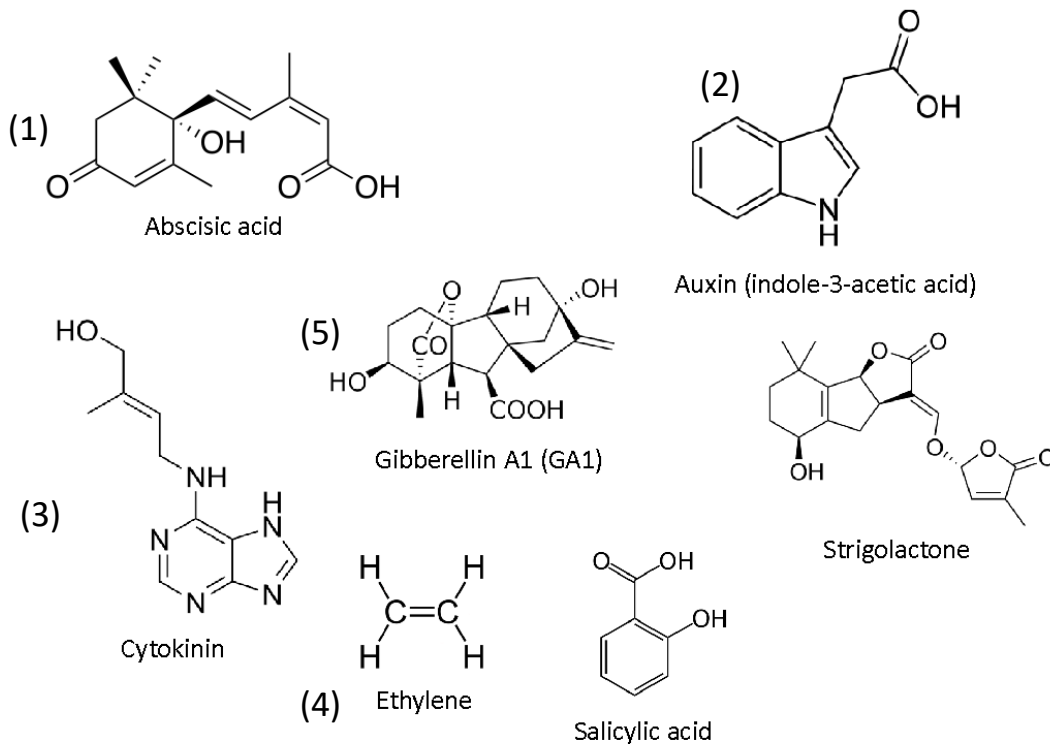


Fig. 1.4. The structures of plant hormones

Ethylene is a hydrocarbon with the formula C_2H_4 . Ethylene is widely used in chemical industry, and it also serves as a plant hormone (Lin et al., 2009). It acts at trace levels throughout the life of the plant by stimulating or regulating the ripening of fruit, the opening of flowers, and the abscission (or shedding) of leaves (Yang & Hoffman, 1984).

Gibberellins (GAs) are plant hormones that regulate growth and influence various developmental

processes, including stem elongation, germination, dormancy, flowering, sex expression, enzyme induction, and leaf and fruit senescence (Fleet & Sun, 2005).

Besides, there still are some other identified plant growth regulators, which are not easily grouped into these five classes, strigolactones, salicylic acid, jasmonates.

Strigolactones are plant hormones that stimulate the branching and growth of symbiotic arbuscular mycorrhizal fungi, increasing the probability of contact and establishment of a symbiotic association between the plant and fungus. And strigolactones also inhibit plant shoot branching and trigger germination of parasitic plant seeds (for example *Striga lutea*) (Akiyama et al., 2005).

Salicylic acid (SA) is phenolic plant hormone, and plays important roles in plant growth, development, photosynthesis, transpiration, ion uptake and transport. SA also induces specific changes in leaf anatomy and chloroplast structure and is involved in endogenous signaling, mediating in plant defense against pathogens (Hayat & Ahmad, 2007). SA also plays a role in the resistance to pathogens by inducing the production of pathogenesis-related proteins; it is involved in the systemic acquired resistance (SAR) in which a pathogenic attack on a certain part of the plant induces resistance in other parts. The signal can also move to nearby plants by SA being converted to the volatile ester, methyl salicylate (Misra & Saxena, 2009).

There is another important plant hormone named as jasmonic acid (JA). The detailed biological activities of jasmonates are described in the following chapters.

1.2 The octadecanoid pathway

The octadecanoid pathway is a well-characterized biosynthetic pathway for jasmonic acid (JA), which is an important plant hormone. When facing the change from the environment (wounding or pest attack), JA is synthesized to maintain plant cellular functions and protect the plant tissue itself. The octadecanoid pathway is important for the plant, and it is responsible for producing JA an

important signaling molecule in plants, which controls the production of variety of secondary metabolites by inducing the defense related genes (Peebles et al., 2009).

In Fig.1.5, the octadecanoid pathway starts from α -linolenic acid, which can be released from the plasma membrane of chloroplasts by certain lipase enzymes. α -Linolenic acid is oxidized by the enzyme 13-lipoxygenase (LOX). This enzyme forms 13(*S*)-hydroperoxyoctadeca-9,11,15-trienoic acid (13-HPOT), which is then converted to 12,13(*S*)-epoxyoctadeca-9,11,15-trienoic acid (12,13-EOT) by allene oxide synthase (AOS). 12,13-EOT undergoes cyclization by allene oxide cyclase (AOC) to form 12-oxo-phytodienoic acid (OPDA). These reactions are carried out in chloroplasts (Romeo et al., 1998, Weber et al., 1997).

After OPDA was transferred from chloroplasts to peroxisomes, the reduction on the olefin of cyclopentenone ring of OPDA was reduced by 12-oxo-phytodienoic acid reductase (OPR) to form 3-oxo-2-(*cis*-2'-pentenyl)-1-cyclopentane-1-octanoic acid (OPC-8:0), and then after three cycles of β -oxidation, the *epi*-JA was produced. Thereafter *epi*-JA is immediately isomerized to JA.

JA itself can be further metabolized into active or inactive derivatives. Methyl jasmonate (MeJA) is a volatile organic compound involved in plant defense and many diverse developmental pathways such as seed germination, root growth, flowering, fruit ripening, and senescence (Cheong & Choi, 2003). Conjugation of JA with isoleucine (Ile) provides JA-Ile, which is currently received to be the only known JA derivative needed for JA signaling (Katsir et al., 2008).

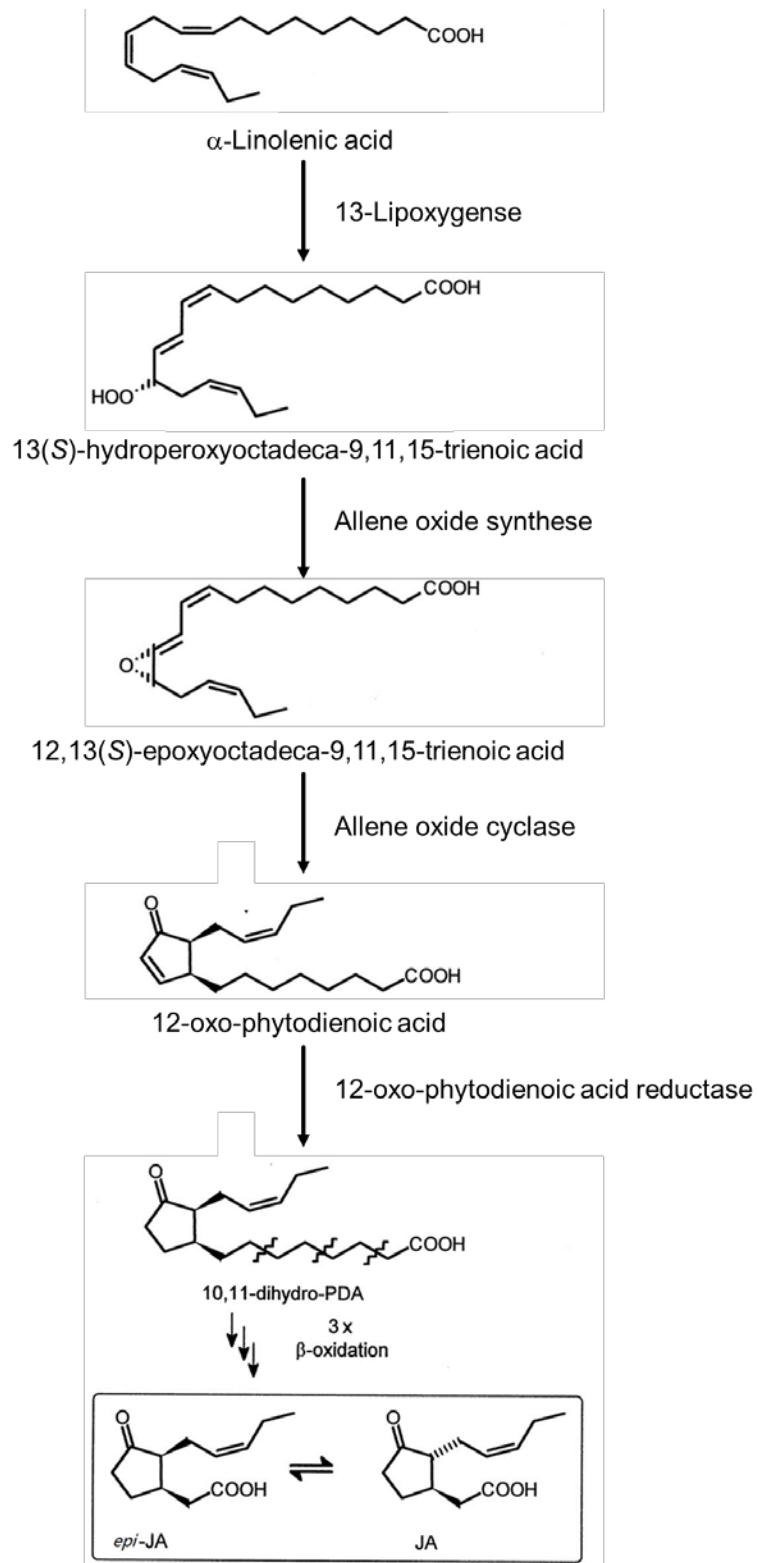


Fig. 1.5. The octadecanoid pathway.

1.3 Jasmonic Acid

Jasmonates are a growing class of lipid-derived signaling molecules with diverse functions such as the initiation of biotic and abiotic stress responses and regulation of plant growth and development (Schaller & Stintzi, 2009). JA (Fig. 1.6) is an important member of jasmonates (JA related compounds). JA is the end product of octadecanoid pathway and it is an important plant signaling molecule (Peebles et al., 2009).

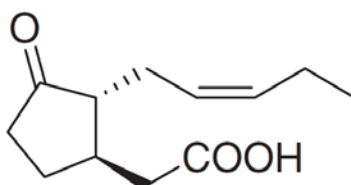


Fig. 1.6. The structure of jasmonic acid.

JA has been shown previously to be a powerful inducer of proteinase inhibitors in tomato (*Lycopersicon esculentum* cultivar Castlemart II) and tobacco (*Nicotiana tabacum* cultivar Xanthi), and alfalfa leaves (*Medicago sativa* line RA3) (Farmer & Ryan, 1990). And when proposed octadecanoid precursors of JA, i.e., linolenic acid, 13-HPOT, and OPDA were applied to the surfaces of tomato leaves, these compounds served as strong inducers to synthesize proteinase inhibitor I and II, a simulation of a wound response. However, the compounds closely related to the precursors, such as hydroperoxyfatty acids, which were not intermediates in the JA synthetic pathway, did not induce proteinase inhibitor synthesis (Farmer & Ryan, 1992). These results suggested that JA plays a role in response to insect and pathogen attack.

JA can influence several aspects of plant growth and development, such as induction of expression of genes encoding vegetative storage protein (*Vsp*), lipoxygenase (*Lox*), ethylene forming enzyme (*EFE*), large subunit of ribulose biphosphate carboxylase (*rbcL*) (Creelman &

Mullet, 1995), and moreover induces to synthesize numerous secondary metabolites, which help plant response to abiotic and biotic stress as well as plant growth and development (Delker et al., 2006). The variety of responses and genes regulated by JA suggests the existence of multiple levels of control over jasmonate biosynthesis, and JA acts with other effectors to potentiate gene expression (Creelman & Mullet, 1995). All these results showed that JA plays an essential role in plant defense such as responses to wounding. Additionally, JA also plays roles in developmental processes such as flower development and seed germination (Creelman & Mullet, 1997).

1.4 12-oxo-Phytodienoic acid (OPDA)

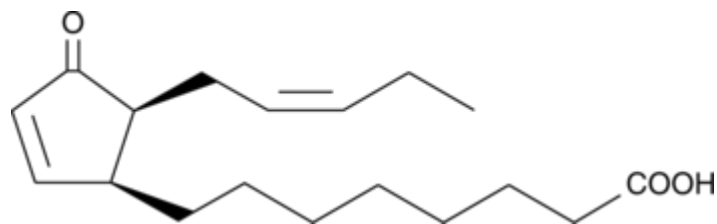


Fig. 1.7. The structure of OPDA.

Jasmonates regulate diverse physiological processes in plants, including to the response to environmental stresses such as wounding, high salinity, and insect attack. As the precursor of the JA, OPDA (Fig.1.7) can also induce gene expression and is known as a signaling molecule distinct from JA. OPDA appears to play an independent role in mediating resistance to pathogens, induction of alkaloid biosynthesis in *Eschscholzia californica* cell cultures, increasing of tendril coiling of *Bryonia dioica*, and suppression of JA-induced programmed cell death in a conditional *Arabidopsis flu* mutant (Bottcher & Pollmann, 2009). According to transcriptome analysis on *Arabidopsis* treated with OPDA and JA, many genes responded identically to both OPDA and JA, there are still a lot of genes specifically respond to OPDA, which were named OPDA-specific response genes (ORGs) (Taki et al., 2005). Moreover, OPDA was shown to interact

with abscisic acid (ABA) and can stimulate the synthesis of ABA INSENSITIVE 5 (ABI5) protein to inhibit seed germination; OPDA plays a significant role in seed germination (Dave & Graham, 2012, Balbi & Devoto, 2008, Bottcher & Pollmann, 2009, Dave et al., 2011).

Previous reports described that the *P. patens* genes encoding LOX, AOS and AOC in the octadecanoid pathway have been cloned and the recombinant proteins of *P. patens* showed enzymatic activities, which were similar to those in flowering plants (Anterola et al., 2009, Hashimoto et al., 2011, Stumpe et al., 2010, Bandara et al., 2009). OPDA was shown to inhibit the growth of *P. patens* (Ponce De Leon et al., 2012). These results suggested that OPDA also plays an important role in response to stresses in *P. patens*.

1.6 Objectives of this study

Proteomic analysis of *P. patens* treated with OPDA in gametophores and protonema stages showed that abundance of the distinct proteins is affected by OPDA in these developmental stages. These results can build a vague vision to understand the functions of OPDA to regulate proteins expressions. Since OPDA, not JA, was accumulated to response to wounding. OPDA is supposed to play an important role involved in the expression of wounding response related genes and proteins in *P. patens*. The detailed function of OPDA is still unknown, so understanding the functions of OPDA in *P. patens* would help to elucidate the OPDA signal transduction pathway in plants. In this research, proteomic analysis of a *PpAOS* knockout mutant and wild type subjected to wounding was conducted. The comparison of proteomic data will reveal OPDA related physiological responses to wounding in *P. patens*.

Chapter 2 Comparative proteomic analysis of wild-type *P. patens* protonema treated with OPDA

2.1 Introduction

Plant hormones regulate a wide variety of physiological events in plants. Many studies have demonstrated that plant hormones, such as auxin, cytokinins, and abscisic acid, also control physiological responses in *P. patens*. In *P. patens*, the first half of the octadecanoid pathway exists, however, JA is not synthesized (Stumpe et al., 2010). OPDA inhibits the growth of *P. patens* (Ponce De Leon et al., 2012). Moreover, wounding induces OPDA accumulation in *P. patens* (Scholz et al., 2012). Thus, OPDA may be an important oxylipin and act as a signaling molecule in *P. patens*. A proteomic analysis of *P. patens* gametophores treated with OPDA was conducted to investigate the function of OPDA (Toshima et al., 2014). A previous report revealed that OPDA treatment of gametophores resulted in the differential accumulation of several proteins, most of which were decreased. The expression of genes and proteins is altered when differentiation from protonema to gametophore occurs (Hiss et al., 2014). To investigate whether the effects of OPDA on protein abundance are different between these protonemata and gametophore, a proteomic analysis of *P. patens* protonemata treated with OPDA was conducted.

2.2 Results

2.2.1 Protein identification and functional categories of differentially expressed proteins

OPDA was shown to suppress the colony growth and rhizoid length of *P. patens* under a concentration of 10 μM (Ponce De Leon et al., 2012), and mechanical stress transiently stimulates OPDA accumulation (Toshima et al., 2014). The morphology of *P. patens* varies over the course of the life cycle. The protonema and gametophore developmental stages are quite different (Roberts et al., 2012). To examine the effects of OPDA on the growth of *P. patens* protonemata, *P. patens* protonemata were incubated in a medium supplemented with OPDA and were then viewed under a microscope (Fig. 2.1). OPDA retarded the growth of protonemata of *P. patens* in a concentration-dependent manner. When OPDA concentration was more than 10 μM , the protonema growth was clearly inhibited by OPDA. In contrast to OPDA, JA did not show significant growth inhibitory effect for *P. patens* protonemata.

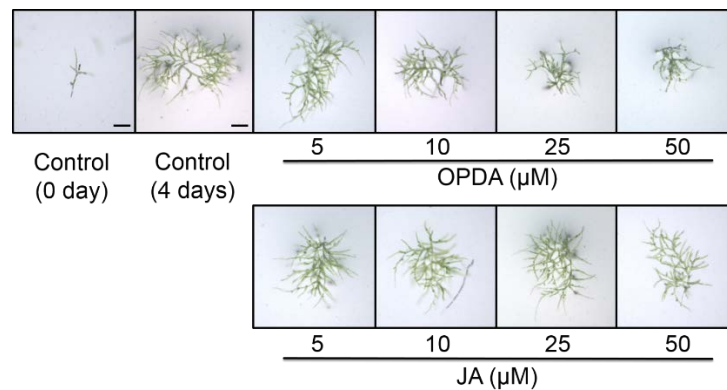


Fig. 2.1. Effects of OPDA on protonema prolongation in *P. patens*.

Protonemata were grown on BCDATG agar plates with OPDA or JA for 4 days. The control showed protonemata on the agar plate without OPDA and JA. Scale bar shows 200 μm .

Analytical data of endogenous OPDA concentration showed that mechanical wounding transiently elevated OPDA concentration in *P. patens* protonema in a similar way with higher plants

(Fig. 2.2). These results strongly suggest OPDA signaling system functions in protonema and gametophore stages in *P. patens*.

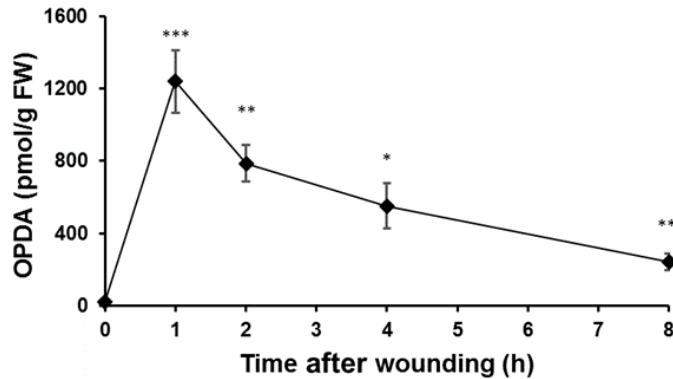


Fig. 2.2. Concentration of OPDA in *P. patens* protonemata after mechanical stress.

P. patens protonemata were grown on BCDATG agar medium for 4 days, and the concentration of endogenous OPDA was analyzed. After *P. patens* protonemata were subjected to wounding for the indicated times, the protonemata were harvested at the indicated time and the OPDA concentration was analyzed using UPLC-MS/MS. The values are the means \pm SD (n = 4). Student's t test, * p < 0.05, ** p < 0.01, *** p < 0.001.

A previous report demonstrated that OPDA alters the abundance of proteins involved in light-dependent reactions, the octadecanoid pathway, carbon fixation, glycolysis and protein synthetic processes in gametophores (Toshima et al., 2014). To examine the effects of OPDA on protein abundance for *P. patens* protonemata, a proteomic analysis of *P. patens* protonemata treated with 10 μ M OPDA for 24 h was performed. The extracted proteins were digested with trypsin and lysyl endopeptidase, and the resulting peptides were analyzed using nano LC-MS/MS. The protein levels were compared based on the area under the curve of each matched peptide using SIEVE software; the number of proteins that were matched with more than two peptides was 2662. A subsequent comparative analysis of OPDA-treated protonemata and OPDA-untreated protonemata revealed

that 41 proteins were differentially altered with fold changes of more than 1.5 ($p < 0.05$) (Table 2.1). The abundance of 40 proteins decreased; only one protein increased in abundance due to OPDA treatment in protonemata.

Based on their biological properties, these differentially changed proteins were grouped into the following six categories: defense, energy and carbohydrate metabolism, photosynthesis, protein metabolism (proteins synthesis, folding and degradation), others and unknown (Fig. 2.3). Twenty-one differentially changed proteins are involved in protein synthesis. One protein is involved in defense, and five proteins are involved in carbohydrate and energy metabolism.

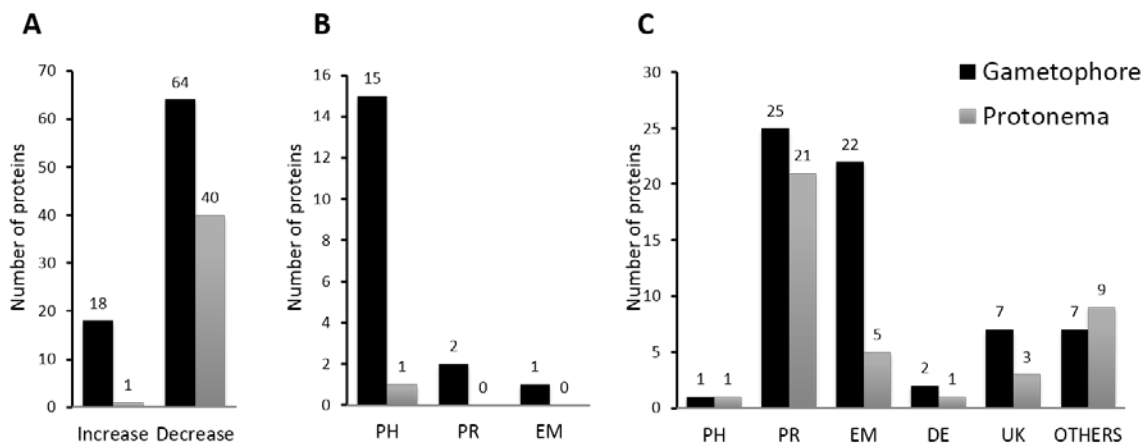


Fig. 2.3. Comparison of proteins changed in gametophore and protonema.

A: comparison of the global protein response to OPDA; B: comparison of proteins increased by OPDA; C: comparison of proteins decreased by OPDA. PH: photosynthesis; PR: protein metabolism (protein synthesis, folding and degradation); EM: energy and carbohydrate metabolism; DE: defense; UK: unknown. Gametophore data are referred from a paper by Toshima et al (2014).

Table 2.1. Proteins identified as responsive to OPDA in *P. patens* protonemata.

Protein ID ¹	Description	Category ²	MP ³	FC ⁴
Pp1s61_321V6.1	oxygen-evolving enhancer protein chloroplast	PH	4	1.60
Pp1s253_38V6.1	40S ribosomal protein S6	PR	3	0.67
Pp1s253_7V6.1	40S ribosomal protein S6	PR	3	0.67
Pp1s311_33V6.1	40S ribosomal protein S6	PR	3	0.67
Pp1s31_322V6.1	40S ribosomal protein S6	PR	3	0.67
Pp1s264_34V6.1	proliferation-associated protein 2g4	PR	2	0.67
Pp1s271_9V6.1	40s ribosomal protein	PR	2	0.66
Pp1s2_233V6.1	60s ribosomal protein 118	PR	2	0.66
Pp1s107_27V6.1	unknown	UK	3	0.66
Pp1s47_196V6.1	apoptosis inhibitor	DE	3	0.65
Pp1s45_11V6.1	60s ribosomal protein 118	PR	2	0.65
Pp1s306_12V6.1	hypothetical PE-PGRS family protein PE_PGRS54 precursor	UK	2	0.64
Pp1s145_142V6.1	phosphoglycerate kinase	EM	2	0.64
Pp1s159_52V6.1	phosphoenolpyruvate carboxykinase	EM	4	0.64
Pp1s60_266V6.1	phosphoenolpyruvate carboxykinase	EM	4	0.64
Pp1s221_62V6.1	formamidopyrimidine-dna glycosylase	Others	5	0.63
Pp1s168_70V6.2	phosphoglucomutase a	EM	7	0.63
Pp1s42_99V6.1	lupus la	PR	2	0.62
Pp1s117_154V6.1	histone h2a	Others	2	0.61
Pp1s219_44V6.1	histone 2	Others	2	0.61
Pp1s376_22V6.1	histone 2	Others	2	0.61
Pp1s46_245V6.1	histone 2	Others	2	0.61
Pp1s72_85V6.1	histone h2a	Others	2	0.61
Pp1s72_86V6.1	histone h2a	Others	2	0.61
Pp1s198_153V6.2	inner membrane protein	Others	3	0.60
Pp1s198_153V6.3	inner membrane protein	Others	3	0.60
Pp1s136_70V6.1	glycine-rich RNA-binding protein	PR	3	0.60
Pp1s311_33V6.2	40S ribosomal protein S6	PR	2	0.59
Pp1s37_67V6.1	translational inhibitor protein	PR	2	0.59
Pp1s37_67V6.2	translational inhibitor protein	PR	2	0.59
Pp1s37_67V6.3	translational inhibitor protein like	PR	2	0.59
Pp1s114_93V6.1	pyruvate kinase	EM	2	0.59
Pp1s247_51V6.1	translation initiation factor	PR	3	0.57
Pp1s97_246V6.1	unknown	UK	5	0.53
Pp1s79_93V6.1	FCAALL.30; lil3 protein	PR	3	0.53
Pp1s165_40V6.1	60s ribosomal protein	PR	3	0.51
Pp1s174_48V6.1	60s ribosomal protein	PR	3	0.51
Pp1s63_162V6.1	60s ribosomal protein	PR	3	0.51
Pp1s80_110V6.1	60s ribosomal protein	PR	3	0.51
Pp1s75_223V6.1	60s ribosomal protein	PR	4	0.51
Pp1s83_99V6.1	plastid-lipid-associated protein 2	PH	2	0.50

¹Protein IDs are from Phytozome ver. 9.1 (<http://www.phytozome.net/>).

²Category: DE, defense; EM, energy and carbohydrate metabolism; PH, photosynthesis; PR, protein metabolism (protein synthesis, folding and degradation); UK, unknown. ³MP indicates the number of matched peptides. ⁴FC indicates the fold change between control and 10 μ M OPDA treatment.

2.2.2 Proteins with increased abundance due to OPDA treatment of protonemata

The abundance of only one protein, oxygen-evolving enhancer protein 2 (OEE2), was increased by OPDA in protonemata. This protein is encoded by the nuclear genome (Table 2.1, Fig. 2.3B). OEE2 is required for high levels of O₂ evolution. Oxygen-evolving enhancer protein (Pp1s61_321V6.1) belongs to the PsbP family, which is required for increased Photosystem II (PSII) affinity for the water oxidation site of Cl⁻ and provides the conditions required for high affinity binding to Ca²⁺ (Kochhar et al., 1996). Both PsbP and PsbQ are necessary regulators of the biogenesis of optically active PSII. The oxygen-evolving complex (OEC) is responsible for catalyzing the splitting of water to O₂ and H⁺. In flowering plants, such as *Arabidopsis*, OPDA plays an important role in response to biotic and abiotic stresses (Bottcher & Pollmann, 2009). OPDA is accumulated in *P. patens* gametophores due to wounding. OPDA accumulation results in the increased protein abundance in the gametophore stage, including PsbC, PsbD, and PsbE and allene oxide cyclase (AOC) (Toshima et al., 2014). Accordingly, OPDA is likely synthesized to stimulate light-dependent reactions in response to wounding stress in *P. patens*.

2.2.3 Decreased proteins involved in carbohydrate metabolism and energy production

OPDA treatment resulted in the decreased abundance of enzymes involved in carbohydrate metabolism, such as phosphoenolpyruvate carboxykinase (PEPC), phosphoglucomutase (PGM), phosphoglycerate kinase and pyruvate kinase (Table 2.1, Fig. 2.3C). PEPC is the bottleneck enzyme for gluconeogenesis, which catalyzes the addition of bicarbonate to phosphoenolpyruvate to form oxaloacetate and inorganic phosphate. PEPC plays a crucial role in modulating the balance of carbon metabolism in *Arabidopsis* (Jianghua et al., 2015). PGM catalyzes the interconversion of glucose 1-phosphate and glucose 6-phosphate; the enzyme exists in both plastidial and cytosolic isoforms. The plastidial isoform is essential for transitory starch synthesis in the chloroplasts of

leaves, whereas the cytosolic counterpart is essential for glucose phosphate partitioning and the synthesis of sucrose and cell wall components. A lack of PGM (both plastidial and cytosolic isoforms) activities in *Arabidopsis* resulted in dwarfed growth, premature death, and an inability to develop a functional inflorescence (Malinova et al., 2014). The synthesis of the enzymes phosphoglycerate kinase and pyruvate kinase was suppressed by OPDA; these enzymes are involved in carbon fixation (Calvin cycle) and energy production. Phosphoglycerate kinase is an essential enzyme in the Calvin cycle; it catalyzes the phosphorylation of 3-phosphoglycerate with ATP, which is produced in the light-dependent stage (Calvin, 1950). Pyruvate kinase catalyzes the transfer of a phosphate group from phosphoenolpyruvate (PEP) to ADP to yield pyruvate and ATP (Romano & Conway, 1996).

2.2.4 Proteins with decreased abundance involved in protein metabolism

OPDA suppressed the abundance of ribosomal proteins, transcriptional initiator and translational inhibitor proteins; these proteins are associated with RNA. Of the 40 proteins with suppressed abundance, over half were involved in protein metabolism (Table 2.1, Fig. 2.3C). OPDA was shown to down-regulate protein synthesis by suppressing transcription and translation activity. Among the OPDA-repressed proteins involved in protein metabolism, ribosomal proteins were mainly identified in protonemata. The repression of ribosomal protein biosynthesis significantly affects various physiological phenomena in cells. Translational inhibitor proteins (endoribonuclease L-PSP) are active on single-stranded mRNA and inhibit protein synthesis by cleaving mRNA (Morishita et al., 1999, Hedegaard et al., 2000). When protein synthesis is suppressed in cells, translational inhibitor proteins might be unnecessary. The repression of protein synthesis likely leads to a decreased abundance of translational inhibitor proteins.

2.2.5 Six histones were suppressed by OPDA

The abundance of six histones was decreased in *P. patens* protonemata treated with OPDA. To our knowledge, this is the first report that OPDA inhibits histone abundance. These histones all belong to the histone H2A group. Histones are the chief components of chromatin and play an important role in the regulation of gene expression. Histone H2A is important for the packaging of DNA into chromatin; this packaging process is believed to affect gene expression (Marino-Ramirez et al., 2006). Considering the function of histones in gene expression, this finding was worthy of further exploration. The qRT-PCR analysis of these six histone genes in *P. patens* treated with OPDA was performed. As a result, 10 μ M OPDA was shown to down-regulate the mRNA accumulation of these histone genes (Fig. 2.4). These results supported the proteomic data in this study. The qRT-PCR data indicate that OPDA regulates the expression of these histone genes at the transcriptional level. It is possible that OPDA affects cell cycle progression at the protonema stage of *P. patens*.

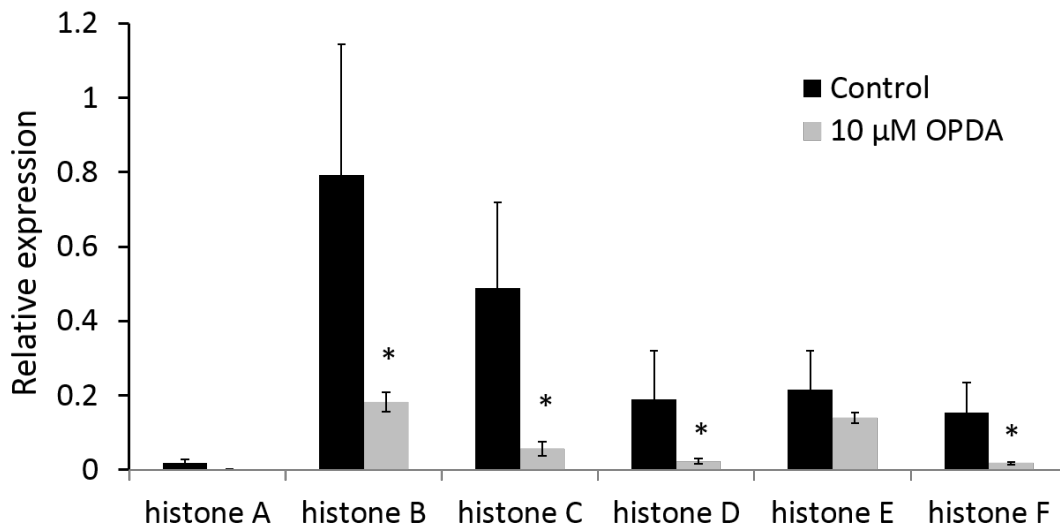


Fig. 2.4. Relative expression of histone genes by qRT-PCR.

Five-day-old *P. patens* protonemata were treated with 10 μ M OPDA or water for 24 h. The expression level of the internal standard gene actin 5 is set to 1.0. The data represent means \pm SD (n=3).

Asterisks represent significant differences between OPDA-treated plants and control plants (Student's t test, $*p < 0.05$). histone A: Pp1s117_154V6.1; histone B: Pp1s219_44V6.1; histone C: Pp1s376_22V6.1; histone D: Pp1s46_245V6.1; histone E: Pp1s72_85V6.1; histone_F: Pp1s72_86V6.1.

2.2.6 Comparison of proteomic data of gametophores and protonemata

The proteome data of gametophores (Toshima et al., 2014) and protonemata of *P. patens* treated with OPDA were compared to analyze the function of OPDA in *P. patens*. As shown in Fig. 2.3, 82 proteins were differentially expressed in response to OPDA treatment in gametophores (threshold level: 2.5-fold change). The amounts of 41 proteins were differentially altered in protonemata (threshold level: 1.5-fold change). The abundance of most proteins decreased following OPDA treatment in both developmental stages.

The proteins that decreased in abundance in protonemata and gametophores accounted for majority of the proteins that were differently altered proteins due to OPDA treatment. Proteins involved in protein metabolism, energy and carbohydrate metabolism accounted for approximately 65 % and 73 % of the proteins that decreased in abundance due to OPDA treatment in protonemata and gametophores, respectively. These results suggest that the primary mode of action of OPDA is the repression of protein metabolism and energy consumption processes at both developmental stages. Proteins involved in photosynthesis accounted for 100 % and 83 % of the proteins that increased abundance due to OPDA treatment in protonemata (one protein) and gametophores, respectively. These results suggest that OPDA would act on photosynthesis in both gametophores and protonemata. The abundance suppression of several histones was notable in *P. patens* protonemata treated with OPDA.

2.3 Discussion

A comparison of the proteome data of OPDA treated-*P. patens* protonemata with those of OPDA-treated *P. patens* gametophores revealed that greater number of proteins were affected in gametophores than in protonemata. Additionally, the magnitude of the changes in protein abundance evoked by OPDA in gametophores was greater than in protonemata. As protonemata differentiate into gametophores, physiological events seem to be more complex in *P. patens*. Complicated physiological reactions may cause OPDA to affect protein abundance more significantly in gametophores. Whereas OPDA elevates the abundance of a set of proteins in Arabidopsis (Dueckershoff et al., 2008), the abundance of most proteins altered by OPDA decreased in *P. patens*. Contrary to the changes in protein due to OPDA observed in Arabidopsis, OPDA mainly decreased the abundance of proteins in both protonemata and gametophores of *P. patens*.

Changes in the abundance of proteins involved in light-dependent reactions were elicited by OPDA in protonemata and gametophores. Accordingly, it was suggested that OPDA enhances light-dependent reactions in *P. patens*. Light-dependent reactions provide oxygen, which is connected to the production of reactive electrophile species (RES). RES and lipid peroxidation appear to be advantageous in plant cells when plants are subjected to stress. RES is presumed to induce the expression of genes related to cell survival (Farmer & Mueller, 2013). As light-dependent reactions are induced by OPDA, redox changes that stimulate signaling cascades to induce the mediators of nuclear transcription may occur (Dueckershoff et al., 2008). OPDA-induced proteins in light-dependent reactions seem to play roles in the stress response at both the protonema and gametophore stages of *P. patens*. In Arabidopsis, OPDA elevates the accumulation of some proteins involved in photosynthesis; however, the abundance of Rubisco was decreased due to the toxicity of 100 μ M OPDA (Dueckershoff et al., 2008). While a high OPDA concentration might give a harmful effect to plants, OPDA treatment resulted in an induction of the synthesis of

photosynthesis-related proteins. Taken together, it is likely that the increased abundance of photosynthesis-related proteins due to OPDA treatment is conserved in land plants.

A previous proteomic analysis of *P. patens* gametophores demonstrated that OPDA treatment induced the abundance of proteins encoded by genes in the chloroplast genome; these proteins were involved in light-dependent reactions (Toshima et al., 2014). In protonemata, no proteins encoded in the chloroplast genome were altered by OPDA treatment. The OPDA-induced accumulation of proteins encoded in the chloroplast genome, which are involved in light-dependent reactions, may be a physiological response of *P. patens* that is specific to gametophores. The abundance of AOC proteins was induced by OPDA in *P. patens* gametophores, indicating the presence of positive feedback regulation on OPDA biosynthesis in *P. patens* gametophores. In contrast, AOC abundance was not increased in *P. patens* protonemata. Protonema stage is an active growing stage in the life cycle of *P. patens*, therefore protonemata grow more rapidly than gametophores. Given that OPDA retards growth in *P. patens*, the positive feedback regulation on OPDA biosynthesis might be suppressed during the protonema stage.

OPDA also reduced the abundance of proteins involved in proteins synthesis and carbohydrate metabolism. More than 50% of the affected proteins were involved in protein metabolism (Table 2.1, Fig. 2.3C). OPDA treatment mainly reduced the abundance of ribosomal proteins in protonemata. Ribosomes are the primary apparatus for biological protein synthesis. The functional repression of ribosomes disrupts the generation of new proteins, thereby arresting the cell growth. As the protonema stage is a period of active growth, more so than the gametophore stage, the growth inhibition observed due to OPDA treatment might be the result of decreased ribosomal protein abundance in *P. patens* protonemata. Whereas OPDA decreased the abundance of proteins involved in protein metabolism in both protonemata and gametophores, the abundance of additional proteins involved in protein metabolism and amino acid synthesis was reduced in gametophores. OPDA likely repressed protein synthesis multilaterally in gametophores.

The abundance of proteins related to carbohydrate metabolism was also suppressed by OPDA treatment in *P. patens* protonemata; these proteins were not identified in a previous study of gametophores. Given that OPDA synthesis is triggered by wounding, the inhibitory effects of OPDA on the abundance of proteins involved in carbohydrate metabolism have likely been adapted to adverse environmental conditions.

OPDA treatment decreased the accumulation of histones in *P. patens* protonemata. The decline in histone accumulation might affect DNA replication, as histones are important components of nucleosomes (Kornberg, 1977). Protonemata grow by apical cell division under the influence of cytokinin; buds are derived from three-faced apical cells that differentiate into gametophores, which contain stem- and leaf-like structures (Roberts et al., 2012). Moreover, cell differentiation is relatively slow in the gametophore stage of *P. patens*. Protonemata grow more rapidly than gametophores. Therefore, suppression of histone expression due to OPDA treatment may retard growth more severely in protonemata than in gametophores.

Genomic analysis revealed that genes homologous to COI and JAZ are also present in *P. patens*. However, JA does not show any significant effect in *P. patens*. It is possible that OPDA and/or an identified OPDA-related compound binds COI for activation of OPDA signaling in *P. patens*. Alternatively, *P. patens* might have a unique OPDA signaling system. In either case, considering that OPDA yields physiological effects in land plants, an OPDA signaling system might have been conserved since the emergence of land plants.

Chapter 3 Comparative proteomic analysis of wild-type *P. patens* and OPDA-deficient *P. patens* mutant after wounding

3.1 Introduction

Transcriptomic and proteomic analyses have been conducted to understand the molecular basis of environmental stress tolerance in *P. patens* (Wang et al., 2008, Wang et al., 2009, Wang et al., 2010, Wang et al., 2012, Luo et al., 2016). Specifically, drought tolerance studies in *P. patens* could help to elucidate how plants acquired drought resistance, thereby permitting their invasion of the terrestrial environment. However, the influence of wounding, a severe environmental stress in plants, has been overlooked in *P. patens* until recently (Toshima et al., 2014). Previous research reported that OPDA and MeJA, but not JA, retards the growth of *P. patens* (Dave et al., 2011, Luo et al., 2016, Ponce De Leon et al., 2012). Unlike vascular plants, *P. patens* produces OPDA, but not JA, in response to wounding and pathogenic infection (Stumpe et al., 2010, Pratiwi et al., 2017, Taki et al., 2005, Ponce De Leon et al., 2012). These findings strongly suggest that the first half of the octadecanoid pathway in chloroplasts is conserved in *P. patens* and OPDA, not JA, functions as a signaling molecule in *P. patens*. The differences of the responses to JA and OPDA between vascular plants and bryophytes are a significant observation in the study of plant evolution. Moreover, understanding the functions of AOS activity in *P. patens* would help to elucidate the OPDA signal transduction pathway in plants. Previous research showed that a *P. patens* mutant with *PpAOS1* disrupted did not increase the endogenous OPDA concentration in response to wounding, and the phenotype of the mutant did not differ significantly from that of wild-type. Two AOS genes, *PpAOS1* and *PpAOS2*, are present in the genome of *P. patens* (Scholz et al., 2012). To investigate the mechanism of the adaptation to wounding and the role of AOS in the response to wounding, wild-type *P. patens* and a mutant with disrupted *PpAOS1* and *PpAOS2* were used in this research. We conducted a research to describe the proteomic analysis of *P. patens* subjected to wounding. A comparative proteomic analysis of wounded wild-type *P. patens* and a mutant in which *PpAOS1* and *PpAOS2* are disrupted, revealed

physiological responses, which is involved in AOS reactions, to wounding in *P. patens*. The detailed procedure was shown as Fig. 3.1.

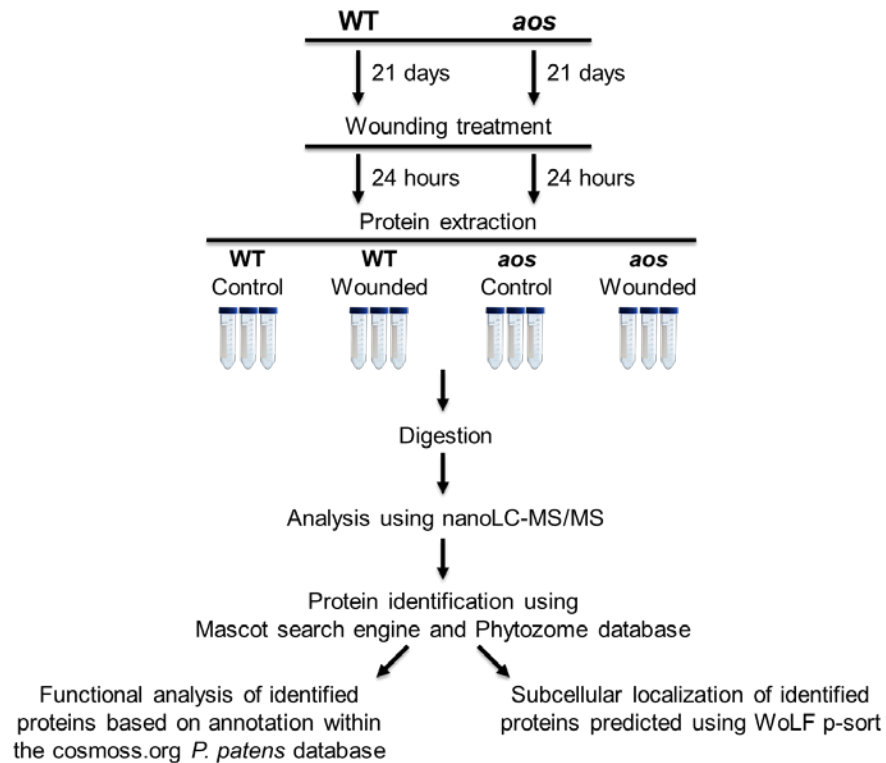


Fig. 3.1. Experimental design for proteomic analysis of

Physcomitrella patens subjected to wounding.

Three-week-old *P. patens* (wild type and the *aos* mutant) were treated without or with wounding treatment. Three-week-old *P. patens* were on gametophore stage. The wounding treatment was conducted by tweezers. *P. patens* (wild type and the *aos* mutant) without wounding were used as control. Extracted proteins were digested, and the obtained peptides were analyzed using nano LC-MS/MS. Three independent experiments were conducted as biological replicates for proteome analysis.

3.2 Results

3.2.1 *P. patens* mutants with disrupted *PpAOS1* and *PpAOS2* genes

To study the difference of physiological responses to wounding with or without OPDA, three *P. patens* OPDA-deficient mutants in which *PpAOS1* and *PpAOS2* were disrupted (A5, A19, and A22) were constructed. Ultra-performance liquid chromatography-tandem mass spectrometry (UPLC-MS/MS) analysis of OPDA in the three mutants revealed that wounding did not induce OPDA accumulation, however, a trace amount of OPDA was found in the *P. patens* mutants in which *PpAOS1* and *PpAOS2* are disrupted (Fig. 3.2).

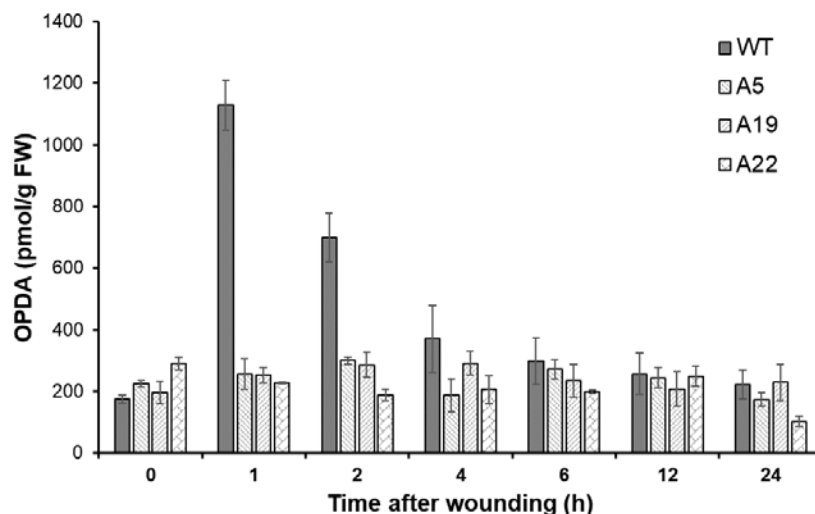


Fig. 3.2. Concentration of OPDA in *P. patens* after wounding.

The wild-type and the *aos* mutant of *P. patens* were grown on BCDATG agar for 3 weeks and then subjected to wounding. The samples were prepared at 1h, 2h, 4h, 6h, 12h and 24h after wounding. Three independent experiments were conducted as biological replicates. The concentrations of OPDA in a wild-type and *aos* mutant (A5, A19, and A22) after wounding were analyzed by UPLC-MS/MS. The values are the means \pm SD ($n = 3$).

The results showed that the OPDA biosynthetic pathway is present in *P. patens* without PpAOS1 and PpAOS2. The growth of the three mutants was almost same as that of the wild-type and no significant difference in phenotype and OPDA production was found between the three mutants (Fig. 3.3). The A5 strain (referred to as the *aos* mutant hereafter) was utilized to investigate the influence of *PpAOS* gene disruption, which suppressed OPDA synthesis, at the protein level in response to wounding. *PpAOS1* and *PpAOS2* genes in *aos* mutant were not induced by wounding (Fig. 3.3).

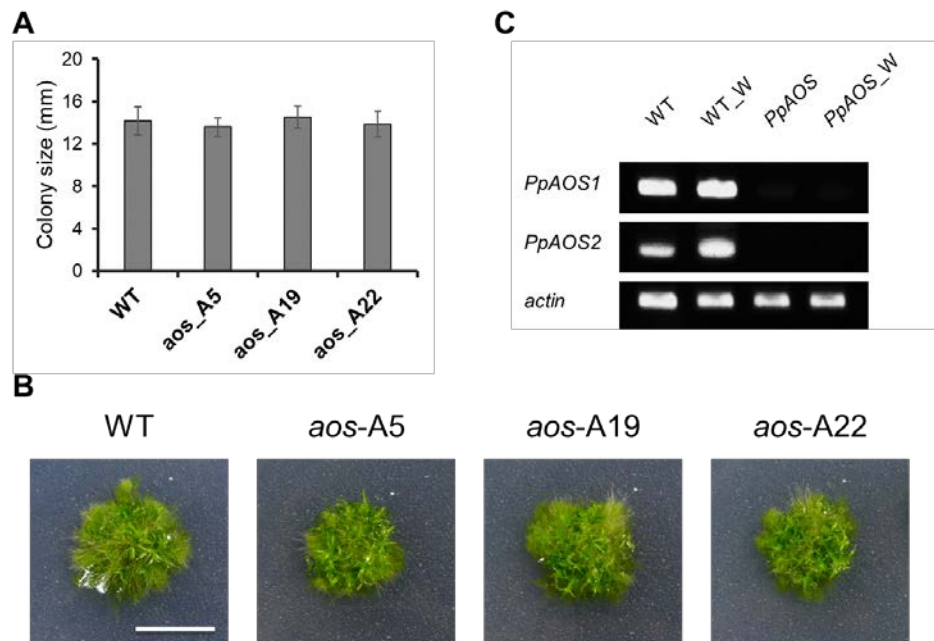


Fig. 3.3. Phenotypic analysis of the wild-type and the *aos* mutant of *P. patens*.

The wild-type and the *aos* mutant of *P. patens* were grown on BCDATG agar for 3 weeks and then their phenotypes were compared. (A) Colony size analysis of *P. patens*. (B) Morphological analysis of the wild-type and the *aos* mutant of *P. patens*. The wild-type and the *aos* mutant of *P. patens* were grown on BCDATG agar for 3 weeks and then their colony size and morphology were compared. The values are the means \pm SD (n = 12). Student *t*'test (* p <0.5, ** p <0.1, *** p <0.001). White bar means 1cm. (C) Semi qRT-PCR of AOS genes

expression after wounding in WT and *aos* mutant (A5). Gametophores of *P. patens*, which were grown on BCDAT agar medium for 3 weeks, wounded by tweezers and harvested 1 hour later after wounding for RNA isolation. PCR was performed using cDNA that was prepared from the total RNA of *P. patens*. WT_W and PpAOS_W mean wild type and *aos* mutant, which were subjected to wounding. The gels were visualized by ethidium bromide staining.

3.2.2 Identification of proteins that are differentially accumulated in response to wounding

To identify *P. patens* proteins that are altered by wounding, gel-free/label-free proteomic analysis was performed. The outline of the procedure used for proteome analysis in this study is illustrated in Fig. 3.1. Proteins were extracted from 3-week-old wild-type *P. patens* and the *aos* mutant with or without wounding. The extracted proteins were digested with trypsin, and the resulting peptides were analyzed by quantitative proteomics using nano-LC-MS/MS (Wang & Komatsu, 2017). Three biological replicates were conducted in this study. The numbers of proteins with >2 matched peptides whose abundance was changed by wounding were 261 and 281 in the wild-type and the *aos* mutant, respectively. Among these proteins, the levels of 136 and 88 proteins were significantly altered more than 1.5-fold in response to wounding in the wild-type and the *aos* mutant, respectively ($p < 0.05$) (Table 3.1 and 3.2). The distributions of the number of peptides, whose abundance were altered, are shown in Fig. 3.4. The identified proteins were compared to show the common proteins and distinct proteins in response to wounding in wild-type and *aos* mutant (Fig. 2.5, Tables 3.3, 3.4 and 3.5). Wounding increased the abundance of 114 proteins in the wild-type and 88 proteins in the *aos* mutant, while the abundance of 22 proteins in the wild-type was decreased due to wounding (Fig. 3.4). Remarkably, the proteins in the *aos* mutant did not decrease significantly in response to wounding. As the *aos* mutant did not exhibit an increase in the OPDA concentration in response to wounding unlike the wild-type (Fig. 3.2), it appears that *PpAOS* gene expression, which leads to increase OPDA, is related to the decrease in protein abundance observed in response to wounding.

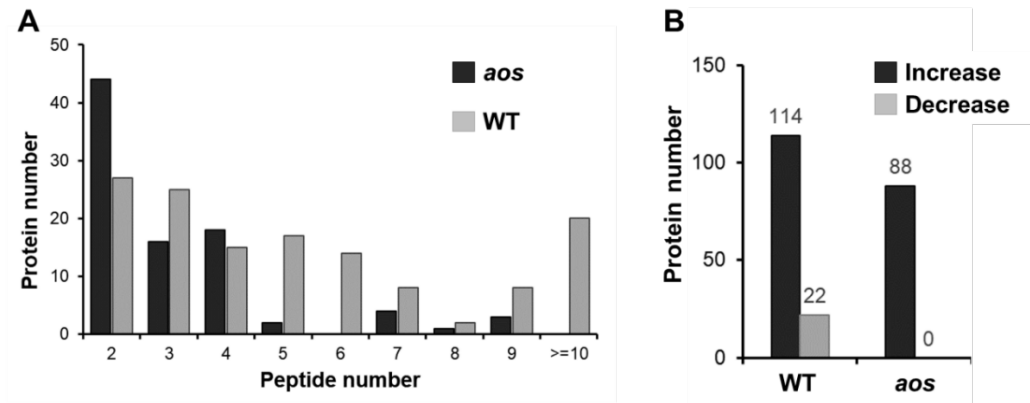


Fig. 3.4. Identification and comparative analysis of the *P. patens* proteome.

(A) The number of peptides that match proteins, as indicated by Mascot search engine. (B) Comparison of the global protein response to wounding in *P. patens* wild-type and the *aos* mutant. The proteins were identified using the Mascot search engine and the *P. patens* database (38,480 protein sequences), which was obtained from the Phytozome database (<http://www.cosmoss.org/>).

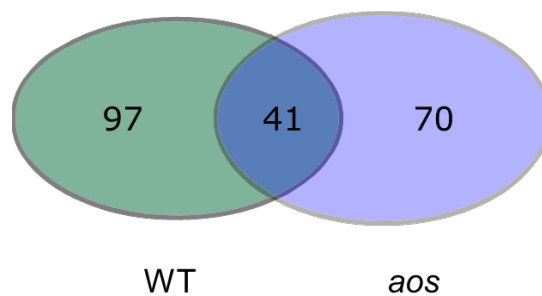


Fig. 3.5. Venn-diagram of identified proteins in WT and *aos* mutant in response to wounding.

Venn-diagram of identified proteins shows the common proteins and distinct proteins in response to wounding in WT and *aos* mutant.

Table 3.1. Identified proteins in response to wounding in wild-type *P. patens*.

Protein ID ¹	Description	Function	Subcellular location	MP ²	Ratio ³
Pp1s141_125V6.1	Chaperonin (Cpn60/TCP-1)	Protein fold	Chloroplast	2	3.13
Pp1s201_109V6.1	Chaperonin (Cpn60/TCP-1)	Protein fold	Chloroplast	2	3.13
Pp1s56_219V6.1	Chaperonin (Cpn60/TCP-1)	Protein fold	Chloroplast	6	3.13
Pp1s434_27V6.1	Lipase/lipoxygenase, PLAT/LH2	Lipid metabolism	Chloroplast	3	2.90
Pp1s207_94V6.1	Protein synthesis factor, GTP-binding	Protein synthesis	Endoplasmic reticulum	3	2.78
Pp1s73_232V6.2	Ribosomal Protein L14b/L23e	Protein synthesis	Endoplasmic reticulum	4	2.73
Pp1s114_79V6.1	Ribosomal Protein L14b/L23e	Protein synthesis	Endoplasmic reticulum	4	2.66
Pp1s16_112V6.1	Ribosomal Protein L14b/L23e	Protein synthesis	Endoplasmic reticulum	4	2.66
Pp1s62_136V6.1	Ribosomal Protein L14b/L23e	Protein synthesis	Endoplasmic reticulum	2	2.66
Pp1s60_179V6.1	Ketol-acid reductoisomerase	Amino acid metabolism	Chloroplast	3	2.37
Pp1s290_40V6.1	Dehydrogenase, multihelical	Amino acid metabolism	Cytoplasm	2	2.37
Pp1s103_66V6.1	ATPase	Energy synthesis	Chloroplast	3	2.32
Pp1s131_71V6.3	Superoxide dismutase	Redox	Chloroplast	2	2.31
Pp1s359_40V6.1	Pyridoxal phosphate-dependent enzyme	Photosystem	Chloroplast	7	2.29
Pp1s78_56V6.2	Dihydrolipoamide acetyltransferase, long form	Photosystem	Chloroplast	7	2.26
Pp1s97_112V6.1	Cytochrome P450 (allene oxide synthase 2)	Lipid metabolism	Chloroplast	4	2.22
Pp1s345_25V6.1	Photosystem I reaction center Protein Psaf, subunit III	Photosystem I	Chloroplast	5	2.20
Pp1s80_23V6.1	Photosystem I reaction center Protein Psaf, subunit III	Photosystem I	Chloroplast	5	2.19
Pp1s251_44V6.1	Ribulose biphosphate carboxylase, small subunit (RuBisCO)	Carbon fixation	Chloroplast	4	2.19
Pp1s38_300V6.1	Malate dehydrogenase	TCA cycle	Cytoplasm	7	2.19
Pp1s98_132V6.1	Dihydrolipoamide dehydrogenase	TCA cycle	Mitochondrial	3	2.16
Pp1s39_428V6.1	Malate dehydrogenase	TCA cycle	Cytoplasm	8	2.15
Pp1s25_66V6.1	Photosystem II manganese-stabilizing Protein PsbO	Photosystem II	Chloroplast	8	2.13
Pp1s121_54V6.1	Photosystem I reaction center Protein Psaf, subunit III	Photosystem I	Chloroplast	5	2.13
Pp1s19_276V6.1	Photosystem I reaction center Protein Psaf, subunit III	Photosystem I	Chloroplast	5	2.13
Pp1s228_3V6.1	Acetohydroxy acid isomeroreductase	Amino acid metabolism	Chloroplast	6	2.12

Continued

Table 3.1. Continued

Protein ID ¹	Description	Function	Subcellular location	MP ²	Ratio ³
Pp1s172_22V6.1	Translation elongation factor EF1B	Protein synthesis	Cytoplasm	3	2.12
Pp1s206_126V6.1	Germin-like Protein GLP2	Photosystem	Chloroplast	2	2.05
Pp1s311_58V6.1	Eukaryotic translation initiation factor	Protein synthesis	Cytoplasm	3	2.02
Pp1s215_81V6.1	Ribosomal Protein S13	Protein synthesis	Endoplasmic reticulum	4	2.02
Pp1s98_250V6.1	GDP-mannose 3-epimerase	Carbohydrate metabolism	Cytoplasm	2	2.01
Pp1s330_36V6.1	Ribosomal Protein L3	Protein synthesis	Endoplasmic reticulum	2	2.01
Pp1s77_207V6.1	Ribosomal Protein L3	Protein synthesis	Endoplasmic reticulum	3	2.01
Pp1s112_169V6.1	Cytochrome b6-f complex iron-sulfur subunit	Photosystem	Chloroplast	3	2.01
Pp1s215_71V6.1	Ribosomal Protein S13	Protein synthesis	Endoplasmic reticulum	3	2.00
Pp1s72_222V6.1	Ribosomal Protein S13	Protein synthesis	Endoplasmic reticulum	7	2.00
Pp1s39_223V6.2	Protein disulfide isomerase	Protein synthesis	Endoplasmic reticulum	3	2.00
Pp1s133_103V6.1	Histone h4	Gene expression	Nuclear	3	1.99
Pp1s269_48V6.1	Histone h5	Gene expression	Nuclear	3	1.99
Pp1s342_32V6.1	Histone h6	Gene expression	Nuclear	5	1.99
Pp1s8_168V6.1	Acetyl-biotin carboxylase	Lipid metabolism	Chloroplast	14	1.96
Pp1s283_22V6.1	UDP-glucose pyrophosphorylase	Carbohydrate metabolism	Cytoplasm	3	1.92
Pp1s154_131V6.1	Ribosomal Protein L3	Protein synthesis	Endoplasmic reticulum	4	1.91
Pp1s40_48V6.3	Multicopper oxidase type 2	Redox	Cytoplasm	6	1.91
Pp1s18_23V6.1	Acetyl-biotin carboxylase	Lipid metabolism	Chloroplast	12	1.90
Pp1s308_11V6.1	L-ascorbate oxidase	Redox	Cytoplasm	3	1.89
Pp1s106_16V6.2	Formate dehydrogenase	Redox	Cytoplasm	4	1.87
Pp1s182_26V6.1	Photosystem II oxygen evolving complex Protein PsbQ	Photosystem II	Chloroplast	3	1.86
Pp1s131_153V6.1	Superoxide dismutase (SOD)	Redox	Chloroplast	11	1.85
Pp1s306_84V6.1	Photosystem II manganese-stabilizing Protein PsbO	Photosystem II	Chloroplast	6	1.84
Pp1s127_74V6.1	Ribosomal Protein S3	Protein synthesis	Endoplasmic reticulum	6	1.79

Continued

Table 3.1. Continued

Protein ID ¹	Description	Function	Subcellular location	MP ²	Ratio ³
Pp1s136_175V6.1	Ribosomal Protein S3	Protein synthesis	Endoplasmic reticulum	4	1.79
Pp1s91_109V6.1	Heat shock Protein, HSP70	Stress	Cytoplasm	3	1.76
Pp1s21_165V6.1	Ribosomal Protein 60S	Protein synthesis	Endoplasmic reticulum	2	1.76
Pp1s14_438V6.1	Ribosomal Protein S13	Protein synthesis	Endoplasmic reticulum	2	1.75
Pp1s185_81V6.1	Non-green plastid inner envelope membrane Protein	Transport	Plasma Membrane	10	1.75
Pp1s258_52V6.1	Heat shock Protein, HSP90	Stress	Cytoplasm	4	1.73
Pp1s26_173V6.2	QuinohemoProtein ethanol dehydrogenase type I (QH-EDH1)	Glycolysis	Plasma Membrane	15	1.72
Pp1s39_82V6.1	UDP-glucose pyrophosphorylase	Carbohydrate metabolism	Cytoplasm	10	1.71
Pp1s79_110V6.1	Malate dehydrogenase	TCA cycle	Cytoplasm	9	1.70
Pp1s21_36V6.1	DJ-1/PfpI family	Protein synthesis	Cytoplasm	10	1.70
Pp1s201_6V6.1	Mitochondrial nad-dependent malate dehydrogenase	Glycolysis	Cytoplasm	2	1.69
Pp1s85_94V6.1	Non-green plastid inner envelope membrane Protein	Transport	Plasma Membrane	9	1.68
Pp1s133_10V6.1	Phosphoenolpyruvate carboxykinase	Gluconeogenesis	Cytoplasm	2	1.67
Pp1s144_37V6.1	Ribosomal Protein L19	Protein synthesis	Endoplasmic reticulum	11	1.65
Pp1s60_65V6.1	Photosystem II manganese-stabilizing Protein PsbO	Photosystem II	Chloroplast	2	1.65
Pp1s294_50V6.1	Dihydroorotate dehydrogenase family Protein	Energy synthesis	Mitochondrial	2	1.64
Pp1s40_57V6.2	Dihydropyrimidine dehydrogenase	Amino acid metabolism	Chloroplast	9	1.64
Pp1s145_172V6.1	Elongation factor 1-delta 1	Protein synthesis	Cytoplasm	16	1.63
Pp1s154_66V6.1	ATP synthase beta chain	Energy synthesis	Mitochondrial	5	1.63
Pp1s12_289V6.1	Pyruvate kinase	Glycolysis	Cytoplasm	5	1.63
Pp1s12_307V6.1	Pyruvate kinase	Glycolysis	Cytoplasm	6	1.63
Pp1s425_20V6.1	Geranylgeranyl reductase	Photosystem	Chloroplast	5	1.62
Pp1s106_68V6.2	ThioRedoxin m	Redox	Mitochondrial	5	1.62
Pp1s23_109V6.1	ThioRedoxin m	Redox	Mitochondrial	5	1.62
Pp1s317_49V6.1	ThioRedoxin m	Redox	Mitochondrial	5	1.62

Continued

Table 3.1. Continued

Protein ID ¹	Description	Function	Subcellular location	MP ²	Ratio ³
Pp1s326_66V6.1	ThioRedoxin m	Redox	Mitochondrial	9	1.62
Pp1s17_59V6.1	Pyridoxal phosphate-dependent enzyme (oas-tl4 cysteine) synthase	Amino acid metabolism	Mitochondrial	11	1.62
Pp1s27_81V6.1	Vitamin-b12 independent methionine 5-methyltetrahydropteroyltriglutamate-homocysteine	Amino acid metabolism	Chloroplast	9	1.62
Pp1s291_62V6.1	Heat shock Protein, HSP90	Stress	Cytoplasm	11	1.61
Pp1s628_7V6.1	Light-harvesting complex ii Protein lhcb5	Photosystem II	Chloroplast	3	1.61
Pp1s156_57V6.1	Pyruvate dehydrogenase e1 component subunit beta	Glycolysis	Cytoplasm	12	1.61
Pp1s6_313V6.1	Light-harvesting complex ii Protein lhcb5	Photosystem II	Chloroplast	11	1.60
Pp1s131_154V6.1	FerRedoxin--nadp+ reductase-like Protein	Photosystem	Chloroplast	2	1.59
Pp1s233_94V6.1	Rnase 1 inhibitor-like Protein	Protein synthesis	Cytoplasm	2	1.59
Pp1s402_8V6.1	Rnase 1 inhibitor-like Protein	Protein synthesis	Cytoplasm	2	1.59
Pp1s425_20V6.2	Geranylgeranyl reductase	Photosystem	Chloroplast	7	1.58
Pp1s348_15V6.1	14-3-3 Protein lil 1433-3	Signaling	Nuclear	7	1.58
Pp1s67_176V6.1	14-3-3 Protein lil 1433-3	Signaling	Nuclear	7	1.58
Pp1s154_69V6.1	ATPase alpha subunit Protein ATPB	Energy synthesis	Mitochondrial	17	1.58
Pp1s310_30V6.1	ATP synthase beta chain	Energy synthesis	Mitochondrial	17	1.58
Pp1s147_10V6.1	Clathrin heavy chain	Transport	Cytoplasm	6	1.57
Pp1s7_102V6.1	Clathrin heavy chain	Transport	Cytoplasm	6	1.57
Pp1s62_236V6.4	Glutamate dehydrogenase	Amino acid metabolism	Mitochondrial	6	1.57
Pp1s20_284V6.1	Geranylgeranyl reductase	Photosystem	Chloroplast	5	1.57
Pp1s62_236V6.7	Glutamate dehydrogenase	Amino acid metabolism	Mitochondrial	4	1.56
Pp1s309_84V6.1	Glyceraldehyde-3-phosphate dehydrogenase (GAPDH)	Glycolysis	Cytoplasm	9	1.55
Pp1s33_110V6.2	Vitamin-b12 independent methionine 5-methyltetrahydropteroyltriglutamate-homocysteine	Amino acid metabolism	Chloroplast	16	1.55
Pp1s419_7V6.1	Lipoxygenase	Lipid metabolism	Chloroplast	26	1.53
NC_005087.1_cdsid_NP_904171.1	Cytochrome b6	Photosystem	Chloroplast	3	1.53

Continued

Table 3.1. Continued

Protein ID ¹	Description	Function	Subcellular location	MP ²	Ratio ³
Pp1s100_117V6.1	ATP synthase subunit beta	Energy synthesis	Mitochondrial	6	1.52
Pp1s425_12V6.1	Vacuolar ATPase b subunit	Energy synthesis	Mitochondrial	6	1.52
Pp1s85_75V6.2	ATP synthase subunit beta	Energy synthesis	Mitochondrial	6	1.52
Pp1s254_25V6.1	Chloroplast precursor (Plastocyanin)	Photosystem II	Chloroplast	5	1.52
Pp1s309_73V6.2	Glyceraldehyde-3-phosphate dehydrogenase (GAPDH)	Glycolysis	Cytoplasm	9	1.52
Pp1s10_102V6.1	Ribosomal Protein L4/L1e	Protein synthesis	Endoplasmic reticulum	9	1.51
Pp1s99_201V6.1	Amino acid binding	Amino acid metabolism	Cytoplasm	4	1.51
Pp1s214_86V6.1	Type iii chlorophyll a b-binding Protein	Photosystem II	Chloroplast	3	1.50
Pp1s214_87V6.1	Type iii chlorophyll a b-binding Protein	Photosystem II	Chloroplast	3	1.50
Pp1s429_33V6.1	Type iii chlorophyll a b-binding Protein	Photosystem II	Chloroplast	3	1.50
Pp1s100_107V6.1	Geranylgeranyl reductase	Photosystem	Chloroplast	5	1.50
Pp1s399_19V6.1	Vitamin-b12 independent methionine 5-methyltetrahydropteroyltriglutamate-homocysteine	Amino acid metabolism	Chloroplast	14	1.50
Pp1s220_79V6.1	Heat shock Protein, HSP90	Stress	Cytoplasm	10	1.50
Pp1s220_83V6.1	Heat shock Protein, HSP90	Stress	Cytoplasm	10	1.50
Pp1s125_81V6.5	Unknown	Unknown	Cytoplasm	5	0.67
Pp1s334_17V6.1	Photosystem I reaction center subunit IV/PsaE	Photosystem I	Chloroplast	4	0.66
Pp1s351_24V6.1	Heat shock Protein, HSP70	Stress	Cytoplasm	5	0.65
Pp1s24_254V6.1	Unknown	Transport	Mitochondrial	4	0.59
Pp1s114_95V6.1	Rubisco subunit-binding Protein alpha subunit	Carbon fixation	Chloroplast	6	0.56
Pp1s125_81V6.2	Unknown	Unknown	Cytoplasm	6	0.54
Pp1s165_12V6.2	Nucleoside diphosphate kinase	Gene expression	Cytoplasm	3	0.54
Pp1s61_17V6.4	S-formylglutathione hydrolase (esterase d)	Stress	Chloroplast	2	0.51
Pp1s259_76V6.1	Photosystem II 5 kDa Protein, chloroplast precursor (PSII-T)	Photosystem II	Chloroplast	2	0.51
Pp1s54_166V6.1	Photosystem II Protein PsbR (Photosystem ii 10 kda polypeptide)	Photosystem II	Chloroplast	3	0.50

Continued

Table 3.1. Continued

Protein ID ¹	Description	Function	Subcellular location	MP ²	Ratio ³
NC_005087.1_cdsid _NP_904203.1	Photosystem I P700 chlorophyll a apoprotein A2	Photosystem I	Chloroplast	7	0.50
Pp1s131_72V6.1	Serine carboxypeptidase	Amino acid metabolism	Chloroplast	2	0.49
Pp1s170_46V6.1	Rubisco subunit-binding Protein alpha subunit	Carbon fixation	Chloroplast	2	0.48
Pp1s200_89V6.1	Uncharacterized Protein family UPF0133	Unknown	Chloroplast	2	0.44
Pp1s475_2V6.1	SucraseferRedoxin-like protein	Hydrolysis	Cytoplasm	2	0.41
Pp1s309_77V6.1	Glycoside hydrolase (chitinase)	Hydrolysis	Extracellular	3	0.40
Pp1s153_153V6.2	Heat shock Protein, HSP70	Stress	Cytoplasm	2	0.39
Pp1s87_57V6.1	Clathrin light chain (expressed Protein)	Transport	Nuclear	2	0.37
Pp1s15_183V6.1	AMP-ACTIVATED Protein KINASE	Energy synthesis	Chloroplast	2	0.35
Pp1s240_68V6.1	Signal-peptide (Unknown)	Signaling	Extracellular	5	0.32
Pp1s77_158V6.2	GY-Box (GY)	Gene expression	Nuclear	4	0.27
Pp1s52_261V6.1	Late embryoGenesis abundant (plants) lea-related	Stress	Nuclear	2	0.25

¹Protein IDs are from Phytozome ver. 11.0.9 (<http://www.phytozome.net/>).

²MP indicates the number of matched peptides.

³The ratio indicates the fold change between the control and wounding treatment group

Table 3.2. Identified proteins in response to wounding in the *aos* mutant of *P. patens*.

Protein ID ¹	Description	Function	Subcellular location	MP ²	Ratio ³
Pp1s306_59V6.1	Signal-peptide (Expressed Protein)	Unknown	Vacuolar	2	4.68
Pp1s52_261V6.1	Late embryoGenesis abundant (plants) lea-related	Stress	Nuclear	2	4.10
Pp1s75_107V6.2	Glutathione S-transferase (glutathione s-transferase)	Detoxification	Chloroplast	2	3.06
Pp1s109_234V6.1	26S proteasome subunit P45 (26s proteasome subunit 4)	Degradation	Cytoplasm	2	2.59
Pp1s12_207V6.1	26S proteasome subunit P45 (26s proteasome subunit 4)	Degradation	Cytoplasm	2	2.59
Pp1s4_277V6.1	26S proteasome subunit P45 (26s proteasome subunit 4)	Degradation	Cytoplasm	2	2.59
Pp1s106_16V6.1	NAD(P)-binding domain (formate dehydrogenase)	Redox	Cytoplasm	2	2.57
Pp1s31_343V6.1	EUKARYOTIC TRANSLATION INITIATION FACTOR 3F, EIF3F	Gene expression	Cytoplasm	2	2.54
Pp1s170_67V6.1	NADH:ubiquinone oxidoreductase, subunit G	Photosystem II	Chloroplast	2	2.31
Pp1s315_40V6.1	Pre-pro-cysteine Proteinase	Protein synthesis	Extracellular	2	2.25
Pp1s33_172V6.1	Leucyl Aminopeptidase-like Protein	Protein synthesis	Cytoplasm	2	2.23
Pp1s215_81V6.1	Ribosomal Protein S13	Protein synthesis	Endoplasmic reticulum	3	2.22
Pp1s6_50V6.1	Glycoside hydrolase, family 31	Hydrolysis	Vacuolar	2	2.18
Pp1s156_53V6.1	Germin-like Protein GLP4	Stress	Cytoplasm	4	2.15
Pp1s121_144V6.1	Ribosomal Protein L19/L19e	Protein synthesis	Nuclear	2	2.08
Pp1s235_118V6.1	Ribosomal Protein L19/L19e	Protein synthesis	Nuclear	2	2.08
Pp1s302_25V6.1	Ribosomal Protein L19/L19e	Protein synthesis	Nuclear	2	2.08
Pp1s3_375V6.1	Ribosomal Protein L19/L19e	Protein synthesis	Nuclear	2	2.08
Pp1s83_173V6.1	Ribosomal Protein L19/L19e	Protein synthesis	Nuclear	2	2.08
Pp1s14_318V6.1	26S PROTEASOME NON-ATPASE REGULATORY SUBUNIT 4	Degradation	Cytoplasm	2	2.07
Pp1s350_23V6.2	Asparagine synthetase	Amino acid metabolism	Cytoplasm	2	2.05
Pp1s58_224V6.1	GY-Box (GY)	Gene expression	Nuclear	7	2.05
Pp1s73_232V6.2	Ribosomal Protein L14b/L23e	Protein synthesis	Endoplasmic reticulum	3	2.05
Pp1s50_102V6.1	Ribosomal Protein L19/L19e	Protein synthesis	Nuclear	3	2.05
Pp1s28_321V6.1	Formate dehydrogenase/DMSO reductase, domains 1-3	Redox	Cytoplasm	3	2.04

Continued

Table 3.2. Continued

Protein ID ¹	Description	Function	Subcellular location	MP ²	Ratio ³
Pp1s75_99V6.1	LATE EMBRYOGeneSIS ABUNDANT (LEA)	Stress	Nuclear	5	2.03
Pp1s9_107V6.2	12-OXOPHYTODIENOATE REDUCTASE OPR	Stress	Chloroplast	2	2.02
Pp1s335_17V6.1	MRO11.7; expressed Protein	Unknown	Chloroplast	2	1.98
Pp1s206_126V6.1	Germin-like Protein GLP2	Photosystem	Chloroplast	2	1.98
Pp1s293_81V6.1	Unknown	Unknown	Nuclear	9	1.97
Pp1s13_231V6.1	Unknown	Unknown	Nuclear	3	1.95
Pp1s252_67V6.2	Gene abcb16 multidrug resistance Protein	Transport	Plasma Membrane	7	1.95
Pp1s86_31V6.1	Germin-like Protein (GLP4) (GLP5)	Stress	Cytoplasm	5	1.92
Pp1s95_65V6.1	Methionine sulfoxide reductase type	Redox	Chloroplast	2	1.89
Pp1s326_44V6.1	12-Oxophytodienoate reductase 2	Stress	Chloroplast	2	1.88
Pp1s17_304V6.2	Ribosomal Protein S27e	Protein synthesis	Chloroplast	2	1.88
Pp1s92_45V6.1	Ribosomal Protein S27e	Protein synthesis	Chloroplast	2	1.88
Pp1s144_37V6.1	Ribosomal Protein L19/L19e	Protein synthesis	Nuclear	3	1.85
Pp1s218_59V6.1	Serine threonine-Protein kinase	Protein synthesis	Cytoskeleton	2	1.84
Pp1s240_91V6.1	Serine threonine-Protein kinase	Protein synthesis	Cytoskeleton	2	1.84
Pp1s75_99V6.2	Unknown	Unknown	Nuclear	4	1.82
NC_007945.1_cdsid _YP_539003.1	ATPase subunit 8	Energy synthesis	Mitochondrial	2	1.82
Pp1s159_85V6.2	SOUL heme-binding Protein (soul-like Protein)	Signaling	Nuclear	2	1.81
Pp1s285_10V6.1	Cysteine protease	Degradation	Vacuolar	3	1.80
Pp1s348_22V6.1	Plastid-Lipid-associated Protein	Transport	Chloroplast	4	1.77
Pp1s69_133V6.1	Putative Protein	Transport	Chloroplast	4	1.76
Pp1s180_8V6.1	Neuromodulin (Growth- associated Protein 43)	Degradation	Cytoplasm	3	1.75
Pp1s44_58V6.1	GTP-binding Protein	Signaling	Cytoplasm	3	1.73
Pp1s214_86V6.1	Type iii chlorophyll a b-binding Protein	Photosystem II	Chloroplast	4	1.72
Pp1s214_87V6.2	Type iii chlorophyll a b-binding Protein	Photosystem II	Chloroplast	4	1.72
Pp1s429_33V6.1	Type iii chlorophyll a b-binding Protein	Photosystem II	Chloroplast	4	1.72

Continued

Table 3.2. Continued

Protein ID ¹	Description	Function	Subcellular location	MP ²	Ratio ³
Pp1s131_107V6.1	Sucrose-phosphate synthase	Glycolysis	Cytoplasm	2	1.70
Pp1s181_57V6.4	Unknown	Lipid metabolism	Vacuolar	4	1.70
Pp1s84_187V6.1	Pirin-like Protein	Signaling	Chloroplast	2	1.69
Pp1s157_11V6.1	Glucan endo- -beta-glucosidase	Signaling	Plasma Membrane	2	1.68
Pp1s121_168V6.1	Glycoside hydrolase family	Hydrolysis	Chloroplast	4	1.67
Pp1s72_222V6.2	Ribosomal Protein S13	Protein synthesis	Endoplasmic reticulum	3	1.64
Pp1s215_71V6.1	Ribosomal Protein S14	Protein synthesis	Endoplasmic reticulum	4	1.63
Pp1s72_222V6.1	Ribosomal Protein S15	Protein synthesis	Endoplasmic reticulum	4	1.63
Pp1s55_66V6.2	Late embryoGenesis abundant (plants) lea-related	Stress	Chloroplast	3	1.63
Pp1s152_13V6.1	26S protease regulatory subunit 7	Degradation	Cytoplasm	4	1.62
Pp1s49_256V6.1	26S protease regulatory subunit 7	Degradation	Cytoplasm	4	1.62
Pp1s235_138V6.1	Lactate dehydrogenase (LDH)	Glycolysis	Cytoplasm	2	1.62
Pp1s140_60V6.1	Eukaryotic translation initiation factor 3	Gene expression	Cytoplasm	2	1.61
Pp1s26_26V6.1	Malate dehydrogenase	TCA cycle	Mitochondrial	7	1.60
Pp1s97_166V6.1	Methionine sulfoxide reductase type	Redox	Chloroplast	2	1.60
Pp1s40_48V6.3	Multicopper type 2(Multicopper oxidase, type 2&3)	Redox	Cytoplasm	4	1.60
Pp1s379_40V6.1	Signal transduction Protein with cbs domains	Protein synthesis	Chloroplast	3	1.59
Pp1s82_6V6.1	Germin-like Protein (GLP4) (GLP5)	Stress	Extracellular	8	1.59
Pp1s2_600V6.1	Mitochondrial phosphate carrier Protein	Transport	Mitochondrial	3	1.58
Pp1s2_605V6.1	Mitochondrial phosphate carrier Protein	Transport	Mitochondrial	3	1.58
Pp1s86_72V6.2	Outer membrane lipoProtein blc	Transport	Chloroplast	4	1.58
Pp1s55_65V6.1	Late embryoGenesis abundant (plants) lea-related	Stress	Chloroplast	2	1.57
Pp1s55_66V6.1	Late embryoGenesis abundant (plants) lea-related	Stress	Chloroplast	2	1.57
Pp1s59_239V6.1	Heat shock Protein, HSP70	Stress	Mitochondrial	9	1.54
Pp1s8_209V6.1	Heat shock Protein, HSP20	Stress	Chloroplast	2	1.53
Pp1s94_106V6.1	Pyrophosphate-fructose-6-phosphate 1-phosphotransferase (PFP)	Carbohydrate metabolism	Cytoplasm	3	1.52

Continued

Table 3.2. Continued

Protein ID ¹	Description	Function	Subcellular location	MP ²	Ratio ³
Pp1s9_103V6.1	Succinate-CoA ligase	TCA cycle	Mitochondrial	2	1.52
Pp1s12_415V6.1	GRAM domain-containing Protein	Signaling	Nuclear	7	1.51
Pp1s333_15V6.1	Pyruvate kinase	Glycolysis	Cytoplasm	2	1.51
Pp1s70_15V6.1	Pyruvate kinase	Glycolysis	Cytoplasm	2	1.51
Pp1s37_247V6.2	60s ribosomal Protein l2	Protein synthesis	Cytoplasm	4	1.50
Pp1s582_3V6.1	60s ribosomal Protein l2	Protein synthesis	Cytoplasm	4	1.50

¹Protein IDs are from Phytozome ver. 11.0.9 (<http://www.phytozome.net/>).

²MP indicates the number of matched peptides.

³The ratio indicates the fold change between the control and wounding treatment group

Table 3.3. Identified proteins in response to wounding both in wild-type *P. patens* and *aos* mutant.

Protein ID ¹	Description	Function	Subcellular location	R_WT ²	R_ao ³
Pp1s73_232V6.2	Ribosomal Protein L14b/L23e	Protein synthesis	Endoplasmic reticulum	2.73	2.05
Pp1s78_56V6.2	Dihydrolipoamide acetyltransferase, long form	Photosystem	Chloroplast	2.26	1.39
Pp1s25_66V6.1	Photosystem II manganese-stabilizing Protein PsbO	Photosystem II	Chloroplast	2.13	1.17
Pp1s172_22V6.1	Translation elongation factor EF1B	Protein synthesis	Cytoplasm	2.12	1.27
Pp1s206_126V6.1	Germin-like Protein GLP2	Photosystem	Chloroplast	2.05	1.98
Pp1s311_58V6.1	Eukaryotic translation initiation factor	Protein synthesis	Cytoplasm	2.02	1.45
Pp1s215_81V6.1	Ribosomal Protein S13	Protein synthesis	Endoplasmic reticulum	2.02	2.22
Pp1s215_71V6.1	Ribosomal Protein S13	Protein synthesis	Endoplasmic reticulum	2.00	1.63
Pp1s72_222V6.1	Ribosomal Protein S13	Protein synthesis	Endoplasmic reticulum	2.00	1.63
Pp1s39_223V6.2	Protein disulfide isomerase	Protein synthesis	Endoplasmic reticulum	2.00	1.23
Pp1s283_22V6.1	UDP-glucose pyrophosphorylase	Carbohydrate metabolism	Cytoplasm	1.92	1.29
Pp1s40_48V6.3	Multicopper oxidase type 2	Redox	Cytoplasm	1.91	1.60
Pp1s18_23V6.1	Acetyl-biotin carboxylase	Lipid metabolism	Chloroplast	1.90	1.45
Pp1s308_11V6.1	L-ascorbate oxidase	Redox	Cytoplasm	1.89	1.32
Pp1s106_16V6.2	Formate dehydrogenase	Redox	Cytoplasm	1.87	2.57
Pp1s106_16V6.2	Formate dehydrogenase	Redox	Cytoplasm	1.87	1.12
Pp1s306_84V6.1	Photosystem II manganese-stabilizing Protein PsbO	Photosystem II	Chloroplast	1.84	1.49
Pp1s79_110V6.1	Malate dehydrogenase	TCA cycle	Cytoplasm	1.70	1.37
Pp1s133_10V6.1	Phosphoenolpyruvate carboxykinase	Gluconeogenesis	Cytoplasm	1.67	1.85
Pp1s144_37V6.1	Ribosomal Protein L19	Protein synthesis	Endoplasmic reticulum	1.65	1.05
Pp1s60_65V6.1	Photosystem II manganese-stabilizing Protein PsbO	Photosystem II	Chloroplast	1.65	1.44
Pp1s145_172V6.1	Elongation factor 1-delta 1	Protein synthesis	Cytoplasm	1.63	1.27
Pp1s154_66V6.1	ATP synthase beta chain	Energy synthesis	Mitochondrial	1.63	1.15
Pp1s17_59V6.1	Pyridoxal phosphate-dependent enzyme (oas-tl4 cysteine) synthase	Amino acid metabolism	Mitochondrial	1.62	1.27
Pp1s628_7V6.1	Light-harvesting complex ii Protein lhcb5	Photosystem II	Chloroplast	1.61	2.05

Continued

Table 3.3. Continued

Protein ID ¹	Description	Function	Subcellular location	R_WT ²	R_ao ³
Pp1s156_57V6.1	Pyruvate dehydrogenase e1 component subunit beta	Glycolysis	Cytoplasm	1.61	1.19
Pp1s6_313V6.1	Light-harvesting complex ii Protein lhcb5	Photosystem II	Chloroplast	1.60	1.27
Pp1s154_69V6.1	ATPase alpha subunit Protein ATPB	Energy synthesis	Mitochondrial	1.58	1.27
Pp1s310_30V6.1	ATP synthase beta chain	Energy synthesis	Mitochondrial	1.58	1.27
Pp1s62_236V6.4	Glutamate dehydrogenase	Amino acid metabolism	Mitochondrial	1.57	1.38
Pp1s33_110V6.2	Vitamin-b12 independent methionine 5-methyltetrahydropteroyltriglutamate-homocysteine	Amino acid metabolism	Chloroplast	1.55	1.44
Pp1s100_117V6.1	ATP synthase subunit beta	Energy synthesis	Mitochondrial	1.52	1.31
Pp1s425_12V6.1	Vacuolar ATPase b subunit	Energy synthesis	Mitochondrial	1.52	1.31
Pp1s85_75V6.2	ATP synthase subunit beta	Energy synthesis	Mitochondrial	1.52	1.30
Pp1s214_86V6.1	Type iii chlorophyll a b-binding Protein	Photosystem II	Chloroplast	1.50	1.72
Pp1s214_87V6.1	Type iii chlorophyll a b-binding Protein	Photosystem II	Chloroplast	1.50	1.72
Pp1s429_33V6.1	Type iii chlorophyll a b-binding Protein	Photosystem II	Chloroplast	1.50	1.72
Pp1s220_79V6.1	Heat shock Protein, HSP90	Stress	Cytoplasm	1.50	1.09
Pp1s220_83V6.1	Heat shock Protein, HSP90	Stress	Cytoplasm	1.50	1.09
Pp1s84_187V6.1	Pirin-like Protein	Signaling	Chloroplast	1.46	1.69
Pp1s52_261V6.1	Late embryoGenesis abundant (plants) lea-related	Stress	Nuclear	0.25	4.10

¹Protein IDs are from Phytozome ver. 11.0.9 (<http://www.phytozome.net/>).

²The ratio indicates the fold change between the control and wounding treatment group in wild type.

³The ratio indicates the fold change between the control and wounding treatment group in *aos* mutant.

Table 3.4. Identified proteins in response to wounding in wild-type *P. patens*, not in *aos* mutant.

Protein ID ¹	Description	Function	Subcellular location	MP ²	Ratio ³
Pp1s141_125V6.1	Chaperonin (Cpn60/TCP-1)	Protein fold	Chloroplast	2	3.13
Pp1s201_109V6.1	Chaperonin (Cpn60/TCP-1)	Protein fold	Chloroplast	2	3.13
Pp1s56_219V6.1	Chaperonin (Cpn60/TCP-1)	Protein fold	Chloroplast	6	3.13
Pp1s434_27V6.1	Lipase/lipoxygenase, PLAT/LH2	Lipid metabolism	Chloroplast	3	2.90
Pp1s207_94V6.1	Protein synthesis factor, GTP-binding	Protein synthesis	Endoplasmic reticulum	3	2.78
Pp1s114_79V6.1	Ribosomal Protein L14b/L23e	Protein synthesis	Endoplasmic reticulum	4	2.66
Pp1s16_112V6.1	Ribosomal Protein L14b/L23e	Protein synthesis	Endoplasmic reticulum	4	2.66
Pp1s62_136V6.1	Ribosomal Protein L14b/L23e	Protein synthesis	Endoplasmic reticulum	2	2.66
Pp1s60_179V6.1	Ketol-acid reductoisomerase	Amino acid metabolism	Chloroplast	3	2.37
Pp1s290_40V6.1	Dehydrogenase, multihelical	Amino acid metabolism	Cytoplasm	2	2.37
Pp1s103_66V6.1	ATPase	Energy synthesis	Chloroplast	3	2.32
Pp1s131_71V6.3	Superoxide dismutase	Redox	Chloroplast	2	2.31
Pp1s359_40V6.1	Pyridoxal phosphate-dependent enzyme	Photosystem	Chloroplast	7	2.29
Pp1s97_112V6.1	Cytochrome P450 (allene oxide synthase 2)	Lipid metabolism	Chloroplast	4	2.22
Pp1s345_25V6.1	Photosystem I reaction center Protein PsaF, subunit III	Photosystem I	Chloroplast	5	2.20
Pp1s80_23V6.1	Photosystem I reaction center Protein PsaF, subunit III	Photosystem I	Chloroplast	5	2.19
Pp1s251_44V6.1	Ribulose biphosphate carboxylase, small subunit (RuBisCO)	Carbon fixation	Chloroplast	4	2.19
Pp1s38_300V6.1	Malate dehydrogenase	TCA cycle	Cytoplasm	7	2.19
Pp1s98_132V6.1	Dihydroliipoamide dehydrogenase	TCA cycle	Mitochondrial	3	2.16
Pp1s39_428V6.1	Malate dehydrogenase	TCA cycle	Cytoplasm	8	2.15
Pp1s121_54V6.1	Photosystem I reaction center Protein PsaF, subunit III	Photosystem I	Chloroplast	5	2.13
Pp1s19_276V6.1	Photosystem I reaction center Protein PsaF, subunit III	Photosystem I	Chloroplast	5	2.13
Pp1s228_3V6.1	Acetohydroxy acid isomeroreductase	Amino acid metabolism	Chloroplast	6	2.12
Pp1s98_250V6.1	GDP-mannose 3-epimerase	Carbohydrate metabolism	Cytoplasm	2	2.01
Pp1s330_36V6.1	Ribosomal Protein L3	Protein synthesis	Endoplasmic reticulum	2	2.01

Continued

Table 3.4. Continued

Protein ID ¹	Description	Function	Subcellular location	MP ²	Ratio ³
Pp1s77_207V6.1	Ribosomal Protein L3	Protein synthesis	Endoplasmic reticulum	3	2.01
Pp1s112_169V6.1	Cytochrome b6-f complex iron-sulfur subunit	Photosystem	Chloroplast	3	2.01
Pp1s133_103V6.1	Histone h4	Gene expression	Nuclear	3	1.99
Pp1s269_48V6.1	Histone h5	Gene expression	Nuclear	3	1.99
Pp1s342_32V6.1	Histone h6	Gene expression	Nuclear	5	1.99
Pp1s8_168V6.1	Acetyl-biotin carboxylase	Lipid metabolism	Chloroplast	14	1.96
Pp1s154_131V6.1	Ribosomal Protein L3	Protein synthesis	Endoplasmic reticulum	4	1.91
Pp1s182_26V6.1	Photosystem II oxygen evolving complex Protein PsbQ	Photosystem II	Chloroplast	3	1.86
Pp1s131_153V6.1	Superoxide dismutase (SOD)	Redox	Chloroplast	11	1.85
Pp1s127_74V6.1	Ribosomal Protein S3	Protein synthesis	Endoplasmic reticulum	6	1.79
Pp1s136_175V6.1	Ribosomal Protein S3	Protein synthesis	Endoplasmic reticulum	4	1.79
Pp1s91_109V6.1	Heat shock Protein, HSP70	Stress	Cytoplasm	3	1.76
Pp1s21_165V6.1	Ribosomal Protein 60S	Protein synthesis	Endoplasmic reticulum	2	1.76
Pp1s14_438V6.1	Ribosomal Protein S13	Protein synthesis	Endoplasmic reticulum	2	1.75
Pp1s185_81V6.1	Non-green plastid inner envelope membrane Protein	Transport	Plasma Membrane	10	1.75
Pp1s258_52V6.1	Heat shock Protein, HSP90	Stress	Cytoplasm	4	1.73
Pp1s26_173V6.2	QuinohemoProtein ethanol dehydrogenase type I (QH-EDH1)	Glycolysis	Plasma Membrane	15	1.72
Pp1s39_82V6.1	UDP-glucose pyrophosphorylase	Carbohydrate metabolism	Cytoplasm	10	1.71
Pp1s21_36V6.1	DJ-1/PfpI family	Protein synthesis	Cytoplasm	10	1.70
Pp1s201_6V6.1	Mitochondrial nad-dependent malate dehydrogenase	Glycolysis	Cytoplasm	2	1.69
Pp1s85_94V6.1	Non-green plastid inner envelope membrane Protein	Transport	Plasma Membrane	9	1.68
Pp1s294_50V6.1	Dihydroorotate dehydrogenase family Protein	Energy synthesis	Mitochondrial	2	1.64
Pp1s40_57V6.2	Dihydropyrimidine dehydrogenase	Amino acid metabolism	Chloroplast	9	1.64
Pp1s12_289V6.1	Pyruvate kinase	Glycolysis	Cytoplasm	5	1.63
Pp1s12_307V6.1	Pyruvate kinase	Glycolysis	Cytoplasm	6	1.63

Continued

Table 3.4. Continued

Protein ID ¹	Description	Function	Subcellular location	MP ²	Ratio ³
Pp1s425_20V6.1	Geranylgeranyl reductase	Photosystem	Chloroplast	5	1.62
Pp1s106_68V6.2	ThioRedoxin m	Redox	Mitochondrial	5	1.62
Pp1s23_109V6.1	ThioRedoxin m	Redox	Mitochondrial	5	1.62
Pp1s317_49V6.1	ThioRedoxin m	Redox	Mitochondrial	5	1.62
Pp1s326_66V6.1	ThioRedoxin m	Redox	Mitochondrial	9	1.62
Pp1s27_81V6.1	Vitamin-b12 independent methionine 5-methyltetrahydropteroyltriglutamate-homocysteine	Amino acid metabolism	Chloroplast	9	1.62
Pp1s291_62V6.1	Heat shock Protein, HSP90	Stress	Cytoplasm	11	1.61
Pp1s131_154V6.1	FerRedoxin--nadp+ reductase-like Protein	Photosystem	Chloroplast	2	1.59
Pp1s233_94V6.1	Rnase 1 inhibitor-like Protein	Protein synthesis	Cytoplasm	2	1.59
Pp1s402_8V6.1	Rnase 1 inhibitor-like Protein	Protein synthesis	Cytoplasm	2	1.59
Pp1s425_20V6.2	Geranylgeranyl reductase	Photosystem	Chloroplast	7	1.58
Pp1s348_15V6.1	14-3-3 Protein lil 1433-3	Signaling	Nuclear	7	1.58
Pp1s67_176V6.1	14-3-3 Protein lil 1433-3	Signaling	Nuclear	7	1.58
Pp1s147_10V6.1	Clathrin heavy chain	Transport	Cytoplasm	6	1.57
Pp1s7_102V6.1	Clathrin heavy chain	Transport	Cytoplasm	6	1.57
Pp1s20_284V6.1	Geranylgeranyl reductase	Photosystem	Chloroplast	5	1.57
Pp1s62_236V6.7	Glutamate dehydrogenase	Amino acid metabolism	Mitochondrial	4	1.56
Pp1s309_84V6.1	Glyceraldehyde-3-phosphate dehydrogenase (GAPDH)	Glycolysis	Cytoplasm	9	1.55
Pp1s419_7V6.1	Lipoxygenase	Lipid metabolism	Chloroplast	26	1.53
NC_005087.1_cdsid_NP_904171.1	Cytochrome b6	Photosystem	Chloroplast	3	1.53
Pp1s254_25V6.1	Chloroplast precursor (Plastocyanin)	Photosystem II	Chloroplast	5	1.52
Pp1s309_73V6.2	Glyceraldehyde-3-phosphate dehydrogenase (GAPDH)	Glycolysis	Cytoplasm	9	1.52
Pp1s10_102V6.1	Ribosomal Protein L4/L1e	Protein synthesis	Endoplasmic reticulum	9	1.51
Pp1s99_201V6.1	Amino acid binding	Amino acid metabolism	Cytoplasm	4	1.51
Pp1s100_107V6.1	Geranylgeranyl reductase	Photosystem	Chloroplast	5	1.50

Continued

Table 3.4. Continued

Protein ID ¹	Description	Function	Subcellular location	MP ²	Ratio ³
Pp1s399_19V6.1	Vitamin-b12 independent methionine 5-methyltetrahydropteroyltriglutamate-homocysteine	Amino acid metabolism	Chloroplast	14	1.50
Pp1s125_81V6.5	Unknown	Unknown	Cytoplasm	5	0.67
Pp1s334_17V6.1	Photosystem I reaction center subunit IV/PsaE	Photosystem I	Chloroplast	4	0.66
Pp1s351_24V6.1	Heat shock Protein, HSP70	Stress	Cytoplasm	5	0.65
Pp1s24_254V6.1	Unknown	Transport	Mitochondrial	4	0.59
Pp1s114_95V6.1	Rubisco subunit-binding Protein alpha subunit	Carbon fixation	Chloroplast	6	0.56
Pp1s125_81V6.2	Unknown	Unknown	Cytoplasm	6	0.54
Pp1s165_12V6.2	Nucleoside diphosphate kinase	Gene expression	Cytoplasm	3	0.54
Pp1s61_17V6.4	S-formylglutathione hydrolase (esterase d)	Stress	Chloroplast	2	0.51
Pp1s259_76V6.1	Photosystem II 5 kDa Protein, chloroplast precursor (PSII-T)	Photosystem II	Chloroplast	2	0.51
Pp1s54_166V6.1	Photosystem II Protein PsbR (Photosystem ii 10 kda polypeptide)	Photosystem II	Chloroplast	3	0.50
NC_005087.1_cdsid_NP_904203.1	Photosystem I P700 chlorophyll a apoprotein A2	Photosystem I	Chloroplast	7	0.50
Pp1s131_72V6.1	Serine carboxypeptidase	Amino acid metabolism	Chloroplast	2	0.49
Pp1s170_46V6.1	Rubisco subunit-binding Protein alpha subunit	Carbon fixation	Chloroplast	2	0.48
Pp1s200_89V6.1	Uncharacterized Protein family UPF0133	Unknown	Chloroplast	2	0.44
Pp1s475_2V6.1	Sucrase/ferRedoxin-like protein	Hydrolysis	Cytoplasm	2	0.41
Pp1s309_77V6.1	Glycoside hydrolase (chitinase)	Hydrolysis	Extracellular	3	0.40
Pp1s153_153V6.2	Heat shock Protein, HSP70	Stress	Cytoplasm	2	0.39
Pp1s87_57V6.1	Clathrin light chain (expressed Protein)	Transport	Nuclear	2	0.37
Pp1s15_183V6.1	AMP-ACTIVATED Protein KINASE	Energy synthesis	Chloroplast	2	0.35
Pp1s240_68V6.1	Signal-peptide (Unknown)	Signaling	Extracellular	5	0.32
Pp1s77_158V6.2	GY-Box (GY)	Gene expression	Nuclear	4	0.27

¹Protein IDs are from Phytozome ver. 11.0.9 (<http://www.phytozome.net/>).

²MP indicates the number of matched peptides.

³The ratio indicates the fold change between the control and wounding treatment group.

Table 3.5. Identified proteins in response to wounding in *aos* mutant, not in wild-type *P. patens*.

Protein ID ¹	Description	Function	Subcellular location	MP ²	Ratio ³
Pp1s306_59V6.1	Signal-peptide (Expressed Protein)	Unknown	Vacuolar	2	4.68
Pp1s75_107V6.2	Glutathione S-transferase (glutathione s-transferase)	Detoxification	Chloroplast	2	3.06
Pp1s109_234V6.1	26S proteasome subunit P45 (26s proteasome subunit 4)	Degradation	Cytoplasm	2	2.59
Pp1s12_207V6.1	26S proteasome subunit P45 (26s proteasome subunit 4)	Degradation	Cytoplasm	2	2.59
Pp1s4_277V6.1	26S proteasome subunit P45 (26s proteasome subunit 4)	Degradation	Cytoplasm	2	2.59
Pp1s31_343V6.1	EUKARYOTIC TRANSLATION INITIATION FACTOR 3F, EIF3F	Gene expression	Cytoplasm	2	2.54
Pp1s170_67V6.1	NADH:ubiquinone oxidoreductase, subunit G	Photosystem II	Chloroplast	2	2.31
Pp1s315_40V6.1	Pre-pro-cysteine Proteinase	Protein synthesis	Extracellular	2	2.25
Pp1s33_172V6.1	Leucyl Aminopeptidase-like Protein	Protein synthesis	Cytoplasm	2	2.23
Pp1s6_50V6.1	Glycoside hydrolase, family 31	Hydrolysis	Vacuolar	2	2.18
Pp1s156_53V6.1	Germin-like Protein GLP4	Stress	Cytoplasm	4	2.15
Pp1s121_144V6.1	Ribosomal Protein L19/L19e	Protein synthesis	Nuclear	2	2.08
Pp1s235_118V6.1	Ribosomal Protein L19/L19e	Protein synthesis	Nuclear	2	2.08
Pp1s302_25V6.1	Ribosomal Protein L19/L19e	Protein synthesis	Nuclear	2	2.08
Pp1s3_375V6.1	Ribosomal Protein L19/L19e	Protein synthesis	Nuclear	2	2.08
Pp1s83_173V6.1	Ribosomal Protein L19/L19e	Protein synthesis	Nuclear	2	2.08
Pp1s14_318V6.1	26S PROTEASOME NON-ATPASE REGULATORY SUBUNIT 4	Degradation	Cytoplasm	2	2.07
Pp1s350_23V6.2	Asparagine synthetase	Amino acid metabolism	Cytoplasm	2	2.05
Pp1s58_224V6.1	GY-Box (GY)	Gene expression	Nuclear	7	2.05
Pp1s50_102V6.1	Ribosomal Protein L19/L19e	Protein synthesis	Nuclear	3	2.05
Pp1s28_321V6.1	Formate dehydrogenase/DMSO reductase, domains 1-3	Redox	Cytoplasm	3	2.04
Pp1s75_99V6.1	LATE EMBRYOGeneSIS ABUNDANT (LEA)	Stress	Nuclear	5	2.03
Pp1s9_107V6.2	12-OXOPHYTODIENOATE REDUCTASE OPR	Stress	Chloroplast	2	2.02
Pp1s335_17V6.1	MRO11.7; expressed Protein	Unknown	Chloroplast	2	1.98
Pp1s293_81V6.1	Unknown	Unknown	Nuclear	9	1.97

Continued

Table 3.5. Continued

Protein ID ¹	Description	Function	Subcellular location	MP ²	Ratio ³
Pp1s13_231V6.1	Unknown	Unknown	Nuclear	3	1.95
Pp1s252_67V6.2	Gene abcb16 multidrug resistance Protein	Transport	Plasma Membrane	7	1.95
Pp1s86_31V6.1	Germin-like Protein (GLP4) (GLP5)	Stress	Cytoplasm	5	1.92
Pp1s95_65V6.1	Methionine sulfoxide reductase type	Redox	Chloroplast	2	1.89
Pp1s326_44V6.1	12-Oxophytodienoate reductase 2	Stress	Chloroplast	2	1.88
Pp1s17_304V6.2	Ribosomal Protein S27e	Protein synthesis	Chloroplast	2	1.88
Pp1s92_45V6.1	Ribosomal Protein S27e	Protein synthesis	Chloroplast	2	1.88
Pp1s218_59V6.1	Serine threonine-Protein kinase	Protein synthesis	Cytoskeleton	2	1.84
Pp1s240_91V6.1	Serine threonine-Protein kinase	Protein synthesis	Cytoskeleton	2	1.84
Pp1s75_99V6.2	Unknown	Unknown	Nuclear	4	1.82
NC_007945.1_cdsid_YP_539003.1	ATPase subunit 8	Energy synthesis	Mitochondrial	2	1.82
Pp1s159_85V6.2	SOUL heme-binding Protein (soul-like Protein)	Signaling	Nuclear	2	1.81
Pp1s285_10V6.1	Cysteine protease	Degradation	Vacuolar	3	1.80
Pp1s348_22V6.1	Plastid-Lipid-associated Protein	Transport	Chloroplast	4	1.77
Pp1s69_133V6.1	Putative Protein	Transport	Chloroplast	4	1.76
Pp1s180_8V6.1	Neuromodulin (Growth-associated Protein 43)	Degradation	Cytoplasm	3	1.75
Pp1s44_58V6.1	GTP-binding Protein	Signaling	Cytoplasm	3	1.73
Pp1s131_107V6.1	Sucrose-phosphate synthase	Glycolysis	Cytoplasm	2	1.70
Pp1s181_57V6.4	Unknown	Lipid metabolism	Vacuolar	4	1.70
Pp1s157_11V6.1	Glucan endo- -beta-glucosidase	Signaling	Plasma Membrane	2	1.68
Pp1s121_168V6.1	Glycoside hydrolase family	Hydrolysis	Chloroplast	4	1.67
Pp1s72_222V6.2	Ribosomal Protein S13	Protein synthesis	Endoplasmic reticulum	3	1.64
Pp1s55_66V6.2	Late embryoGenesis abundant (plants) lea-related	Stress	Chloroplast	3	1.63
Pp1s152_13V6.1	26S protease regulatory subunit 7	Degradation	Cytoplasm	4	1.62
Pp1s49_256V6.1	26S protease regulatory subunit 7	Degradation	Cytoplasm	4	1.62
Pp1s235_138V6.1	Lactate dehydrogenase (LDH)	Glycolysis	Cytoplasm	2	1.62
Pp1s140_60V6.1	Eukaryotic translation initiation factor 3	Gene expression	Cytoplasm	2	1.61
Pp1s26_26V6.1	Malate dehydrogenase	TCA cycle	Mitochondrial	7	1.60
Pp1s97_166V6.1	Methionine sulfoxide reductase type	Redox	Chloroplast	2	1.60
Pp1s379_40V6.1	Signal transduction Protein with cbs domains	Protein synthesis	Chloroplast	3	1.59
Pp1s82_6V6.1	Germin-like Protein (GLP4) (GLP5)	Stress	Extracellular	8	1.59

Continued

Table 3.5. Continued

Protein ID ¹	Description	Function	Subcellular location	MP ²	Ratio ³
Pp1s2_600V6.1	Mitochondrial phosphate carrier Protein	Transport	Mitochondrial	3	1.58
Pp1s2_605V6.1	Mitochondrial phosphate carrier Protein	Transport	Mitochondrial	3	1.58
Pp1s86_72V6.2	Outer membrane lipoProtein blc	Transport	Chloroplast	4	1.58
Pp1s55_65V6.1	Late embryoGenesis abundant (plants) lea-related	Stress	Chloroplast	2	1.57
Pp1s55_66V6.1	Late embryoGenesis abundant (plants) lea-related	Stress	Chloroplast	2	1.57
Pp1s59_239V6.1	Heat shock Protein, HSP70	Stress	Mitochondrial	9	1.54
Pp1s8_209V6.1	Heat shock Protein, HSP20	Stress	Chloroplast	2	1.53
Pp1s94_106V6.1	Pyrophosphate-fructose-6-phosphate 1-phosphotransferase (PF6)	Carbohydrate metabolism	Cytoplasm	3	1.52
Pp1s9_103V6.1	Succinate-CoA ligase	TCA cycle	Mitochondrial	2	1.52
Pp1s12_415V6.1	GRAM domain-containing Protein	Signaling	Nuclear	7	1.51
Pp1s333_15V6.1	Pyruvate kinase	Glycolysis	Cytoplasm	2	1.51
Pp1s70_15V6.1	Pyruvate kinase	Glycolysis	Cytoplasm	2	1.51
Pp1s37_247V6.2	60s ribosomal Protein l2	Protein synthesis	Cytoplasm	4	1.50
Pp1s582_3V6.1	60s ribosomal Protein l2	Protein synthesis	Cytoplasm	4	1.50

¹Protein IDs are from Phytozome ver. 11.0.9 (<http://www.phytozome.net/>).

²MP indicates the number of matched peptides.

³The ratio indicates the fold change between the control and wounding treatment group.

3.2.3 Functional categories and subcellular localization of identified wounding-responsive proteins

To determine the functions of the identified proteins, the proteins were annotated using Phytozome (<https://phytozome.jgi.doe.gov/pz/portal.html>) and functionally categorized (Fig. 3.6). Our data showed that various proteins were significantly altered by wounding in the wild-type and the *aos* mutant. In the wild-type, wounding predominantly increased the abundance of proteins related to protein synthesis (27 proteins), photosystems (24 proteins), amino acid metabolism (11 proteins), redox (9 proteins), and energy synthesis (8 proteins). Flowering plants accumulate proteins involved in photosynthesis and protein synthesis under adverse environmental conditions (Kosova et al., 2011). The increases in the proteins, which were involved in protein synthesis and photosystem, in response to wounding are probably conserved in land plants. The *aos* mutant largely accumulated proteins related to protein synthesis (21 proteins), stress (15 proteins) and protein degradation (10 proteins) in response to wounding. The number of accumulated proteins related to protein synthesis in the wild-type was comparable to that in the *aos* mutant. Under wounding stress, the abundance of proteins related to photosystems, amino acid metabolism, redox, and energy synthesis significantly increased in the wild-type compared to those in the *aos* mutant. In contrast, the accumulation of proteins involved in stress and protein degradation in the *aos* mutant was greater than that in the wild-type. *PpAOS* gene disruption affected the difference of protein abundance between the wild-type and the *aos* mutant in response to wounding. It is likely that OPDA is involved in the differential abundance of proteins between the wild-type and the *aos* mutant.

To predict the subcellular localization of the proteins, whose abundance was altered, in the wild-type and the *aos* mutant under wounding stress, bioinformatic analysis was conducted (Martinez-Cortes et al., 2014). Subcellular localization data revealed that more than 30% of the proteins with changes in abundance in response to wounding, including 52 proteins in the wild-type and 27 proteins in the *aos* mutant, are predicted to be localized in the chloroplast (Fig. 3.7). Moreover, 15 proteins with increased abundance are predicted to be localized in the nucleus of the *aos* mutant, and 8 proteins

are speculated to be localized in the nucleus of the wild-type. The bioinformatic findings indicated that proteins in chloroplasts may play an important role in the physiological response to wounding in *P. patens*.

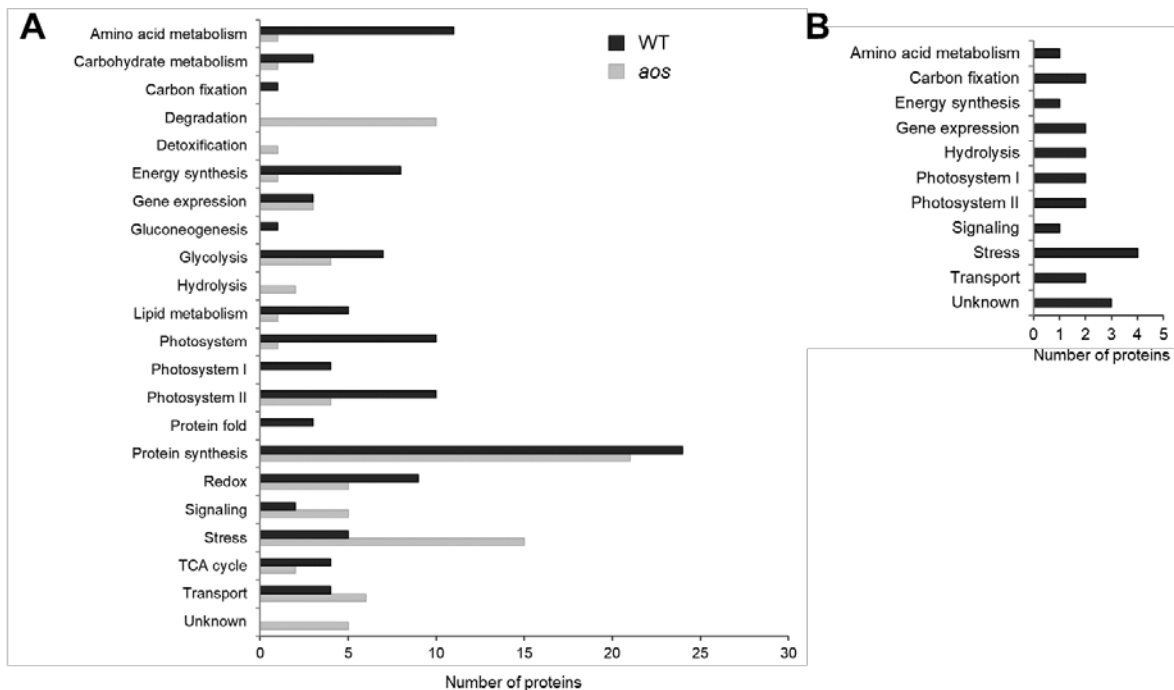


Fig. 3.6. Functional categorization of proteins identified in response to wounding stress in *P. patens* wild-type and the *aos* mutant.

(A) Functional categorization of proteins that accumulated in response to wounding in *P. patens* wild-type and the *aos* mutant. (B) Functional categorization of proteins that decreased in response to wounding in the wild-type *P. patens*. Three-week-old *P. patens* tissues were wounded using tweezers. After 24 h, proteins were extracted from the tissue and analyzed using a gel-free/label-free proteomic technique, and significantly changed proteins ($p < 0.05$) were identified using two-way ANOVA. The identified proteins were functionally categorized.

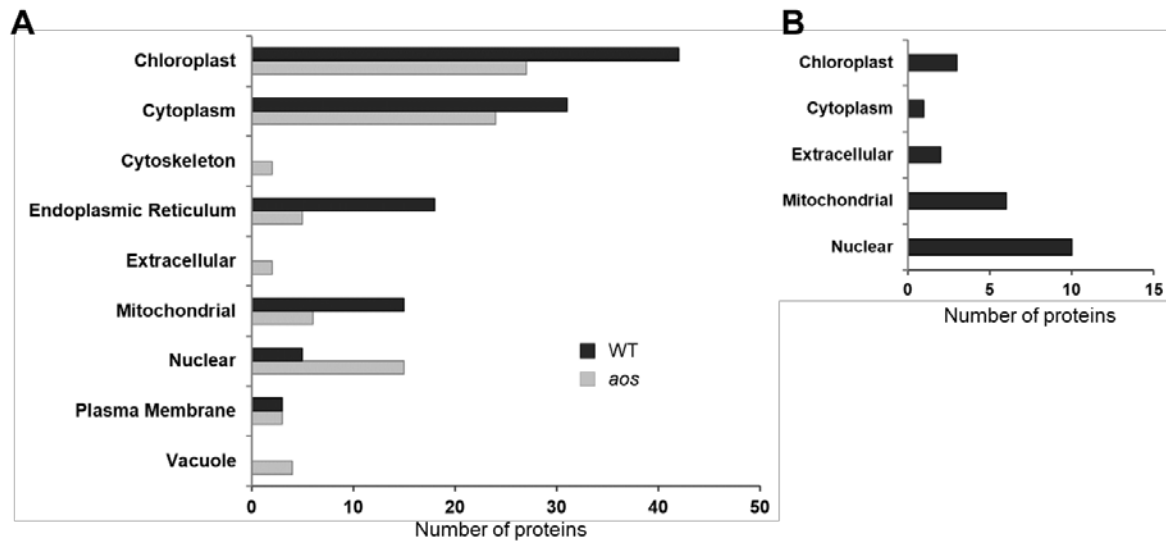


Fig. 3.7. Subcellular localization of proteins whose abundance were changed in response to wounding in *P. patens* wild-type and the *aos* mutant.

(A) Increased proteins. (B) Decreased proteins. The subcellular localization of the identified proteins was predicted using TargetP (<http://www.cbs.dtu.dk/services/TargetP/>), Bacello (<http://gpcr2.biocomp.unibo.it/bacello/index.htm>) and WoLF PSORT (<http://wolfpsort.org/>).

The common proteins and distinct proteins in wild-type and the *aos* mutant in response to wounding were categorized by proteins' function and subcellular localization (Fig. 3.8 and Fig. 3.9).

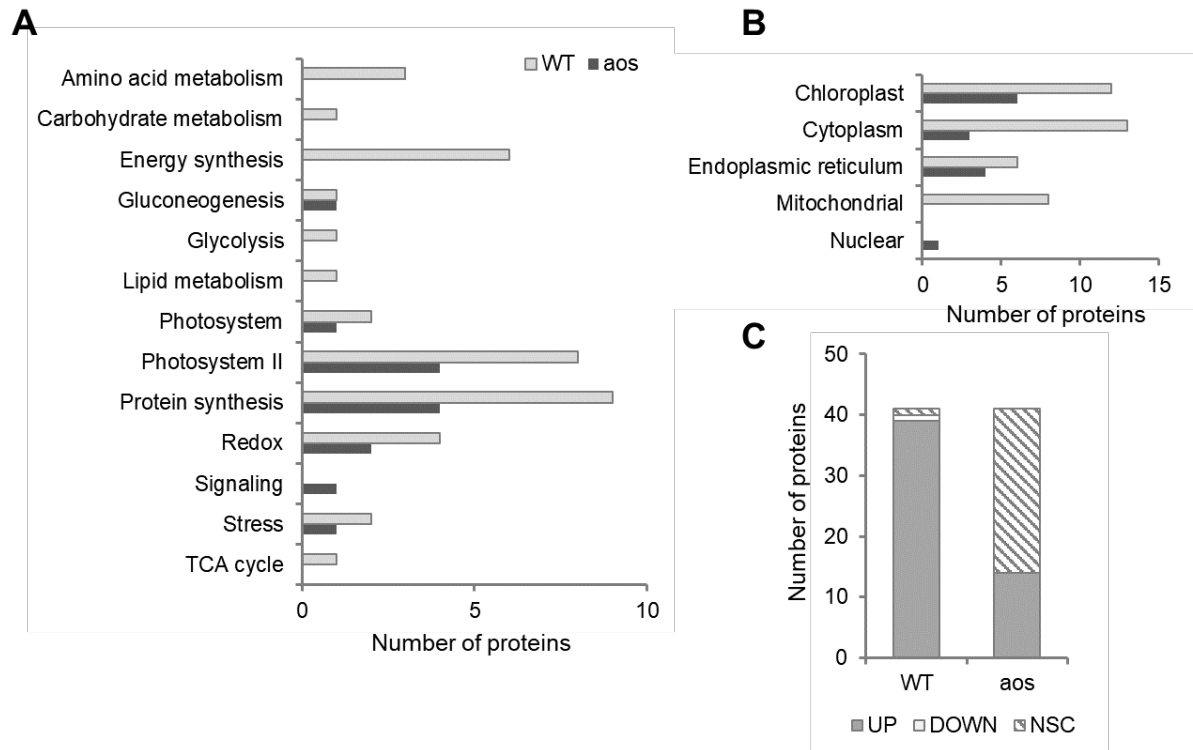


Fig. 3.8. Comparison of common proteins accumulated both in wild type *P. patens* and the *aos* mutant in response to wounding stress.

(A) Functional categorization of common proteins that significantly accumulated in response to wounding in *P. patens* wild-type and the *aos* mutant. (B) Subcellular localization of common proteins that accumulated in response to wounding in *P. patens* wild-type and the *aos* mutant. (C) Comparison of the global common protein response to wounding in *P. patens* wild-type and the *aos* mutant. UP, significantly accumulated proteins; DOWN, significantly decreased proteins; NSC, no significantly changed proteins.

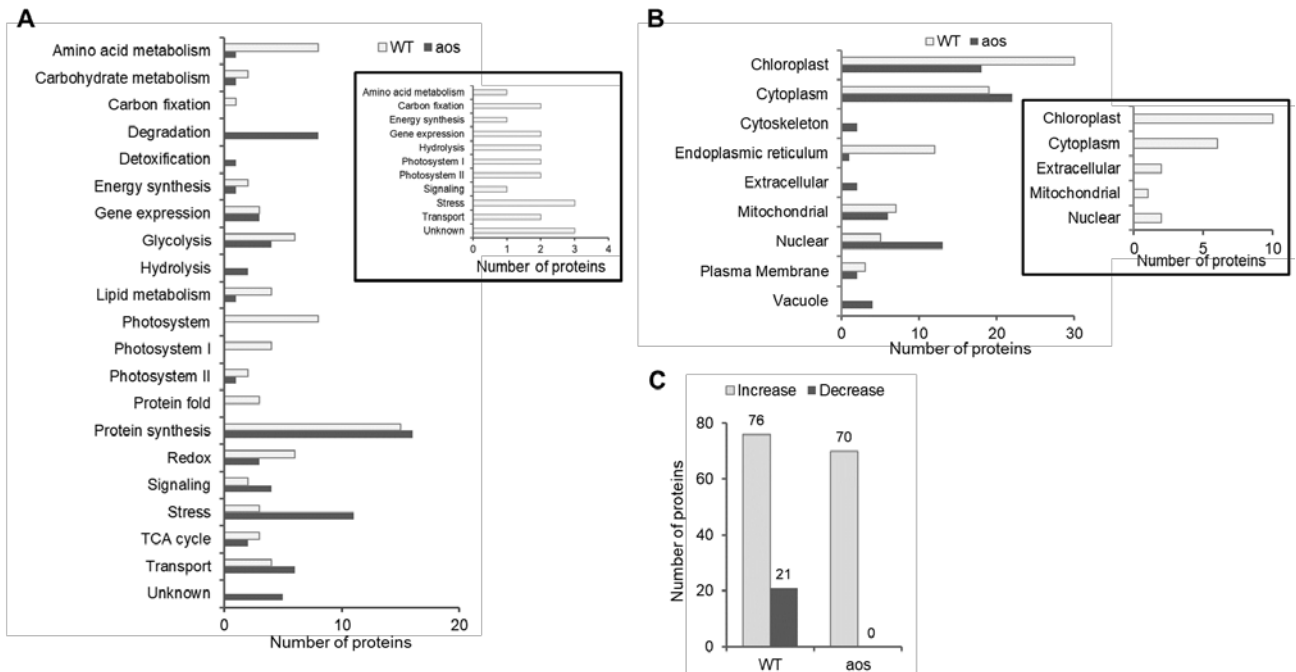


Fig. 3.9. Comparison of distinct proteins accumulated in wild type *P. patens* and the *aos* mutant in response to wounding stress.

(A) Functional categorization of distinct proteins that significantly accumulated in response to wounding in *P. patens* wild-type and the *aos* mutant. Inner small black frame shows functional categorization of distinct proteins that significantly decreased in response to wounding in *P. patens* wild-type. (B) Subcellular localization of distinct proteins that accumulated in response to wounding in *P. patens* wild-type and the *aos* mutant. Inner small black frame shows subcellular localization of distinct proteins that significantly decreased in response to wounding in *P. patens* wild-type (C) Comparison of the global distinct proteins response to wounding in *P. patens* wild-type and the *aos* mutant.

To investigate the functional relationship of the proteins identified in *P. patens* (wild-type and *aos* mutant) in response to wounding, significantly enriched Gene Ontology (GO) terms and Kyoto Encyclopedia of Genes and Genomes (KEGG) pathways were identified according to the *P* value and enrichment factor. The significantly enriched GO terms in each group and the significantly enriched KEGG pathways in each comparison are summarized in Table 3.6. To further analyze the correlations of the differentially expressed proteins, protein-protein interactions were determined, and pathway prediction was performed. The STRING (Search Tool or the Retrieval of Interacting Genes) database was used to calculate all direct interactions between the 136 and 88 proteins identified in the wild-type and the *aos* mutant. As shown in Fig. 3.10, a complicated network of protein-protein interactions was found in the wild-type. The proteins categorized in each group were closely related each other. In contrast to the wild-type, the interactions between each protein group, which were clustered based on functions, were remotely related in the *aos* mutant. These data suggested that *PpAOS* gene disruption, which lowered the concentration of OPDA, reduces multiple protein-protein interactions in response to wounding stress.

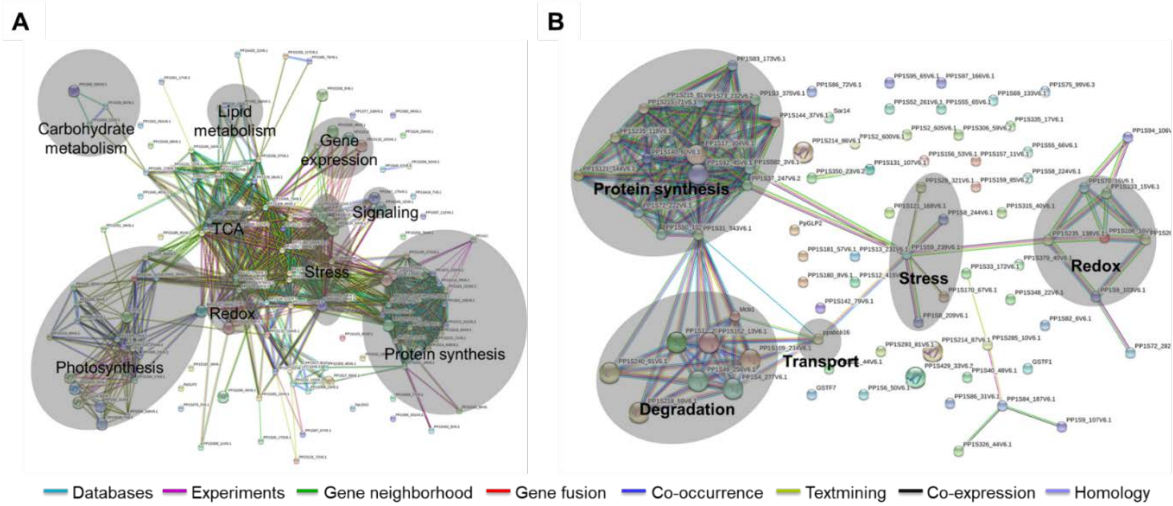


Fig. 3.10. STRING bioinformatic analysis of significantly differentially accumulated proteins in *P. patens* after wounding.

(A) Visualization of the protein interaction network of significantly differentially accumulated proteins in wild-type *P. patens* after wounding. The shaded analysis networks are for photosynthesis, carbohydrate metabolism, lipid metabolism, TCA, redox, stress, gene expression, signaling and protein synthesis. Databases and text-mining were chosen as the active prediction methods. (B) Visualization of the protein interaction network of significantly differentially accumulated proteins in the *aos* mutant after wounding. The shaded analysis networks are for protein synthesis, degradation, transport, stress and redox. Databases and text-mining were chosen as the active prediction methods.

Table 3.6. GO and pathway enrichment analysis of identified proteins in *P. patens* in response to wounding.

Analysis Type:	PANTHER Overrepresentation Test (release 20170413)
Annotation Version and Release Date:	GO Ontology database Released 2017-06-29
Analyzed List:	Differentially expressed proteins response to wounding in wild type
Reference List:	Physcomitrella patens (all genes in database)
Bonferroni correction:	TRUE

GO Terms		Allgenes_with_Go_annotation	Count	expected	over/under	fold Enrichment	P-value	-LOG10(p-value)
GO:0045550	geranylgeranyl reductase activity	3	3	0.01	+	> 100	3.52E-05	4.453457337
GO:0003871	5-methyltetrahydropteroyltriglutamate-homocysteine S-methyltransferase activity	4	3	0.01	+	> 100	8.34E-05	4.078833949
GO:0042085	5-methyltetrahydropteroyltri-L-glutamate-dependent methyltransferase activity	4	3	0.01	+	> 100	8.34E-05	4.078833949
GO:0042084	5-methyltetrahydrofolate-dependent methyltransferase activity	4	3	0.01	+	> 100	8.34E-05	4.078833949
GO:0008705	methionine synthase activity	4	3	0.01	+	> 100	8.34E-05	4.078833949
GO:0008534	oxidized purine nucleobase lesion DNA N-glycosylase activity	3	2	0.01	+	> 100	2.01E-02	1.696803943
GO:0032051	clathrin light chain binding	4	2	0.01	+	> 100	3.57E-02	1.447331784
GO:0008172	S-methyltransferase activity	8	3	0.01	+	> 100	6.64E-04	3.177831921
GO:0016628	oxidoreductase activity, acting on the CH-CH group of donors, NAD or NADP as acceptor	13	3	0.02	+	> 100	2.83E-03	2.548213564
GO:0071949	FAD binding	24	3	0.04	+	69.03	1.76E-02	1.754487332
GO:0051082	unfolded protein binding	119	5	0.22	+	23.2	3.88E-03	2.411168274
GO:0003735	structural constituent of ribosome	477	13	0.86	+	15.05	4.64E-09	8.333482019
GO:0005198	structural molecule activity	567	15	1.03	+	14.61	1.23E-10	9.910094889
GO:0050662	coenzyme binding	273	6	0.49	+	12.14	1.50E-02	1.823908741
GO:0048037	cofactor binding	421	7	0.76	+	9.18	1.61E-02	1.793174124
GO:0003723	RNA binding	1025	14	1.86	+	7.54	4.94E-06	5.306273051
GO:0005515	protein binding	1059	11	1.92	+	5.74	4.12E-03	2.385102784
GO:0016491	oxidoreductase activity	1189	12	2.15	+	5.57	1.85E-03	2.732828272
GO:0000166	nucleotide binding	2254	17	4.08	+	4.16	4.89E-04	3.310691141
GO:1901265	nucleoside phosphate binding	2254	17	4.08	+	4.16	4.89E-04	3.310691141
GO:0036094	small molecule binding	2420	18	4.38	+	4.11	2.47E-04	3.607303047
GO:0043167	ion binding	4040	29	7.32	+	3.96	1.42E-08	7.847711656
GO:0005488	binding	7288	51	13.2	+	3.86	5.63E-21	20.24949161
GO:0043168	anion binding	2322	16	4.2	+	3.81	3.81E-03	2.419075024
GO:0046872	metal ion binding	1904	13	3.45	+	3.77	4.32E-02	1.364516253
GO:0043169	cation binding	1916	13	3.47	+	3.75	4.61E-02	1.336299075
GO:1901363	heterocyclic compound binding	5186	35	9.39	+	3.73	1.29E-10	9.88941029
GO:0097159	organic cyclic compound binding	5188	35	9.4	+	3.73	1.30E-10	9.886056648
GO:0003676	nucleic acid binding	2779	16	5.03	+	3.18	3.65E-02	1.437707136
GO:0003674	molecular_function	12215	59	22.12	+	2.67	2.31E-19	18.63638802

	GO:0003824	catalytic activity	7241	28	13.11	+	2.14	2.94E-02	1.53165267
biological process	GO:0042549	photosystem II stabilization	8	3	0.01	+	> 100	7.73E-04	3.111820506
	GO:0050667	homocysteine metabolic process	8	3	0.01	+	> 100	7.73E-04	3.111820506
	GO:0042548	regulation of photosynthesis, light reaction	11	3	0.02	+	> 100	2.00E-03	2.698970004
	GO:0043467	regulation of generation of precursor metabolites and energy	11	3	0.02	+	> 100	2.00E-03	2.698970004
	GO:0010109	regulation of photosynthesis	14	3	0.03	+	> 100	4.11E-03	2.386158178
	GO:0015995	chlorophyll biosynthetic process	16	3	0.03	+	> 100	6.12E-03	2.213248578
	GO:0015994	chlorophyll metabolic process	22	3	0.04	+	75.3	1.58E-02	1.801342913
	GO:0009086	methionine biosynthetic process	24	3	0.04	+	69.03	2.05E-02	1.688246139
	GO:0000097	sulfur amino acid biosynthetic process	35	4	0.06	+	63.11	9.42E-04	3.025949097
	GO:0000096	sulfur amino acid metabolic process	47	4	0.09	+	47	3.01E-03	2.521433504
	GO:0044272	sulfur compound biosynthetic process	91	4	0.16	+	24.27	3.99E-02	1.399027104
	GO:0015979	photosynthesis	188	8	0.34	+	23.5	3.50E-06	5.455931956
	GO:0009205	purine ribonucleoside triphosphate metabolic process	186	6	0.34	+	17.81	1.98E-03	2.70333481
	GO:0009144	purine nucleoside triphosphate metabolic process	187	6	0.34	+	17.72	2.04E-03	2.690369833
	GO:0009199	ribonucleoside triphosphate metabolic process	191	6	0.35	+	17.35	2.30E-03	2.638272164
	GO:0006457	protein folding	197	6	0.36	+	16.82	2.75E-03	2.560667306
	GO:0009141	nucleoside triphosphate metabolic process	198	6	0.36	+	16.73	2.83E-03	2.548213564
	GO:0046034	ATP metabolic process	172	5	0.31	+	16.05	2.65E-02	1.576754126
	GO:0008652	cellular amino acid biosynthetic process	179	5	0.32	+	15.42	3.20E-02	1.494850022
	GO:0006790	sulfur compound metabolic process	194	5	0.35	+	14.23	4.69E-02	1.328827157
	GO:0009150	purine ribonucleotide metabolic process	236	6	0.43	+	14.04	7.69E-03	2.11407366
	GO:0006163	purine nucleotide metabolic process	239	6	0.43	+	13.86	8.26E-03	2.083019953
	GO:0009259	ribonucleotide metabolic process	257	6	0.47	+	12.89	1.25E-02	1.903089987
	GO:0072521	purine-containing compound metabolic process	268	6	0.49	+	12.36	1.58E-02	1.801342913
	GO:0006412	translation	687	15	1.24	+	12.06	2.19E-09	8.659555885
	GO:0043043	peptide biosynthetic process	691	15	1.25	+	11.99	2.37E-09	8.625251654
	GO:0019693	ribose phosphate metabolic process	287	6	0.52	+	11.54	2.32E-02	1.634512015
	GO:0043604	amide biosynthetic process	732	15	1.33	+	11.32	5.34E-09	8.272458743
	GO:0006518	peptide metabolic process	760	15	1.38	+	10.9	9.03E-09	8.04431225
	GO:1901566	organonitrogen compound biosynthetic process	1303	25	2.36	+	10.59	2.14E-16	15.66958623
	GO:0042254	ribosome biogenesis	380	7	0.69	+	10.17	9.72E-03	2.012333735
	GO:0043603	cellular amide metabolic process	827	15	1.5	+	10.02	2.94E-08	7.53165267
	GO:0034622	cellular macromolecular complex assembly	405	7	0.73	+	9.54	1.47E-02	1.832682665
	GO:0065003	macromolecular complex assembly	422	7	0.76	+	9.16	1.91E-02	1.718966633
	GO:0019752	carboxylic acid metabolic process	668	10	1.21	+	8.27	5.56E-04	3.254925208
	GO:0043933	macromolecular complex subunit organization	468	7	0.85	+	8.26	3.69E-02	1.432973634
	GO:0043436	oxoacid metabolic process	681	10	1.23	+	8.11	6.62E-04	3.179142011
	GO:0006082	organic acid metabolic process	684	10	1.24	+	8.07	6.89E-04	3.161780778
	GO:0022613	ribonucleoprotein complex biogenesis	482	7	0.87	+	8.02	4.45E-02	1.351639989
	GO:0044085	cellular component biogenesis	863	11	1.56	+	7.04	6.63E-04	3.178486472
GO:0044281	small molecule metabolic process	1190	15	2.15	+	6.96	4.27E-06	5.369572125	

	GO:0044271	cellular nitrogen compound biosynthetic process	1717	20	3.11	+	6.43	2.04E-08	7.690369833
	GO:0055114	oxidation-reduction process	1320	14	2.39	+	5.86	1.34E-04	3.872895202
	GO:0044249	cellular biosynthetic process	2537	25	4.59	+	5.44	9.37E-10	9.028260409
	GO:0044711	single-organism biosynthetic process	1029	10	1.86	+	5.37	2.52E-02	1.598599459
	GO:1901576	organic substance biosynthetic process	2591	25	4.69	+	5.33	1.49E-09	8.826813732
	GO:0009058	biosynthetic process	2777	25	5.03	+	4.97	6.85E-09	8.164309429
	GO:0034645	cellular macromolecule biosynthetic process	1681	15	3.04	+	4.93	3.94E-04	3.404503778
	GO:0009059	macromolecule biosynthetic process	1712	15	3.1	+	4.84	4.98E-04	3.302770657
	GO:0044710	single-organism metabolic process	2903	24	5.26	+	4.57	1.28E-07	6.89279003
	GO:0034641	cellular nitrogen compound metabolic process	3103	25	5.62	+	4.45	7.59E-08	7.119758224
	GO:0010467	gene expression	1881	15	3.41	+	4.4	1.63E-03	2.787812396
	GO:0044763	single-organism cellular process	2783	21	5.04	+	4.17	1.48E-05	4.829738285
	GO:1901564	organonitrogen compound metabolic process	3936	29	7.13	+	4.07	8.68E-09	8.061480275
	GO:0009987	cellular process	7959	50	14.41	+	3.47	5.85E-18	17.23284413
	GO:0044237	cellular metabolic process	6372	38	11.54	+	3.29	2.85E-10	9.54515514
	GO:0008152	metabolic process	8109	44	14.68	+	3	1.09E-11	10.9625735
	GO:0006807	nitrogen compound metabolic process	5588	30	10.12	+	2.96	8.06E-06	5.093664958
	GO:0044699	single-organism process	4729	25	8.56	+	2.92	4.27E-04	3.369572125
	GO:0071704	organic substance metabolic process	6791	35	12.3	+	2.85	4.20E-07	6.37675071
	GO:0008150	biological_process	11260	54	20.39	+	2.65	4.31E-15	14.36552273
	GO:0044238	primary metabolic process	6447	30	11.67	+	2.57	2.30E-04	3.638272164
cellular component	GO:0000788	nuclear nucleosome	3	2	0.01	+	> 100	8.02E-03	2.095825632
	GO:0071439	clathrin complex	4	2	0.01	+	> 100	1.42E-02	1.847711656
	GO:0009654	photosystem II oxygen evolving complex	28	5	0.05	+	98.61	1.26E-06	5.899629455
	GO:0019898	extrinsic component of membrane	47	4	0.09	+	47	1.03E-03	2.987162775
	GO:0033178	proton-transporting two-sector ATPase complex, catalytic domain	37	3	0.07	+	44.77	2.52E-02	1.598599459
	GO:1990204	oxidoreductase complex	90	5	0.16	+	30.68	3.98E-04	3.400116928
	GO:0009523	photosystem II	94	5	0.17	+	29.37	4.92E-04	3.308034897
	GO:0009521	photosystem	123	5	0.22	+	22.45	1.81E-03	2.742321425
	GO:0015935	small ribosomal subunit	160	6	0.29	+	20.71	2.85E-04	3.54515514
	GO:0042651	thylakoid membrane	171	6	0.31	+	19.38	4.18E-04	3.378823718
	GO:0022625	cytosolic large ribosomal subunit	207	7	0.37	+	18.67	6.05E-05	4.218244625
	GO:0044391	ribosomal subunit	406	13	0.74	+	17.68	2.51E-10	9.600326279
	GO:0034357	photosynthetic membrane	200	6	0.36	+	16.57	1.03E-03	2.987162775
	GO:0044436	thylakoid part	204	6	0.37	+	16.24	1.15E-03	2.93930216
	GO:0015934	large ribosomal subunit	241	7	0.44	+	16.04	1.67E-04	3.777283529
	GO:0044445	cytosolic part	394	11	0.71	+	15.42	7.80E-08	7.107905397
	GO:0009579	thylakoid	217	6	0.39	+	15.27	1.63E-03	2.787812396
	GO:0022626	cytosolic ribosome	342	9	0.62	+	14.53	6.97E-06	5.156767222
	GO:0005840	ribosome	505	13	0.91	+	14.22	3.74E-09	8.427128398
	GO:0005829	cytosol	788	18	1.43	+	12.61	1.33E-12	11.87614836
	GO:0098796	membrane protein complex	496	10	0.9	+	11.13	1.23E-05	4.910094889

GO:1990904	ribonucleoprotein complex	856	13	1.55	+	8.39	2.22E-06	5.653647026
GO:0030529	intracellular ribonucleoprotein complex	856	13	1.55	+	8.39	2.22E-06	5.653647026
GO:0043232	intracellular non-membrane-bounded organelle	1256	15	2.27	+	6.59	3.01E-06	5.521433504
GO:0043228	non-membrane-bounded organelle	1256	15	2.27	+	6.59	3.01E-06	5.521433504
GO:0032991	macromolecular complex	2592	28	4.69	+	5.97	6.78E-13	12.16877031
GO:0043234	protein complex	1383	13	2.5	+	5.19	5.53E-04	3.257274869
GO:0044444	cytoplasmic part	3011	24	5.45	+	4.4	9.30E-08	7.031517051
GO:0005737	cytoplasm	4342	30	7.86	+	3.82	5.32E-09	8.274088368
GO:0044446	intracellular organelle part	2626	18	4.76	+	3.79	3.28E-04	3.484126156
GO:0044422	organelle part	2626	18	4.76	+	3.79	3.28E-04	3.484126156
GO:0044424	intracellular part	6548	38	11.86	+	3.2	2.37E-10	9.625251654
GO:0005622	intracellular	6886	39	12.47	+	3.13	1.87E-10	9.728158393
GO:0005623	cell	7621	41	13.8	+	2.97	1.36E-10	9.866461092
GO:0044464	cell part	7557	40	13.69	+	2.92	6.59E-10	9.181114585
GO:0005575	cellular_component	10822	43	19.6	+	2.19	8.47E-07	6.07211659

pathway ID	pathway description	observed gene count	false discovery rate	matching proteins in your network (IDs)	matching proteins in your network (labels)
01100	Metabolic pathways	46	1.02E-22	PP1S100_107V6.1,PP1S100_117V6.1,PP1S106_16V6.2,PP1S112_169V6.1,PP1S12_289V6.1,PP1S12_307V6.1,PP1S133_10V6.1,PP1S156_57V6.1,PP1S17_59V6.1,PP1S182_26V6.1,PP1S18_23V6.1,PP1S201_6V6.1,PP1S20_284V6.1,PP1S251_44V6.1,PP1S25_66V6.2,PP1S27_81V6.1,PP1S283_22V6.1,PP1S290_40V6.1,PP1S294_50V6.1,PP1S306_84V6.1,PP1S308_11V6.1,PP1S309_73V6.1,PP1S309_84V6.1,PP1S310_30V6.1,PP1S334_17V6.1,PP1S33_110V6.1,PP1S345_25V6.1,PP1S38_300V6.1,PP1S399_19V6.1,PP1S39_428V6.1,PP1S39_82V6.1,PP1S40_57V6.1,PP1S425_20V6.2,PP1S54_166V6.1,PP1S60_65V6.1,PP1S628_7V6.1,PP1S62_236V6.1,PP1S6_313V6.1,PP1S78_56V6.1,PP1S79_110V6.1,PP1S80_23V6.1,PP1S85_75V6.1,PP1S8_168V6.1,PP1S97_112V6.1,PP1S98_132V6.1,PP1S98_250V6.1	PP1S100_107V6.1,PP1S100_117V6.1,PP1S106_16V6.2,PP1S112_169V6.1,PP1S12_289V6.1,PP1S12_307V6.1,PP1S133_10V6.1,PP1S156_57V6.1,PP1S17_59V6.1,PP1S182_26V6.1,PP1S18_23V6.1,PP1S201_6V6.1,PP1S20_284V6.1,PP1S251_44V6.1,PP1S25_66V6.2,PP1S27_81V6.1,PP1S283_22V6.1,PP1S290_40V6.1,PP1S294_50V6.1,PP1S306_84V6.1,PP1S308_11V6.1,PP1S309_73V6.1,PP1S309_84V6.1,PP1S310_30V6.1,PP1S334_17V6.1,PP1S33_110V6.1,PP1S345_25V6.1,PP1S38_300V6.1,PP1S399_19V6.1,PP1S39_82V6.1,PP1S40_57V6.1,PP1S425_20V6.2,PP1S54_166V6.1,PP1S60_65V6.1,PP1S628_7V6.1,PP1S62_236V6.1,PP1S6_313V6.1,PP1S78_56V6.1,PP1S79_110V6.1,PP1S80_23V6.1,PP1S85_75V6.1,PP1S8_168V6.1,PP1S97_112V6.1,PP1S98_132V6.1,PP1S98_250V6.1
01200	Carbon metabolism	18	7.12E-14	PP1S106_16V6.2,PP1S12_289V6.1,PP1S12_307V6.1,PP1S133_10V6.1,PP1S156_57V6.1,PP1S17_59V6.1,PP1S18_23V6.1,PP1S201_6V6.1,PP1S251_44V6.1,PP1S309_73V6.1,PP1S309_84V6.1,PP1S38_300V6.1,PP1S39_428V6.1,PP1S61_17V6.2,PP1S78_56V6.1,PP1S79_110V6.1,PP1S8_168V6.1,PP1S98_132V6.1	PP1S106_16V6.2,PP1S12_289V6.1,PP1S12_307V6.1,PP1S133_10V6.1,PP1S156_57V6.1,PP1S17_59V6.1,PP1S18_23V6.1,PP1S201_6V6.1,PP1S251_44V6.1,PP1S309_73V6.1,PP1S309_84V6.1,PP1S38_300V6.1,PP1S39_428V6.1,PP1S61_17V6.2,PP1S78_56V6.1,PP1S79_110V6.1,PP1S8_168V6.1,PP1S98_132V6.1
01110	Biosynthesis of secondary metabolites	25	3.17E-13	PP1S100_107V6.1,PP1S12_289V6.1,PP1S12_307V6.1,PP1S133_10V6.1,PP1S156_57V6.1,PP1S18_23V6.1,PP1S201_6V6.1,PP1S20_284V6.1,PP1S27_81V6.1,PP1S283_22V6.1,PP1S290_40V6.1,PP1S309_73V6.1,PP1S309_77V6.1,PP1S309_84V6.1,PP1S33_110V6.1,PP1S38_300V6.1,PP1S399_19V6.1,PP1S39_428V6.1,PP1S39_82V6.1,PP1S425_20V6.2,PP1S78_56V6.1,PP1S79_110V6.1,PP1S8_168V6.1,PP1S98_132V6.1,PP1S98_250V6.1	PP1S100_107V6.1,PP1S12_289V6.1,PP1S12_307V6.1,PP1S133_10V6.1,PP1S156_57V6.1,PP1S18_23V6.1,PP1S201_6V6.1,PP1S20_284V6.1,PP1S27_81V6.1,PP1S283_22V6.1,PP1S290_40V6.1,PP1S309_73V6.1,PP1S309_77V6.1,PP1S309_84V6.1,PP1S33_110V6.1,PP1S38_300V6.1,PP1S399_19V6.1,PP1S39_82V6.1,PP1S425_20V6.2,PP1S78_56V6.1,PP1S79_110V6.1,PP1S8_168V6.1,PP1S98_132V6.1,PP1S98_250V6.1
00620	Pyruvate metabolism	12	4.15E-13	PP1S12_289V6.1,PP1S12_307V6.1,PP1S133_10V6.1,PP1S156_57V6.1,PP1S18_23V6.1,PP1S201_6V6.1,PP1S39_428V6.1,PP1S78_56V6.1,PP1S79_110V6.1,PP1S8_168V6.1,PP1S98_132V6.1	PP1S12_289V6.1,PP1S12_307V6.1,PP1S133_10V6.1,PP1S156_57V6.1,PP1S18_23V6.1,PP1S201_6V6.1,PP1S39_428V6.1,PP1S78_56V6.1,PP1S79_110V6.1,PP1S8_168V6.1,PP1S98_132V6.1
01120	Microbial metabolism in diverse environments	17	8.65E-13	PP1S106_16V6.2,PP1S12_289V6.1,PP1S133_10V6.1,PP1S156_57V6.1,PP1S17_59V6.1,PP1S18_23V6.1,PP1S201_6V6.1,PP1S251_44V6.1,PP1S309_73V6.1,PP1S309_84V6.1,PP1S38_300V6.1,PP1S39_428V6.1,PP1S61_17V6.2,PP1S78_56V6.1,PP1S79_110V6.1,PP1S8_168V6.1,PP1S98_132V6.1	PP1S106_16V6.2,PP1S12_289V6.1,PP1S133_10V6.1,PP1S156_57V6.1,PP1S17_59V6.1,PP1S18_23V6.1,PP1S201_6V6.1,PP1S251_44V6.1,PP1S309_73V6.1,PP1S309_84V6.1,PP1S38_300V6.1,PP1S39_428V6.1,PP1S61_17V6.2,PP1S78_56V6.1,PP1S79_110V6.1,PP1S8_168V6.1,PP1S98_132V6.1
00195	Photosynthesis	10	4.21E-12	PP1S112_169V6.1,PP1S182_26V6.1,PP1S254_25V6.1,PP1S2_56V6.2,PP1S306_84V6.1,PP1S334_17V6.1,PP1S345_25V6.1,PP1S54_166V6.1,PP1S60_65V6.1,PP1S80_23V6.1	PETE,PP1S112_169V6.1,PP1S182_26V6.1,PP1S25_66V6.2,PP1S306_84V6.1,PP1S334_17V6.1,PP1S345_25V6.1,PP1S54_166V6.1,PP1S60_65V6.1,PP1S80_23V6.1
00020	Citrate cycle (TCA cycle)	8	3.85E-09	PP1S133_10V6.1,PP1S156_57V6.1,PP1S201_6V6.1,PP1S38_300V6.1,PP1S39_428V6.1,PP1S78_56V6.1,PP1S79_110V6.1,PP1S98_132V6.1	PP1S133_10V6.1,PP1S156_57V6.1,PP1S201_6V6.1,PP1S38_300V6.1,PP1S39_428V6.1,PP1S78_56V6.1,PP1S79_110V6.1,PP1S98_132V6.1

00270	Cysteine and methionine metabolism	8	1.11E-08	PP1S17_59V6.1,PP1S201_6V6.1,PP1S27_81V6.1,PP1S33_110V6.1,PP1S38_300V6.1,PP1S399_19V6.1,PP1S39_428V6.1,PP1S79_110V6.1	PP1S17_59V6.1,PP1S201_6V6.1,PP1S27_81V6.1,PP1S33_110V6.1,PP1S38_300V6.1,PP1S399_19V6.1,PP1S39_428V6.1,PP1S79_110V6.1
00710	Carbon fixation in photosynthetic organisms	8	3.14E-07	PP1S133_10V6.1,PP1S201_6V6.1,PP1S251_44V6.1,PP1S309_73V6.1,PP1S309_84V6.1,PP1S38_300V6.1,PP1S39_428V6.1,PP1S79_110V6.1	PP1S133_10V6.1,PP1S201_6V6.1,PP1S251_44V6.1,PP1S309_73V6.1,PP1S309_84V6.1,PP1S38_300V6.1,PP1S39_428V6.1,PP1S79_110V6.1
00010	Glycolysis / Gluconeogenesis	8	3.73E-06	PP1S12_289V6.1,PP1S12_307V6.1,PP1S133_10V6.1,PP1S156_57V6.1,PP1S309_73V6.1,PP1S309_84V6.1,PP1S78_56V6.1,PP1S98_132V6.1	PP1S12_289V6.1,PP1S12_307V6.1,PP1S133_10V6.1,PP1S156_57V6.1,PP1S309_73V6.1,PP1S309_84V6.1,PP1S78_56V6.1,PP1S98_132V6.1
01230	Biosynthesis of amino acids	9	1.28E-05	PP1S12_289V6.1,PP1S12_307V6.1,PP1S17_59V6.1,PP1S27_81V6.1,PP1S290_40V6.1,PP1S309_73V6.1,PP1S309_84V6.1,PP1S33_110V6.1,PP1S399_19V6.1	PP1S12_289V6.1,PP1S12_307V6.1,PP1S17_59V6.1,PP1S27_81V6.1,PP1S290_40V6.1,PP1S309_73V6.1,PP1S309_84V6.1,PP1S33_110V6.1,PP1S399_19V6.1
00630	Glyoxylate and dicarboxylate metabolism	6	1.39E-05	PP1S106_16V6.2,PP1S201_6V6.1,PP1S251_44V6.1,PP1S38_300V6.1,PP1S39_428V6.1,PP1S79_110V6.1	PP1S106_16V6.2,PP1S201_6V6.1,PP1S251_44V6.1,PP1S38_300V6.1,PP1S39_428V6.1,PP1S79_110V6.1
03010	Ribosome	10	3.54E-05	PP1S10_102V6.1,PP1S14_438V6.1,PP1S16_112V6.1,PP1S21_5_81V6.1,PP1S21_165V6.1,PP1S330_36V6.1,PP1S62_136V6.1,PP1S72_222V6.1,PP1S73_232V6.2,PP1S77_207V6.1	PP1S10_102V6.1,PP1S14_438V6.1,PP1S16_112V6.1,PP1S21_5_81V6.1,PP1S21_165V6.1,PP1S330_36V6.1,PP1S62_136V6.1,PP1S72_222V6.1,PP1S73_232V6.2,PP1S77_207V6.1
04141	Protein processing in endoplasmic reticulum	7	2.04E-04	PP1S220_79V6.1,PP1S220_83V6.1,PP1S258_52V6.1,PP1S291_62V6.1,PP1S351_24V6.1,PP1S39_223V6.1,PP1S91_109V6.1	PP1S220_79V6.1,PP1S220_83V6.1,PP1S258_52V6.1,PP1S291_62V6.1,PP1S351_24V6.1,PP1S39_223V6.1,PP1S91_109V6.1
00450	Selenocompound metabolism	3	6.81E-04	PP1S27_81V6.1,PP1S33_110V6.1,PP1S399_19V6.1	PP1S27_81V6.1,PP1S33_110V6.1,PP1S399_19V6.1
00196	Photosynthesis - antenna proteins	3	1.71E-03	PP1S429_33V6.2,PP1S628_7V6.1,PP1S6_313V6.1	PP1S429_33V6.2,PP1S628_7V6.1,PP1S6_313V6.1
00770	Pantothenate and CoA biosynthesis	3	1.79E-03	PP1S290_40V6.1,PP1S294_50V6.1,PP1S40_57V6.1	PP1S290_40V6.1,PP1S294_50V6.1,PP1S40_57V6.1
04144	Endocytosis	4	5.38E-03	PP1S147_10V6.1,PP1S351_24V6.1,PP1S7_102V6.1,PP1S91_109V6.1	PP1S147_10V6.1,PP1S351_24V6.1,PP1S7_102V6.1,PP1S91_109V6.1
00900	Terpenoid backbone biosynthesis	3	7.27E-03	PP1S100_107V6.1,PP1S20_284V6.1,PP1S425_20V6.2	PP1S100_107V6.1,PP1S20_284V6.1,PP1S425_20V6.2
00860	Porphyrin and chlorophyll metabolism	3	8.18E-03	PP1S100_107V6.1,PP1S20_284V6.1,PP1S425_20V6.2	PP1S100_107V6.1,PP1S20_284V6.1,PP1S425_20V6.2
00520	Amino sugar and nucleotide sugar metabolism	4	9.29E-03	PP1S283_22V6.1,PP1S309_77V6.1,PP1S39_82V6.1,PP1S98_250V6.1	PP1S283_22V6.1,PP1S309_77V6.1,PP1S39_82V6.1,PP1S98_250V6.1
00061	Fatty acid biosynthesis	2	4.75E-02	PP1S18_23V6.1,PP1S8_168V6.1	PP1S18_23V6.1,PP1S8_168V6.1

Analysis Type:	PANTHER Overrepresentation Test (release 20170413)
Annotation Version and Release Date:	GO Ontology database Released 2017-06-29
Analyzed List:	Differentially expressed proteins response to wounding in the <i>aos</i> mutant
Reference List:	Physcomitrella patens (all genes in database)
Bonferroni correction:	TRUE

GO Terms	Allgenes_with_Go_ annotation	Co unt	expec ted	over/u nder	fold Enrich ment	P- value	- LOG1 0(p- value)
molecular function	GO:0036402 proteasome-activating ATPase activity	17	5	0.02	+	> 100	3.24E-08 7.489455
	GO:0017025 TBP-class protein binding	24	5	0.03	+	> 100	1.81E-07 6.742321
	GO:0008134 transcription factor binding	45	5	0.05	+	92.03	4.11E-06 5.386158
	GO:0003735 structural constituent of ribosome	477	13	0.58	+	22.57	1.48E-11 10.82974
	GO:0005198 structural molecule activity	567	13	0.68	+	18.99	1.30E-10 9.886057
	GO:0042623 ATPase activity, coupled	380	6	0.46	+	13.08	8.83E-03 2.054039
	GO:0003723 RNA binding	1025	12	1.24	+	9.7	2.88E-06 5.540608
	GO:0016887 ATPase activity	513	6	0.62	+	9.69	4.75E-02 1.323306
	GO:0005515 protein binding	1059	8	1.28	+	6.26	4.78E-02 1.320572
	GO:1901363 heterocyclic compound binding	5186	21	6.26	+	3.35	1.32E-04 3.879426
	GO:0097159 organic cyclic compound binding	5188	21	6.26	+	3.35	1.33E-04 3.876148
	GO:0005488 binding	7288	28	8.8	+	3.18	3.07E-07 6.512862
GO:0003674 molecular_function	12215	37	14.8	+	2.51	2.22E-09 8.653647	
biological process	GO:0045899 positive regulation of RNA polymerase II transcriptional preinitiation complex assembly	17	5	0.02	+	> 100	3.78E-08 7.422508
	GO:0045898 regulation of RNA polymerase II transcriptional preinitiation complex assembly	17	5	0.02	+	> 100	3.78E-08 7.422508
	GO:0060261 positive regulation of transcription initiation from RNA polymerase II promoter	21	5	0.03	+	> 100	1.08E-07 6.966576
	GO:0060260 regulation of transcription initiation from RNA polymerase II promoter	21	5	0.03	+	> 100	1.08E-07 6.966576
	GO:2000144 positive regulation of DNA-templated transcription, initiation	21	5	0.03	+	> 100	1.08E-07 6.966576
	GO:2000142 regulation of DNA-templated transcription, initiation	21	5	0.03	+	> 100	1.08E-07 6.966576
	GO:0061136 regulation of proteasomal protein catabolic process	26	5	0.03	+	> 100	3.14E-07 6.50307
	GO:1901800 positive regulation of proteasomal protein catabolic process	26	5	0.03	+	> 100	3.14E-07 6.50307
	GO:1903364 positive regulation of cellular protein catabolic process	27	5	0.03	+	> 100	3.78E-07 6.422508
	GO:1903362 regulation of cellular protein catabolic process	27	5	0.03	+	> 100	3.78E-07 6.422508
	GO:0045732 positive regulation of protein catabolic process	27	5	0.03	+	> 100	3.78E-07 6.422508
	GO:1903052 positive regulation of proteolysis involved in cellular protein catabolic process	27	5	0.03	+	> 100	3.78E-07 6.422508
	GO:1903050 regulation of proteolysis involved in cellular protein catabolic process	27	5	0.03	+	> 100	3.78E-07 6.422508
	GO:0045862 positive regulation of proteolysis	28	5	0.03	+	> 100	4.53E-07 6.343902
	GO:0031331 positive regulation of cellular catabolic process	30	5	0.04	+	> 100	6.39E-07 6.194499
	GO:0009896 positive regulation of catabolic process	30	5	0.04	+	> 100	6.39E-07 6.194499
	GO:0031334 positive regulation of protein complex assembly	33	5	0.04	+	> 100	1.03E-06 5.987163
	GO:0044089 positive regulation of cellular component biogenesis	35	5	0.04	+	> 100	1.38E-06 5.860121
	GO:0042176 regulation of protein catabolic process	35	5	0.04	+	> 100	1.38E-06 5.860121
	GO:0031329 regulation of cellular catabolic process	36	5	0.04	+	> 100	1.58E-06 5.801343
GO:0036503 ERAD pathway	38	5	0.05	+	> 100	2.07E-06 5.68403	
GO:0030433 ubiquitin-dependent ERAD pathway	38	5	0.05	+	> 100	2.07E-06 5.68403	

GO:0051130	positive regulation of cellular component organization	40	5	0.05	+	> 100	2.67E-06	5.573489
GO:0009894	regulation of catabolic process	44	5	0.05	+	94.13	4.28E-06	5.368556
GO:0043254	regulation of protein complex assembly	46	5	0.06	+	90.03	5.34E-06	5.272459
GO:0034976	response to endoplasmic reticulum stress	58	5	0.07	+	71.41	1.68E-05	4.774691
GO:0044087	regulation of cellular component biogenesis	58	5	0.07	+	71.41	1.68E-05	4.774691
GO:0010243	response to organonitrogen compound	59	5	0.07	+	70.2	1.83E-05	4.737549
GO:0030162	regulation of proteolysis	64	5	0.08	+	64.71	2.74E-05	4.562249
GO:1901698	response to nitrogen compound	84	5	0.1	+	49.3	1.05E-04	3.978811
GO:0045944	positive regulation of transcription from RNA polymerase II promoter	110	5	0.13	+	37.65	3.95E-04	3.403403
GO:0045893	positive regulation of transcription, DNA-templated	126	5	0.15	+	32.87	7.67E-04	3.115205
GO:1902680	positive regulation of RNA biosynthetic process	126	5	0.15	+	32.87	7.67E-04	3.115205
GO:1903508	positive regulation of nucleic acid-templated transcription	126	5	0.15	+	32.87	7.67E-04	3.115205
GO:0051254	positive regulation of RNA metabolic process	129	5	0.16	+	32.11	8.61E-04	3.064997
GO:0045935	positive regulation of nucleobase-containing compound metabolic process	134	5	0.16	+	30.91	1.04E-03	2.982967
GO:0051247	positive regulation of protein metabolic process	137	5	0.17	+	30.23	1.15E-03	2.939302
GO:0032270	positive regulation of cellular protein metabolic process	137	5	0.17	+	30.23	1.15E-03	2.939302
GO:0031328	positive regulation of cellular biosynthetic process	140	5	0.17	+	29.58	1.28E-03	2.89279
GO:0010628	positive regulation of gene expression	140	5	0.17	+	29.58	1.28E-03	2.89279
GO:0010557	positive regulation of macromolecule biosynthetic process	140	5	0.17	+	29.58	1.28E-03	2.89279
GO:0009891	positive regulation of biosynthetic process	140	5	0.17	+	29.58	1.28E-03	2.89279
GO:0051128	regulation of cellular component organization	158	5	0.19	+	26.21	2.31E-03	2.636388
GO:0010033	response to organic substance	207	5	0.25	+	20.01	8.55E-03	2.068034
GO:0032268	regulation of cellular protein metabolic process	257	6	0.31	+	19.34	1.10E-03	2.958607
GO:0043161	proteasome-mediated ubiquitin-dependent protein catabolic process	277	6	0.33	+	17.94	1.69E-03	2.772113
GO:0010498	proteasomal protein catabolic process	277	6	0.33	+	17.94	1.69E-03	2.772113
GO:0006518	peptide metabolic process	760	16	0.92	+	17.44	4.23E-13	12.37366
GO:0051246	regulation of protein metabolic process	288	6	0.35	+	17.26	2.12E-03	2.673664
GO:0051173	positive regulation of nitrogen compound metabolic process	240	5	0.29	+	17.26	1.74E-02	1.759451
GO:0010604	positive regulation of macromolecule metabolic process	240	5	0.29	+	17.26	1.74E-02	1.759451
GO:0043603	cellular amide metabolic process	827	17	1	+	17.03	5.78E-14	13.23807
GO:0043604	amide biosynthetic process	732	15	0.88	+	16.97	6.54E-12	11.18442
GO:0031325	positive regulation of cellular metabolic process	245	5	0.3	+	16.9	1.92E-02	1.716699
GO:0009893	positive regulation of metabolic process	245	5	0.3	+	16.9	1.92E-02	1.716699
GO:0006412	translation	687	14	0.83	+	16.88	6.97E-11	10.15677
GO:0043043	peptide biosynthetic process	691	14	0.83	+	16.78	7.54E-11	10.12263
GO:0006357	regulation of transcription from RNA polymerase II promoter	251	5	0.3	+	16.5	2.15E-02	1.667562
GO:0044712	single-organism catabolic process	311	6	0.38	+	15.98	3.29E-03	2.482804
GO:0048522	positive regulation of cellular process	274	5	0.33	+	15.12	3.27E-02	1.485452
GO:0051603	proteolysis involved in cellular protein catabolic process	440	8	0.53	+	15.06	8.52E-05	4.06956
GO:0044257	cellular protein catabolic process	446	8	0.54	+	14.86	9.45E-05	4.024568
GO:0048518	positive regulation of biological process	279	5	0.34	+	14.84	3.57E-02	1.447332
GO:0030163	protein catabolic process	490	8	0.59	+	13.52	1.93E-04	3.714443

	GO:0006511	ubiquitin-dependent protein catabolic process	386	6	0.47	+	12.88	1.12E-02	1.950782
	GO:0019941	modification-dependent protein catabolic process	387	6	0.47	+	12.84	1.14E-02	1.943095
	GO:0043632	modification-dependent macromolecule catabolic process	393	6	0.47	+	12.65	1.24E-02	1.906578
	GO:0044265	cellular macromolecule catabolic process	545	8	0.66	+	12.16	4.31E-04	3.365523
	GO:1901565	organonitrogen compound catabolic process	583	8	0.7	+	11.37	7.14E-04	3.146302
	GO:0009057	macromolecule catabolic process	713	9	0.86	+	10.46	2.49E-04	3.603801
	GO:0022613	ribonucleoprotein complex biogenesis	482	6	0.58	+	10.31	3.91E-02	1.407823
	GO:1901566	organonitrogen compound biosynthetic process	1303	15	1.57	+	9.54	2.44E-08	7.61261
	GO:0044248	cellular catabolic process	813	9	0.98	+	9.17	7.46E-04	3.127261
	GO:0006508	proteolysis	771	8	0.93	+	8.59	5.67E-03	2.246417
	GO:1901575	organic substance catabolic process	984	10	1.19	+	8.42	3.40E-04	3.468521
	GO:0009056	catabolic process	1089	10	1.31	+	7.61	8.57E-04	3.067019
	GO:0044271	cellular nitrogen compound biosynthetic process	1717	15	2.07	+	7.24	1.12E-06	5.950782
	GO:0044267	cellular protein metabolic process	2760	24	3.33	+	7.2	5.32E-13	12.27409
	GO:0034645	cellular macromolecule biosynthetic process	1681	14	2.03	+	6.9	8.92E-06	5.049635
	GO:0009059	macromolecule biosynthetic process	1712	14	2.07	+	6.77	1.12E-05	4.950782
	GO:0019538	protein metabolic process	3056	24	3.69	+	6.51	5.24E-12	11.28067
	GO:0010467	gene expression	1881	14	2.27	+	6.16	3.68E-05	4.434152
	GO:1901564	organonitrogen compound metabolic process	3936	28	4.75	+	5.89	5.38E-14	13.26922
	GO:0044249	cellular biosynthetic process	2537	15	3.06	+	4.9	2.09E-04	3.679854
	GO:0034641	cellular nitrogen compound metabolic process	3103	18	3.75	+	4.8	8.84E-06	5.053548
	GO:1901576	organic substance biosynthetic process	2591	15	3.13	+	4.8	2.74E-04	3.562249
	GO:0009058	biosynthetic process	2777	15	3.35	+	4.47	6.72E-04	3.172631
	GO:0044260	cellular macromolecule metabolic process	4524	24	5.46	+	4.39	2.85E-08	7.545155
	GO:0043170	macromolecule metabolic process	4964	25	5.99	+	4.17	2.44E-08	7.61261
	GO:0006807	nitrogen compound metabolic process	5588	28	6.75	+	4.15	4.70E-10	9.327902
	GO:0044237	cellular metabolic process	6372	31	7.69	+	4.03	1.14E-11	10.9431
	GO:0071704	organic substance metabolic process	6791	32	8.2	+	3.9	5.78E-12	11.23807
	GO:0044238	primary metabolic process	6447	29	7.78	+	3.73	1.87E-09	8.728158
	GO:0008152	metabolic process	8109	33	9.79	+	3.37	9.67E-11	10.01457
	GO:0009987	cellular process	7959	31	9.61	+	3.23	6.13E-09	8.21254
	GO:0008150	biological_process	11260	35	13.6	+	2.57	2.22E-08	7.653647
cellular component	GO:0031595	nuclear proteasome complex	19	5	0.02	+	> 100	2.25E-08	7.647817
	GO:0008540	proteasome regulatory particle, base subcomplex	26	6	0.03	+	> 100	4.95E-10	9.305395
	GO:0031597	cytosolic proteasome complex	26	5	0.03	+	> 100	1.07E-07	6.970616
	GO:0022624	proteasome accessory complex	41	6	0.05	+	> 100	7.51E-09	8.12436
	GO:0005838	proteasome regulatory particle	41	6	0.05	+	> 100	7.51E-09	8.12436
	GO:1905369	endopeptidase complex	84	6	0.1	+	59.16	5.35E-07	6.271646
	GO:0000502	proteasome complex	84	6	0.1	+	59.16	5.35E-07	6.271646
	GO:1905368	peptidase complex	100	6	0.12	+	49.7	1.50E-06	5.823909
	GO:0022625	cytosolic large ribosomal subunit	207	8	0.25	+	32.01	8.58E-08	7.066513
	GO:0044445	cytosolic part	394	15	0.48	+	31.53	2.65E-16	15.57675

GO:0015934	large ribosomal subunit	241	8	0.29	+	27.5	2.81E-07	6.551294
GO:0044391	ribosomal subunit	406	13	0.49	+	26.52	7.68E-13	12.11464
GO:0015935	small ribosomal subunit	160	5	0.19	+	25.88	8.42E-04	3.074688
GO:0022626	cytosolic ribosome	342	10	0.41	+	24.22	5.16E-09	8.28735
GO:0005840	ribosome	505	13	0.61	+	21.32	1.21E-11	10.91721
GO:0005829	cytosol	788	19	0.95	+	19.97	8.38E-18	17.07676
GO:1990904	ribonucleoprotein complex	856	14	1.03	+	13.55	4.56E-10	9.341035
GO:0030529	intracellular ribonucleoprotein complex	856	14	1.03	+	13.55	4.56E-10	9.341035
GO:0043232	intracellular non-membrane-bounded organelle	1256	13	1.52	+	8.57	9.34E-07	6.029653
GO:0043228	non-membrane-bounded organelle	1256	13	1.52	+	8.57	9.34E-07	6.029653
GO:1902494	catalytic complex	781	7	0.94	+	7.42	2.15E-02	1.667562
GO:0044444	cytoplasmic part	3011	26	3.64	+	7.15	5.37E-15	14.27003
GO:0032991	macromolecular complex	2592	21	3.13	+	6.71	1.31E-10	9.882729
GO:0044446	intracellular organelle part	2626	21	3.17	+	6.62	1.69E-10	9.772113
GO:0044422	organelle part	2626	21	3.17	+	6.62	1.69E-10	9.772113
GO:0005737	cytoplasm	4342	31	5.24	+	5.91	5.54E-17	16.25649
GO:0043229	intracellular organelle	4967	27	6	+	4.5	8.91E-11	10.05012
GO:0043226	organelle	4984	27	6.02	+	4.49	9.69E-11	10.01368
GO:0044424	intracellular part	6548	31	7.91	+	3.92	8.50E-12	11.07058
GO:0005622	intracellular	6886	31	8.31	+	3.73	3.56E-11	10.44855
GO:0044464	cell part	7557	33	9.12	+	3.62	3.86E-12	11.41341
GO:0005623	cell	7621	33	9.2	+	3.59	4.99E-12	11.3019
GO:0005575	cellular_component	10822	35	13.1	+	2.68	2.14E-09	8.669586

pathway ID	pathway description	observed gene count	false discovery rate	matching proteins in your network (IDs)	matching proteins in your network (labels)
03010	Ribosome	10	3.59E-06	PP1S121_144V6.1,PP1S215_81V6.1,PP1S235_118V6.1,PP1S302_25V6.1,PP1S3_375V6.1,PP1S50_102V6.1,PP1S72_222V6.1,PP1S73_232V6.2,PP1S83_173V6.1,PP1S92_45V6.1	PP1S121_144V6.1,PP1S215_81V6.1,PP1S235_118V6.1,PP1S302_25V6.1,PP1S3_375V6.1,PP1S50_102V6.1,PP1S72_222V6.1,PP1S73_232V6.2,PP1S83_173V6.1,PP1S92_45V6.1
03050	Proteasome	6	3.59E-06	PP1S109_234V6.1,PP1S12_207V6.1,PP1S14_318V6.1,PP1S152_13V6.1,PP1S49_256V6.1,PP1S4_277V6.1	Mcb1,PP1S109_234V6.1,PP1S12_207V6.1,PP1S152_13V6.1,PP1S49_256V6.1,PP1S4_277V6.1
01120	Microbial metabolism in diverse environments	7	1.09E-03	PP1S106_16V6.2,PP1S235_138V6.1,PP1S26_26V6.1,PP1S333_15V6.1,PP1S350_23V6.2,PP1S94_106V6.1,PP1S9_103V6.1	PP1S106_16V6.2,PP1S235_138V6.1,PP1S26_26V6.1,PP1S333_15V6.1,PP1S350_23V6.2,PP1S94_106V6.1,PP1S9_103V6.1
00620	Pyruvate metabolism	4	4.70E-03	PP1S235_138V6.1,PP1S26_26V6.1,PP1S333_15V6.1,PP1S70_15V6.1	PP1S235_138V6.1,PP1S26_26V6.1,PP1S333_15V6.1,PP1S70_15V6.1
01100	Metabolic pathways	14	4.70E-03	PP1S106_16V6.2,PP1S121_168V6.1,PP1S131_107V6.1,PP1S170_67V6.1,PP1S235_138V6.1,PP1S26_26V6.1,PP1S326_44V6.1,PP1S333_15V6.1,PP1S33_172V6.1,PP1S350_23V6.2,PP1S70_15V6.1,PP1S94_106V6.1,PP1S9_103V6.1,PP1S9_107V6.1	PP1S106_16V6.2,PP1S121_168V6.1,PP1S131_107V6.1,PP1S170_67V6.1,PP1S235_138V6.1,PP1S26_26V6.1,PP1S326_44V6.1,PP1S333_15V6.1,PP1S33_172V6.1,PP1S350_23V6.2,PP1S70_15V6.1,PP1S94_106V6.1,PP1S9_103V6.1,PP1S9_107V6.1
01200	Carbon metabolism	6	4.70E-03	PP1S106_16V6.2,PP1S26_26V6.1,PP1S333_15V6.1,PP1S70_15V6.1,PP1S94_106V6.1,PP1S9_103V6.1	PP1S106_16V6.2,PP1S26_26V6.1,PP1S333_15V6.1,PP1S70_15V6.1,PP1S94_106V6.1,PP1S9_103V6.1
00010	Glycolysis / Gluconeogenesis	4	1.27E-02	PP1S235_138V6.1,PP1S333_15V6.1,PP1S70_15V6.1,PP1S94_106V6.1	PP1S235_138V6.1,PP1S333_15V6.1,PP1S70_15V6.1,PP1S94_106V6.1
00480	Glutathione metabolism	3	1.27E-02	PP1S33_172V6.1,PP1S66_172V6.1,PP1S75_107V6.1	GSTF1,GSTF7,PP1S33_172V6.1

3.2.4 Proteins involved in protein synthesis

The abundance of 27 proteins involved in protein synthesis was increased in response to wounding in the wild-type (Fig. 3.6, Table 3.1). The proteins mainly included ribosomal proteins (60S ribosomal proteins L23, 60S ribosomal proteins L4, 40S ribosomal protein S18, ribosomal protein L3, ribosomal protein L19 and other ribosomal proteins), translation elongation factors and eukaryotic translation initiation factor. In the *aos* mutant, ribosomal proteins (60S ribosomal proteins L23, 40S ribosomal proteins S27, 40S ribosomal protein S18, ribosomal protein L2, ribosomal protein L19 and other ribosomal proteins) were also increased (Fig. 3.6, Table 3.2). The number of proteins related to protein synthesis that accumulated in the *aos* mutant was comparable to that in the wild-type. Even though the abundance of common proteins related to protein synthesis accumulated in wild-type was a little more than that accumulated in the *aos* mutant (Fig. 3.8). The abundance of distinct proteins related to protein synthesis accumulated in wild-type was almost as same as that accumulated in the *aos* mutant (Fig. 3.9). The data indicated the *AOS* genes disruption was not related to the accumulation of proteins involved in protein synthesis. Because OPDA did not accumulated in response to wounding in the *aos* mutant, it is likely that OPDA is unrelated to the wound-induced accumulation of proteins involved in proteins synthesis.

3.2.5 Proteins involved in protein degradation

Interestingly, the levels of 10 identified proteins related to protein degradation (26S proteasome-related proteins) were increased in only the *aos* mutant (Fig. 3.6, Fig. 3.9). In contrast, increased abundance of proteins involved in protein degradation was not observed in the wild-type. Proteasomes are protein complexes that degrade unnecessary or damaged proteins via proteolysis (Vitlin Gruber et al., 2013, Hartl et al., 2011). Protein degradation plays a major role in regulating cell physiology. Because the increase in the 26S proteasome-related proteins was observed only in the *aos* mutant, *PpAOS* gene expression, which leads to OPDA synthesis, is suggested to suppress the accumulation of 26S proteasome-related proteins in the wild-type.

3.2.6 Proteins involved in amino acid metabolism

The abundance of more than 10 proteins (common proteins and distinct proteins) related to amino acid metabolism was increased after wounding in the wild-type: ketol-acid reductoisomerase, acetohydroxy acid isomeroeductase, dihydropyrimidine dehydrogenase, pyridoxal phosphate-dependent enzyme synthase, vitamin-B12 independent methionine 5-methyltetrahydropteroyltriglutamate-homocysteine, glutamate dehydrogenase and amino acid binding protein (Fig. 3.6, Fig. 3.8 and Fig. 3.9). In contrast to the wild-type, only one protein, asparagine synthetase, accumulated in the *aos* mutant in response to wounding (Fig. 3.6, Fig. 3.8 and Fig. 3.9). Overall, the numbers of increased proteins involved in amino acid synthesis were much greater in the wild-type than in the *aos* mutant. These results suggest that *PpAOS* gene expression, which leads to OPDA synthesis was involved in the induction of amino acid synthesis to maintain adequate protein synthesis in response to wounding in *P. patens*.

3.2.7 Proteins involved in protein folding

Proteins involved in the correct folding of other proteins such as heat shock proteins (HSPs), which are classified as stress proteins in this report, accumulated in both the wild-type and the *aos* mutant of *P. patens* after wounding (Fig. 3.6, Fig. 3.8 and Fig. 3.9). These proteins are involved in spatial structural changes in a protein, which can trigger signaling that activates and/or deactivates a function (Tsan & Gao, 2009, Yang et al., 2016, Binder, 2014, Luo et al., 2016). However, the chaperonins were shown to be the highest-abundance proteins in the wild-type and were the most abundant among the identified wound-induced proteins. The Cpn60 chaperonins are suggested to correctly fold chloroplast proteins (Wasternack & Hause, 2013). In contrast to chaperonins identified in the wild-type, embryogenesis abundant proteins (LEAs), which suppress protein aggregation, accumulated in the *aos* mutant (Wise & Tunnacliffe, 2004, Huang et al., 2012, Minami et al., 2003). These proteins are categorized as stress proteins in this report (Fig. 3.6, Fig. 3.8 and Fig. 3.9). Taken together, these

results imply that *PpAOS* gene disruption reduces the expression of protein related to protein folding in response to wounding.

3.2.8 Proteins involved in photosystems

Proteins involved in photosystems were a major protein group induced by wounding in the wild-type (Fig. 3.6, Fig. 3.8, Fig. 3.9 and Fig. 3.11), including the photosystem I reaction center protein PsaF subunit III, the photosystem II manganese-stabilizing protein PsbO, oxygen-evolving enhancer protein I, the light-harvesting complex II protein lhcb5 (chlorophyll a/b-binding protein), type III chlorophyll a/b-binding protein, and the small subunit of Rubisco. Wounding is suggested to accumulate proteins involved in photosystems to provide energy for various stress responses. The abundance of accumulated common proteins in wild-type are more than those in *aos* mutant. However, the abundance of distinct proteins involved in photosynthesis in wild-type are almost same with that in the *aos* mutant (Fig. 3.8, Fig. 3.9). Wounding induced the accumulation of fewer photosystem proteins in the *aos* mutant than in the wild-type. These results are in accordance with the accumulation of a protein related to photosystems in OPDA-treated *P. patens* (Toshima et al., 2014, Luo et al., 2016). These data also indicate the presence of several regulatory pathways to induce the expression of photosynthesis related proteins in response to wounding in *P. patens*.

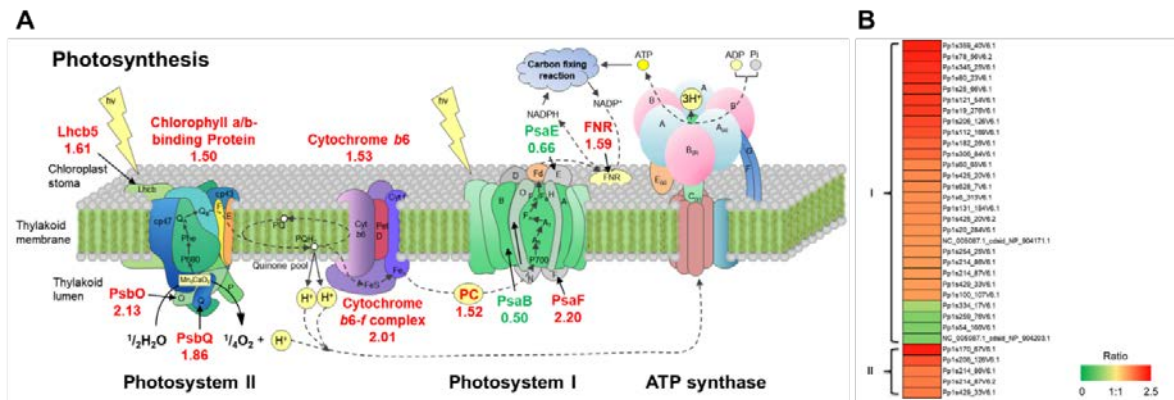


Fig. 3.11. Differentially accumulated proteins involved in photosynthesis.

(A) Proteins involved in photosynthesis were differentially accumulated in response to wounding stress in wild-type *P. patens*. Red and green numbers represent the relative abundance of proteins related to photosynthesis in response to wounding in the wild-type. Lhcb5 (Pp1s628_7V6.1, Pp1s6_313V6.1), light-harvesting complex II protein Lhcb5; chlorophyll a/b-binding protein (Pp1s214_86V6.1, Pp1s214_87V6.1, Pp1s429_33V6.1), type III chlorophyll a/b-binding protein; cytochrome b6 (NC_005087.1_cdsid_NP_904171.1), cytochrome b6; PsbO (Pp1s25_66V6.1, Pp1s306_84V6.1, Pp1s60_65V6.1), photosystem II manganese-stabilizing protein PsbO; PsbQ (Pp1s182_26V6.1), photosystem II oxygen-evolving complex protein PsbQ; cytochrome b6-f complex (Pp1s112_169V6.1), cytochrome b6-f complex iron-sulfur subunit; PC (Pp1s254_25V6.1), plastocyanin; PsaB (NC_005087.1_cdsid_NP_904203.1), photosystem I P700 chlorophyll a apoprotein A2 (PsaB); PsaF (Pp1s345_25V6.1, Pp1s80_23V6.1, Pp1s121_54V6.1, Pp1s19_276V6.1), photosystem I reaction center protein PsaF; PsaE (Pp1s334_17V6.1), photosystem I reaction center subunit IV (PsaE); FNR (Pp1s131_154V6.1), ferredoxin-NADP+ reductase. (B) Heat map representing the profile of differentially accumulated photosystem-related proteins induced by wounding in *P. patens* (I represents wild-type, II represents the *aos* mutant). Red indicates high accumulation, whereas green indicates low accumulation.

3.2.9 Proteins involved in glycolysis, the TCA cycle, and energy synthesis

Wounding caused the accumulation of proteins involved in glycolysis, the TCA cycle, and energy synthesis in the wild-type (Fig. 3.8, Fig. 3.9 and Fig. 3.12); these proteins included pyruvate kinase, UDP-glucose pyrophosphorylase, malate dehydrogenase, phosphoenolpyruvate carboxykinase, pyruvate dehydrogenase E1 component subunit β , glyceraldehyde-3-phosphate dehydrogenase (GAPDH), ATPase, ATP synthase β chain, and vacuolar ATPase β subunit. Glycolysis and the TCA cycle are required for the efficient conversion of photosynthetic products to ATP. Proteins involved in energy synthesis, such as ATPase and ATP synthase, are related to the release of energy. Wounding seems to induce proteins involved in glycolysis and the TCA cycle to readily provide usable chemical energy such as ATP, and energy is released from ATP by proteins associated with energy synthesis. The abundance of proteins involved in glycolysis, the TCA cycle, and energy synthesis was greater in the wild-type than in the *aos* mutant in response to wounding (Fig. 3.6). But there still have a comparative abundance of distinct proteins involved in glycolysis, the TCA cycle, and energy synthesis in the *aos* mutant compare to that in wild-type (Fig. 3.12). These data suggest that *PpAOS* gene expression is suggested to be important for effective energy synthesis against wounding stress.

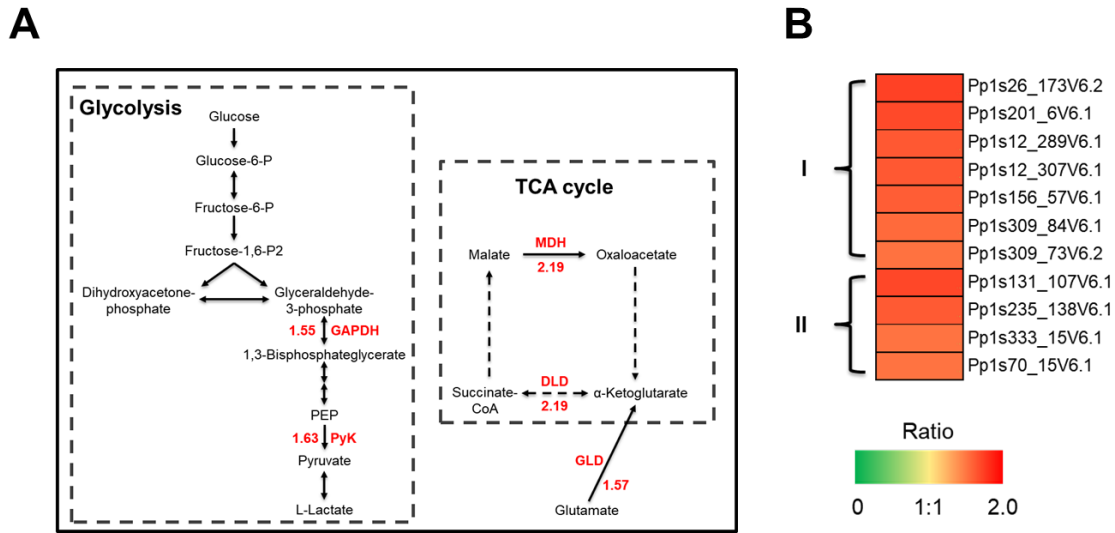


Fig. 3.12. Differentially accumulated proteins involved in glycolysis and the TCA cycle.

(A) Proteins involved in glycolysis and the TCA cycle were all up-regulated in response to wounding stress in wild-type *P. patens*. Red numbers represent the relative abundance of proteins related to glycolysis and the TCA cycle in response to wounding in the wild-type. GAPDH (Pp1s309_84V6.1, Pp1s309_73V6.2), glyceraldehyde-3-phosphate dehydrogenase; PyK (Pp1s12_289V6.1, Pp1s12_307V6.1), pyruvate kinase; MDH (Pp1s38_300V6.1, Pp1s39_428V6.1, Pp1s79_110V6.1), malate dehydrogenase; DLD (Pp1s98_132V6.1), dihydrolipoamide dehydrogenase; GLD (Pp1s62_236V6.4), glutamate dehydrogenase. (B) Heat map representing the profile of differentially accumulated glycolysis and TCA cycle-related proteins induced by wounding in *P. patens* (I represents wild-type, II represents the *aos* mutant). Red indicates high accumulation, whereas green indicates low accumulation.

3.2.10 Proteins for reactive oxygen scavenging

Wounding-enhanced reactive oxygen scavenging enzymes, especially superoxide dismutase (SOD) and thioredoxins, showed increased abundance in response to wounding in the wild-type but not in the *aos* mutant (Fig. 3.6). Glutathione *S*-transferase (GST) was induced by wounding in the *aos* mutant. SOD catalyzes the dismutation of the superoxide ($O_2^{\cdot-}$) radical into oxygen (O_2) or hydrogen peroxide (H_2O_2). Photosynthesis is enhanced by wounding but also produces ROS, which is likely harmful to cells. The accumulation of SOD, which acts as an antioxidant, protects the cellular components from oxidation by ROS. Therefore, wounding likely induces SOD to reduce the accumulated ROS produced by photosynthesis to decrease oxidative stress.

3.2.11 Real -time quantitative PCR analysis of chaperonin genes in *P. patens*

To examine the correlation between proteins abundance and gene expression level, three chaperonin genes (Pp1s141_125V6.1, Pp1s201_109V6.1, Pp1s56_219V6.1) were selected to conduct quantitative real-time PCR (qRT-PCR) to analyze its expression level in response to wounding in *P. patens* (Fig. 3.13). These three chaperonins showed highest abundance level in wild-type in response to wounding, but not accumulated in *aos* mutant (Table 3.1). The transcription levels of three chaperonin genes were increased after wounding in wild type. However, wounding did not induce the expressions levels of three chaperonin genes in wounded *aos* mutant. But when the *aos* mutant treated with wounding and 10 μ M OPDA at the same time, the transcriptional levels of three chaperonin genes was significantly increased. These results indicate that OPDA, which synthesized via AOS reaction, played an import role to regulate the expression of chaperonin in response to wounding stress in *P. patens*.

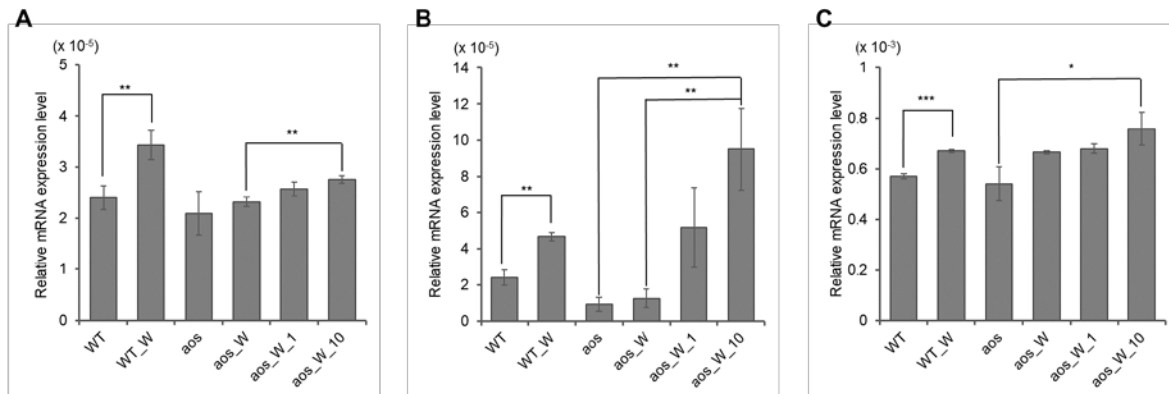


Fig. 3.13. RT-PCR analysis of chaperonin transcription in response to wounding in *P. patens*.

The tissue of 3-week-old *P. patens* was used. The transcription levels of chaperonins (Pp1s141_125V6.1 (A), Pp1s201_109V6.1 (B), and Pp1s56_219V6.1 (C)) were analyzed after wounding for 3 hours. Three independent biological replicates were performed. WT, wild-type control; WT_W, wild-type treated with wounding for 3 hours; aos, mutant control; aos_W mutant treated with wounding for 3 hours; aos_W_1, mutant treated with wounding and supplied with 1 μ M OPDA for 3 hours; aos_W_10, mutant treated with wounding and supplied with 10 μ M OPDA for 3 hours. The values are the means \pm SD (n=3). Student *t*-test (* p <0.05, ** p <0.01, *** p <0.001).

3.3 Discussion

3.3.1 Phenotype of *P. patens* mutants with disrupted *PpAOS1* and *PpAOS2* genes

A *P. patens* mutant in which *PpAOS1* was disrupted showed no increase in the endogenous OPDA concentration in response to wounding, and the phenotype of the mutant was not significantly different from that of the wild-type (Scholz et al., 2012). Hence, *P. patens* mutants in which both the *PpAOS1* and *PpAOS2* genes were disrupted were constructed, and the phenotypes of the mutants were subsequently observed. The OPDA concentration in these mutants was much lower than that in the wild-type after wounding, however, the disruption of these two *PpAOS* genes did not completely prevent OPDA synthesis (Fig. 3.2). Because hydroperoxide lyases show weak AOS activities in *P. patens* (PpHPLs), it is highly likely that OPDA detected in the mutants was produced by PpHPLs (Scholz et al., 2012). A morphogenetic analysis of the mutants revealed that there was no significant phenotypic difference between the mutants with disruption of *PpAOS* genes and the wild-type under conventional growth conditions (Figs. 3.3), implying that the trace amount of OPDA detected in the mutants maybe was sufficient for normal growth of *P. patens*.

3.3.2 Proteins involved in protein metabolism

The number of proteins related to protein synthesis, whose abundance was increased by wounding, was highest among the groups categorized by protein function in both wild-type and the *aos* mutant and was comparable between the two strains (Fig. 3.6, Fig. 3.10, Table 3.1 and Table 3.2). As expression of the *PpAOS* genes and OPDA also did not accumulate in response to wounding in the *aos* mutant, wound-induced signaling, which was no related to OPDA, is probably important for the accumulation of proteins associated with protein synthesis. Since wounding causes serious damage to plants and protein synthesis is necessary to alleviate the effects of these stresses, various signaling mechanisms are integrated. Therefore, these mechanisms induce proteins involved in proteins synthesis to allow adaptation in response to wounding. The representative physiological reactions to

wounding in plants include increases in cell-wall integrity, pathogenesis-related protein synthesis, secondary metabolite synthesis and stress-related plant hormone synthesis (Ge et al., 2015). Furthermore, many metabolic pathways are activated. Before the induction of adaptive responses to wounding stress, *de novo* production of proteins associated with those physiological events is required. Therefore, increasing the abundance of proteins involved in protein synthesis is a significant physiological response in the adaptation to wounding in *P. patens*.

Proteins involved in protein degradation (26S proteasome-related proteins) accumulated in only the *aos* mutant when subjected to wounding, and not in wild-type. The *aos* gene disruption, which did not induce OPDA synthesis, was suggested to be associated with the accumulation of 26S proteasome-related proteins. Wounding causes proteins to promote protein synthesis, thus proteins involved in stress adaptation are more necessary under adverse environmental conditions than under normal conditions. The suppression of the 26S proteasome, which was induced through *PpAOS* expression in response to wounding, possibly causes the accumulation of proteins related to stress adaptation in the wild-type. Therefore, the abundance of proteins related to protein degradation increases little in the wild-type.

Besides, the number of proteins involved in amino acid synthesis whose abundance was increased was much greater in the wild-type than in the *aos* mutant. *PpAOS* gene expression, which resulted in OPDA production, is suggested to participate in the synthesis of amino acids in response to wounding. Amino acids are the basic units of proteins and are thus required for protein synthesis. Simultaneous increases in the abundance of proteins related to both amino acid production and protein synthesis is necessary to maintain efficient and adequate protein synthesis for stress adaptation in response to wounding. These data implied that the decrease in the abundance of proteins involved in protein degradation and the increase in the level of proteins associated with amino acid synthesis are regulated by an *AOS*-related physiological action, such as OPDA synthesis.

3.3.3 Proteins involved in protein folding

As mentioned above, protein synthesis is activated in response to wounding stress. Therefore, correct protein folding in wounded plants is more important than in untreated plants. This study revealed wound-stimulated increases of proteins involved in protein folding, which may be accompanied by enhanced protein synthesis. Increased protein synthesis could require more proteins related to protein folding in wounded *P. patens*.

Chaperonins were the highest increased proteins in wounded wild-type *P. patens* (Table 3.1). The Cpn60 chaperonins are homologous to GroEL in *E. coli*, which participates in the assembly of bacteriophage proteins and is suggested to correctly fold chloroplast proteins which are translocated from the cytosol (Vitlin Gruber et al., 2013, Hartl et al., 2011). The increase in chloroplast proteins encoded in the nuclear genome indicated that proteins translocated from the cytosol to the chloroplast were increased in wounded wild-type *P. patens*. Additionally, the transcription levels of three chaperonin genes were increased after wounding in wild type, but not in *aos* mutant. The transcriptional levels of three chaperonin genes were significantly increased when the *aos* mutant subjected to wounding and treatment with 10 μ M OPDA at the same time. Thus, chaperonins appear to play an important role in the native folding of chloroplast proteins and in adaptation to wounding in *P. patens*. Moreover, as chaperonins were not induced by wounding in the *aos* mutant, the wound-induced accumulation of chaperonins is inferred to depend on *PpAOS* gene expression in *P. patens*. In contrast to the chaperonins detected in the wild-type, LEA proteins accumulated in the *aos* mutant. These proteins are categorized as stress proteins in this report (Fig. 3.6, Table 3.2). LEA proteins suppress protein aggregation, which is promoted by abiotic stresses (Wise & Tunnacliffe, 2004, Huang et al., 2012, Minami et al., 2003). Although the *aos* mutant is unable to accumulate chaperonins, it is possible that induction of LEA proteins, whose functions are similar to chaperonins, possibly to efficiently complement chaperonin functions.

3.3.4 Photosystem proteins and proteins involved in energy synthesis

Photosynthesis, which is one of the most important plant physiological processes, converts light energy to chemical energy and produces carbohydrates, such as sucrose and starch, from water and carbon dioxide using light energy. The activation of the defense system, including protein synthesis, requires additional energy in plants. Thus, enhancement of the photosynthetic capacity in response to wounding is suggested to be crucial for stress adaptation in *P. patens*. Our results show that wounding induced more proteins related to photosystems in wild-type than in the *aos* mutant. These results are in accordance with the accumulation of photosystem proteins observed in OPDA-treated *P. patens* (Luo et al., 2016). These data suggest that *PpAOS* gene expression, which is involved in OPDA synthesis, activate photosynthesis. The genes encoding the photosystem proteins, which significantly increases in response to wounding, are encoded in the chloroplast genome. Given that OPDA is biosynthesized in chloroplasts, OPDA appears to play a role of regulating gene expression in chloroplasts under wounding stress, leading to elevation of protein levels.

Photosynthesis produces oxygen, which causes the production of reactive electrophile species (RES). A recent study suggested that RES and lipid peroxidation are beneficial to plant cells during stress and moreover RES might up-regulate many genes involved in cell survival (Farmer & Mueller, 2013). Thus, the proteins involved in photosystems that are induced by wounding might promote adaptation to wounding stress via RES. From the perspective of OPDA biosynthesis, hydroperoxidation of *a*-linolenic acid is required to increase the accumulation of OPDA. Since the increased abundance of proteins related to photosystems leads to the production of ROS, which can oxidize polyunsaturated lipids in plastid membranes, wound-induced proteins that are associated with photosystems may be involved in supplying oxygen for OPDA biosynthesis (Wasternack & Hause, 2013).

In glycolysis and the TCA cycle, glucose, which is produced by photosynthesis, is metabolized to organic acids, and ATP is subsequently produced. Proteins related to energy synthesis, such as

ATPase, release energy from ATP. The increase in photosystem-related proteins causes increased energy production, and effective energy release is needed for various physiological responses to stress. The orchestrated accumulation of proteins involved in glycolysis, the TCA cycle, and energy synthesis, accompanied by the accumulation of photosystem-related proteins, is suggested to promote the effective utilization of light energy in *P. patens*.

3.3.5 Comparison of proteomic data in this study with those in *P. patens* protonema treated with OPDA

OPDA treatment and wounding induced the expression of many proteins related to photosystems in wild-type (Toshima et al., 2014), however, the abundance of photosystem related proteins was not significantly increased by wounding in the *aos* mutant. Therefore, OPDA signaling is probably involved in the wound-induced protein expression for photosystems. In this study, among 124 proteins, whose abundance were changed in wounded wild-type, the abundance of 22 proteins is reduced in response to wounding. In contrast to wild-type, protein expression is not significantly decreased in the *aos* mutant in response to wounding. Given that OPDA treatment largely decreased the expression of proteins in wild-type *P. patens* (Toshima et al., 2014), OPDA is likely involved in the decreased abundance of proteins caused by wounding.

3.3.6 Comparison of proteomic data in this study

The comparison of proteomic data of wild type *P. patens* and the *aos* mutant, which were subjected to wounding, revealed the common proteins and distinct proteins, whose abundance were altered, in response to wounding in these strains (Figs. 3.6, 3.8 and 3.9). Among the common proteins, the increase ratios of the most proteins in wild type was higher than those in *aos* mutant. These results

also indicated that the disruption of *PpAOS1* and *PpAOS2* primarily decreased the magnitudes of these proteins in *P. patens*.

On the other hand, wounding significantly reduced the abundance of LEA protein (Pp1s52_261V6.1) in wild-type, however, predominantly increased that in *aos* mutant. Increase of LEA proteins in *aos* mutant is suggested to be complementary action for increase of chaperonin in wild-type. However, the detailed mechanism remains elusive. Further study is needed for elucidation of decreasing an LEA protein in wild-type by wounding.

For the distinct proteins, the levels of 76 proteins were increased and those of 21 proteins were decreased in wild type in response to wounding. In *aos* mutant the abundance of 70 proteins were increased in response to wounding (Fig. 3.9). A comparable abundance of the distinct proteins categorized in wild type and the *aos* mutant were categorized to protein synthesis, respectively. Wounding induced More than twenty proteins responsible for protein synthesis in wild-type and *aos* mutant. Among the proteins responsible for protein synthesis were distinct, therefore wound-stimulated protein synthesis was indicated as a common physiological process in response to wounding in wild-type and *aos* mutant. This data implied that disruption of *PpAOS1* and *PpAOS2* did not significantly affect overall accumulation of proteins involved in proteins synthesis. It is possible that the presence of a signal triggered by wounding to increase proteins for proteins synthesis, which was less relevant to OPDA signaling.

Our results also show that the abundance of common proteins and distinct proteins involved in photosynthesis was increased in wild type *P. patens* in response to wounding. In contrast, the number of increased proteins related to photosystems in response to wounding in *aos* mutant was less than that in wild-type (Fig. 3.6, Fig. 3.8 and 3.9). OPDA treatment and wounding increased the levels of many proteins related to photosystems in the wild-type (Toshima et al., 2014). Taken together, the expression of *PpAOS1* and *PpAOS2* is suggested to be need for the wound-induced increase of

proteins related to photosynthesis. Accordingly, OPDA may functions as a signaling compound to potentiate photosynthesis.

Chapter 4 General conclusions

Comparative proteomic analysis of wild-type *P. patens* protonema treated with OPDA shows that OPDA results in the decreased abundance of proteins involved in the metabolism of proteins and carbohydrates at both protonema and gametophore developmental stages. The inhibition of protein synthesis is likely one of significant physiological functions of OPDA in *P. patens*. This study demonstrated that OPDA suppressed histones expression at both protein level and gene transcriptional level at the protonema stage. The elucidation of the detailed OPDA signaling mechanism would shed light on *P. patens* physiology and plant evolution. This study will support to advance the knowledge of how OPDA regulates physiology in *P. patens* and increases our understanding of the function of OPDA as a signaling compound in plants.

Comparative proteomic analysis of wild-type *P. patens* and OPDA-deficient *P. patens* mutant after wounding revealed that wounding mainly promoted the accumulation of proteins involved in protein synthesis, amino acid synthesis, photosynthesis, protein folding, and glycolysis. Since these wounding-responsive proteins in *P. patens* are also accumulated in response to wounding in flowering plants, the accumulation of these proteins in response to wounding may be a conserved physiological event in land plants. The comparison of proteomic data from wild type and the *aos* mutant suggested that the expression of *PpAOS1* and *PpAOS2* is involved in photosynthesis and effective energy utilization in response to wounding in *P. patens*. Additionally, these data also suggested that OPDA plays an important role in these processes. The present data could enhance our understanding of adaptive signaling in response to wounding in land plants as well as OPDA functions in *P. patens*.

Wounding stimulates a wide variety of signaling systems. OPDA-mediated signaling pathway is considered to be one of a number of wound-induced physiological responses in *P. patens*. Various types of signaling triggered by wounding are probably involved in crosstalk with OPDA signaling in

P. patens (Fig. 4.1). Therefore, the proteins that are presumably regulated by OPDA in wounded *P. patens* do not completely correspond to the proteins whose abundance is altered in *P. patens* treated with OPDA.

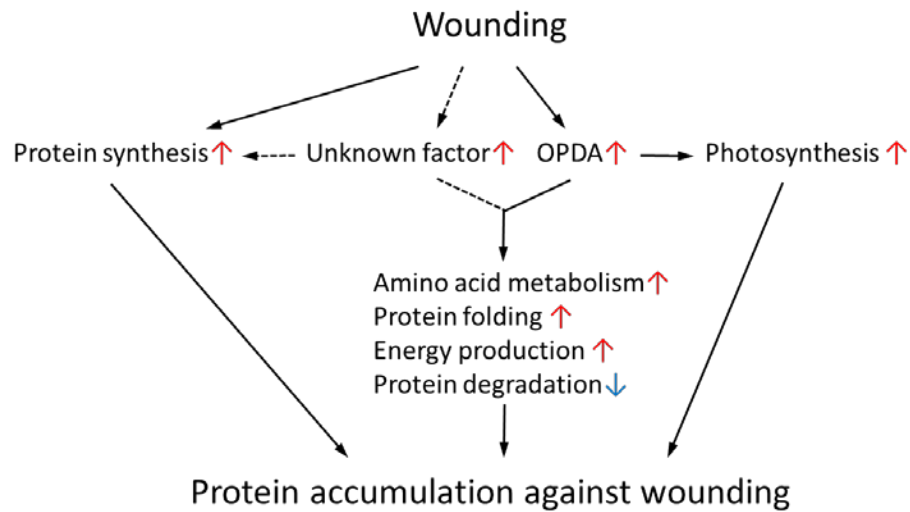


Fig. 4.1. Proposed model for protein accumulation in response to wounding in *P. patens*.

Red or blue arrows indicate an increase or decrease, respectively

Chapter 5 General method

5.1 Plant growth and treatment

In this study, the wild-type strain of *P. patens* subsp. *patens* was used (Ashton & Cove, 1977), which was grown on BCDATG agar medium under continuous white fluorescent light for 5 days at 25 °C. After incubating 5 days, most cells of *P. patens* are in protonemata stage.

P. patens was grown on 20 mL of BCDATG agar medium in a 9-cm petri dish under continuous white fluorescent light at 25 °C (Toshima et al., 2014). For the microscopic analysis of protonema growth, protonemata grown on the agar plate for 4 days were cut into small pieces using a homogenizer (Polytoron PT-10, Kinematica AG, Luzern, Switzerland). After being transferred onto agar supplemented OPDA at various concentrations, protonemata were incubated for 4 days with JA at 50 µM, or OPDA at 5 µM, 10 µM, 25 µM, and 50 µM after which the phenotypes were observed with a microscope (BZ-9000 fluorescence microscope, Keyence, Osaka, Japan).

P. patens was grown on 20 mL of BCDAT agar medium in a Petri dish (9 cm) under continuous white fluorescent light at 25 °C. After 3 weeks incubation, the *P. patens* are in gametophore stage. To generate wounding stress, the gametophore was wounded with tweezers.

5.2 Prepare the BCDATG medium

The component of the medium is showed in the Table. 2.2.

Table 2.2. Components of the BCDATG medium

	1000 ml (All)
H ₂ O	900 ml
Stock B	10 ml
Stock C	10 ml
Stock D	10 ml

Alternative TES	1 ml
Ammonium tartrate (500 mM)	10 ml
CaCl ₂ ·3H ₂ O (50 mM)	20 ml
Agar (NO. 01028-85)	8 g
Glucose	5 g

Table 2.3. The components of Stock B (x 100)

MgSO ₄ 7H ₂ O	25 g (0.1 mM)
Fill up to 1000 ml with H ₂ O	

Table 2.4. The components of Stock C (x 100)

KH ₂ PO ₄	25 g (1.84 mM)
Adjust to pH6.5 with 4M KOH	
Fill up to 1000 ml with H ₂ O	

Table 2.5. The components of Stock D (x 100)

KNO ₃	101 g (1 M)
FeSO ₄ 7H ₂ O	1.25 g (4.5 mM)
Fill up to 1000 ml with H ₂ O	

Table 2.6. The components of Alternative TES (x 1000)

CuSO ₄ 5H ₂ O	55 mg	(0.22 mM)
H ₃ BO ₃	614 mg	(10 mM)
CoCl ₂ 6H ₂ O	55 mg	(0.23 mM)
Na ₂ MoO ₄ 2H ₂ O	25 mg	(0.1 mM)
ZnSO ₄ 7H ₂ O	55 mg	(0.19 mM)
MnCl ₂ 4H ₂ O	389 mg	(2 mM)
KI	28 mg	(0.17 mM)
Fill up to 1000 ml with H ₂ O		

5.3 Synthesis of OPDA

(+)-*cis*-OPDA synthesis was conducted according to the method described by Kajiwara et al (Kajiwara et al., 2012). The synthesis of (+)-*cis*-OPDA was performed according to the method of

previous report (Kajiwara et al., 2012). The reaction mixture contained 46 mg of linoleic acid, and 100 µg/mL of PpAOC2 in the supernatant of flaxseed extract (10 mL). A reaction to synthesize OPDA for 3 hours was performed. After reaction was terminated, the reaction solution was adjusted at approximately pH 3 by addition of 1 M HCl. The reaction mixture was extracted with ethyl acetate, and then the resultant ethyl acetate extract was evaporated. The preparative TLC purification of the ethyl acetate extract (silica gel plate, 0.5 mm x 20 cm x 20 cm, Merck) afforded 17.6 mg of (+)-*cis*-OPDA.

5.4 Analysis of OPDA concentration in *P. patens*

P. patens was grown on BCDATG agar medium for 5 days, and the concentration of endogenous OPDA was analyzed. Protonemata (approximately 200 mg) were frozen in liquid nitrogen and extracted with 10 mL of ethanol. The OPDA analysis was performed as described by Yamamoto et al (Yamamoto et al., 2015). For mechanical stress, the protonemata (approximately 200 mg) were soaked in 2 mL of water and subsequently treated with ultrasonication (Sonifier250, Branson, USA). The samples were directly extracted with 10 mL of ethanol.

Gametophores of *P. patens* (approximately 200 mg), which were grown on BCDAT agar medium for 3 weeks, were frozen in liquid nitrogen and extracted with 10 mL of ethanol. The OPDA analysis was performed as described by Matsuura et al (Matsuura et al., 2000). Four independent experiments were conducted as biological replicates.

5.5 Generation of a *P. patens* mutant with disrupted *PpAOS1* and *PpAOS2*

The detailed methods to generate mutants was described on Tatsuya Abe's master thesis (Abe, 2011). To construct a vector for *PpAOS1* gene disruption, a 1.0-kb genomic DNA fragment beginning 5' to *PpAOS1* was amplified using KOD FX DNA polymerase (Toyobo, Osaka, Japan) and the primers PpAOS1KO5' -F and PpAOS1KO5' -R. A 1.0-kb genomic DNA fragment ending

3' to *PpAOS1* was also amplified using primers PpAOS1KO3' -F and PpAOS1KO3' -R. Each fragment was cloned into the vector pBluescript SKII (+) (Merck, Darmstadt, Germany). The 5' *PpAOS1* genomic fragment was digested with *XbaI* and *EcoRI* and inserted into pTN182, which carries a G418-resistant cassette, digested with *XbaI* and *EcoRI* to obtain pTN182-PpAOS1KO5'. Similarly, the 3' *PpAOS1* genomic fragment was inserted into pTN182-PpAOS1KO5', which had been digested with *SphI* and *NdeI*, to yield pTN182-PpAOS1KO.

A vector for *PpAOS2* gene disruption was constructed using pTN182-PpAOS1KO. A 1.0-kb genomic DNA fragment beginning 5' to *PpAOS2* was amplified using KOD FX DNA polymerase and primers PpAOS2KO5' -F and PpAOS2KO5' -R. A 1.0-kb genomic DNA fragment ending 3' to *PpAOS2* was also amplified using primers PpAOS2KO3' -F and PpAOS2KO3' -R. Each fragment was cloned into pBluescript SKII (+) (Merck, Darmstadt, Germany). The 5' *PpAOS2* genomic fragment was digested with *KpnI* and *HindIII* and inserted into pTN186, which contained a hygromycin resistance cassette and had been digested with *KpnI* and *HindIII* to obtain pTN186-PpAOS2KO5'. The 3' *PpAOS2* genomic fragment was inserted into pTN186-PpAOS2KO5', which had been digested with *SphI* and *SacI*, to yield pTN186-PpAOS2KO.

These plasmids, pTN182-PpAOS1KO and pTN186-PpAOS2KO, had *BamHI* and *KpnI*, restriction sites, respectively. Polyethylene glycol-mediated transformation was conducted as reported previously by Nishiyama et al (Nishiyama et al., 2000). The selected plants were incubated for an additional week without antibiotics and then transferred again onto selection medium. Stable transformants were chosen by PCR using appropriate primer sets (5' end of *PpAOS1*: PpAOS2KO5' -F2 and Pcmv-R; 3' end of *PpAOS1*: 35SPS-F and PpAOS2KO3'-R2; 5' end of *PpAOS2*: PpAOS1KO5'-F2 and Pcmv-R; 3' end of *PpAOS2*: 35SPS-F and PpAOS1KO3'-R2) to confirm integration of the selectable marker into the targeted genes *PpAOS1* and *PpAOS2*. The primers used in this experiment are listed in Table 5.1.

5.6 Protein extraction

(1) *P. patens* protonemata were grown on BCDATG agar plates for 5 days and then treated with 10 μ M OPDA (1 mL of an OPDA solution was sprayed directly onto *P. patens* tissues). *P. patens* protonemata were grown under continuous white fluorescent light at 25°C for 24 h. A portion (approximately 2.5 g) of samples (wet *P. patens* tissue) was ground into powder in liquid nitrogen using a mortar and pestle.

(2) *P. patens* gametophores were grown for 3 weeks and then wounded with tweezers. At 24 hours after wounding, approximately 500 mg of *P. patens* fresh tissue was ground into powder in liquid nitrogen using a mortar and pestle.

The powder was transferred into a solution of 10% trichloroacetic acid and 0.07% 2-mercaptoethanol in acetone and mixed. The suspension was sonicated for 5 min and then incubated for 45 min at -20 °C. After this incubation, the suspension was centrifuged at 9,000 \times g for 20 min at 4 °C. The resulting supernatant was discarded, and the pellet was washed three times with 3 mL of acetone containing 0.07% 2-mercaptoethanol. The final pellet was dried using a vacuum pump. The pellet was resuspended by vortexing for 1 h at 25 °C in 5 mL of lysis buffer consisting of 100 mM Tris-HCl (pH 8.5), 2% SDS, and 50 mM dithiothreitol (DTT). The suspension was then centrifuged at 20,000 \times g for 20 min at 25 °C. The resulting supernatant was collected as the total protein solution. Three independent experiments were conducted as biological replicates. The concentration of the protein solution was measured using the Lowry method (Komatsu et al., 2013).

5.7 Digestion of proteins

For in-solution digestion, 100 μ g of protein was subjected to chloroform/methanol extraction.(Nanjo et al., 2012). The pellet was resuspended with 50 mM NH_4HCO_3 . The solution was reduced with 50 mM DTT and then alkylated with 50 mM iodoacetamide. Proteins were digested

using trypsin and lysyl endopeptidase at a 1:100 enzyme/protein ratio at 37 °C for 16 h (Wang & Komatsu, 2017).

5.8 Nano-liquid chromatography-tandem MS analysis

Peptide separation and detection were performed using an Ultimate 3000 nano LC (Thermo Fisher Scientific, San Jose, CA, USA) and an LTQ Orbitrap mass spectrometer (Thermo Fisher Scientific). The system was operated in data-dependent acquisition mode with XCalibur software (ver. 2.0.7, Thermo Fisher Scientific). The peptides were loaded onto a C18 PepMap trap column (300 µm ID × 5 mm, Dionex). The peptides were eluted with a linear acetonitrile gradient (8–30% over 150 min) in 0.1% formic acid in acetonitrile at a flow rate of 200 nl/min and were loaded and separated on a C18 capillary Tip column (75 µm ID × 120 mm, nano HPLC capillary column, NTTC-360/75-3, Nikkyo Technos, Tokyo, Japan) with a spray voltage of 1.5 kV. Elution was performed with a linear acetonitrile gradient (5-25% in 120 min) in 0.1% formic acid. Full-scan mass spectra were acquired in the Orbitrap over 400 -1,500 m/z with a resolution of 30,000. A lock mass function was used to obtain high mass accuracy (Olsen et al., 2005). The top ten most intense precursor ions were selected for collision-induced fragmentation in the linear ion trap at a normalized collision energy of 35%. Dynamic exclusion was employed within 90 s to prevent the repetitive selection of the peptides (Zhang et al., 2009).

5.9 Protein identification using Mascot

Proteins were identified from the acquired MS/MS spectra using Mascot software (ver. 2.5.1, Matrix Science, London, UK) and the *P. patens* database (38,480 protein sequences) with Proteome Discoverer (ver. 1.4.0.288, Thermo Fisher Scientific). The *P. patens* database was obtained from the Phytozome database (ver. 11. 0. 9, <http://www.phytozome.net/>). The parameters used in the Mascot searches were as follows: the carbamidomethylation of cysteine was set as a fixed modification; the

oxidation of methionine was set as a variable modification; trypsin was specified as the proteolytic enzyme; and one missed cleavage was allowed. The peptide mass tolerance was set at 10 ppm. The fragment mass tolerance was set at 0.8 Da, and the peptide charge was set at +2, +3, and +4. An automatic decoy database search was performed within the search. The Mascot results were filtered using the percolator function in Proteome Discoverer to improve the accuracy and sensitivity of peptide identification (Brosch et al., 2009). False discovery rates for the identification of all searches were less than 1.0%. Peptides with a percolator ion score of more than 13 ($p < 0.05$) were used for protein identification.

5.10 Analysis of differentially accumulated proteins using the acquired MS data

For differential analyses, the commercial label-free quantification package SIEVE (ver. 2.1, Thermo Fisher Scientific) was used to compare the relative abundance of peptides and proteins between the control and experimental groups. The chromatographic peaks detected by MS were aligned, and the peptide peaks were detected as frames using the following settings: the frame time width was 5.0 min; the frame m/z width was 10 ppm, and frames were produced on all parent ions subjected to MS/MS scanning. The frames with MS/MS scans were matched to the imported Mascot results. In the analysis of differential protein abundance, the total ion current was used for normalization. The minimum requirement for the identification of a protein was two matched peptides and a p value of < 0.05 .

5.11 Classification of proteins and bioinformatic analysis

The functions of the identified proteins were categorized according to the annotations of the cosmass.org *P. patens* database (<http://www.cosmass.org/>) and the EU *Arabidopsis thaliana* genome project (Bevan et al., 1998). The functional interactions of the identified proteins were examined using STRING (version 10.5, <http://string-db.org/>) (Szklarczyk et al., 2011). Briefly, the

protein list was subjected to Blast searches against the *Physcomitrella patens* STRING database, which includes the physical and functional relationships of protein molecules, supported by associations derived from eight lines of evidence: the neighborhood in the genome; gene fusions; co-occurrence across the genome; co-expression; experimental/biochemical data; information in databases (associations in curated databases); text-mining (co-mentioned in PubMed abstracts); and homology (Szkarczyk et al., 2017). The biological pathways of the identified proteins were deduced from KEGG analysis (<http://www.genome.jp/kegg/>). The results of Gene Ontology functional and pathway enrichment analysis and the pathway enrichment of the identified proteins were analyzed using an international standardized gene functional classification system (GO, <http://www.geneontology.org/>), employing settings in reference to previous reports (Xiao et al., 2012, Ashburner et al., 2000).

Protein subcellular localization was predicted using TargetP (<http://www.cbs.dtu.dk/services/TargetP/>), Bacello (<http://gpcr2.biocomp.unibo.it/bacello/index.htm>) and WoLF PSORT (<http://wolfspsort.org/>) (Martinez-Cortes et al., 2014). Multiple sequence alignments were conducted by using Clustal Omega (<http://www.ebi.ac.uk/Tools/msa/clustalo/>).

5.12 Extraction of RNA and qRT-PCR analysis

Quantitative reverse transcription polymerase chain reaction (qRT-PCR) was used to analyze the mRNA accumulation of chaperonin genes in response to wounding in wild type *P. patens*. Total RNA was isolated from *P. patens* samples (wild type and the *aos* mutant) with ISOSPIN Plant RNA kit (NIPPON GENE) according to the manufacturer's instructions. RNA solution (2 μ L) were used for first-strand cDNA synthesis with M-MLV reverse transcriptase (Invitrogen, Carlsbad, California, USA) according to the manufacturer's instructions. Gene-specific primers were designed according to expressed sequence tag data available for *P. patens*. The sequences of the

primers are listed in Table 5.2. qRT-PCR analysis was performed following the manufacturer's protocol (KOD SYBR® qPCR Mix, Toyobo Co., Ltd., Osaka, Japan). Each reaction mixture contained 12.5 µl of KOD SYBR® qPCR Mix, 1 µl of each primer (10 mM), 1 µl of cDNA, and 9.5 µl of MilliQ water qRT-PCR was performed on a Thermal Cycler Dice Real Time system (Takara TP800, Japan). The qRT-PCR conditions were as follows: pre-incubation at 95°C for 30 s, followed by 40 cycles of 95°C for 5 s and 60°C for 30 s. The specificity of each PCR amplicon was assessed with a dissociation curve (95°C for 15 s, 60°C for 30 s, and 95°C at 15 s). All RT-PCR reactions were run with three biological replicates on a Thermal Cycler Dice TP800 real-time PCR system (software ver.5.11B, Takara, Japan). To normalize gene expression, actin (accession no.: AW698983) was used as an internal standard set to 1.0 (Le Bail et al., 2013).

5.13 Statistical analysis

Student's *t*-test was used for comparisons between two groups. A *P* value of < 0.05 was considered statistically significant (**p* < 0.05, ***p* < 0.01, ****p* < 0.001).

Table 5.1. List of primers used to construct the double knockout mutant.

Primer name	Primer sequence (5'–3')
PpAOS1KO5'-F	5'-ATCTCGAGGGATCCCATAGGAATAGG-3'
PpAOS1KO5'-R	5'-ATGAATTTCGCTTGCCCAACTACCA-3'
PpAOS1KO3'-F	5'-ATGCATGCGGAGTTCGTCTCCGAGAAC-3'
PpAOS1KO3'-R	5'-ATCATATGCACAACCTTCACAGCCTCGTT-3'
PpAOS2KO5'-F	5'-ATAGGTACCAAGCCAGTAGATTGC-3'
PpAOS2KO5'-R	5'-TATAAGCTTGCACAACACATTTGGC-3'
PpAOS2KO3'-F	5'-TAGCATGCAGGATTGGAGCAAGTG-3'
PpAOS2KO3'-R	5'-TGAGCTCGGTACCTCAAATCGAATCATG-3'
PpAOS1KO5'-F2	5'-TCAACGAATCCACAGAACGTGAAGTG-3'
PpAOS1KO3'-R2	5'-GCAACACCATATGCCATCACATC-3'
PpAOS2KO5'-F2	5'-AGAGCCAAGTTCGAAACAAGACTGCG-3'
PpAOS2KO3'-R2	5'-TGTTTGTAAACACCATCCTTGCAGCG-3'
Pcmv-R	5'-GAGGAAGGGTCTTGCGAAGGATAGTG-3'
35SPA-F	5'-AGGAGGAAGACAAGGAAGGATAAGG-3'

Table 5.2. List of primer used in real-time quantitative RT-PCR.

Primer name	Accession NO.	Primer sequence (5'–3')
Histone_A_F	Pp1s117_154V6.1	TAAGACAATACGAACGGGCGGTGT
Histone_A_R	Pp1s117_154V6.1	AGGCGTGCTTCCTAACATTCACAG
Histone_B_F	Pp1s219_44V6.1	CCTTCAGATCCTTACTAGCGTTTCC
Histone_B_R	Pp1s219_44V6.1	CATCTCGTGCTGGTCTTCAGTTCC
Histone_C_F	Pp1s376_22V6.1	GAAGTAGGCTTCTTCTTATCCTTGTTTT
Histone_C_R	Pp1s376_22V6.1	TTAGTTGTGAAGTGCTCGGTTGGT
Histone_D_F	Pp1s46_245V6.1	GAACACCCAGACAGTAGTTAGTTGAAAA
Histone_D_R	Pp1s46_245V6.1	TCGTTACGCTGAGATCATGTGAGGC
Histone_E_F	Pp1s72_85V6.1	GGGAGAATGCCTTGGTGCTGAA
Histone_E_R	Pp1s72_85V6.1	TGATTGGACCTGCGATCTTGAC
Histone_F_F	Pp1s72_86V6.1	CTCAAGGACCTCAGCAGCCAGA
Histone_F_R	Pp1s72_86V6.1	CGTTCGTTTATTGTTGTGATAGGGTTA
Ppactin-3U1_F	AW698983	ACCAGCCGTTAGAATTGAGCCCAG
Ppactin-3U1_R	AW698983	CGGAGAGGAAGTACAGTGTGTGGA
Chaperonin1_F	Pp1s141_125V6.1	GCCGGAGTTTGAAGCCCTAT
Chaperonin1_R	Pp1s141_125V6.1	CATCTGCCACCGCCTTAGAG
Chaperonin2_F	Pp1s201_109V6.1	GGCTGGTATTAGTGCGATTC
Chaperonin2_R	Pp1s201_109V6.1	AGTTACGCTCCACCTCATT
Chaperonin3_F	Pp1s56_219V6.1	GCGACGGAAGATTCTAAACC
Chaperonin3_R	Pp1s56_219V6.1	TGTGAAGCCAGATCACTCAA

Chapter 6 Acknowledgments

Foremost, I would like to express my greatest gratitude to my awesome supervisor, Dr. Kosaku Takahashi, Laboratory of Natural Products Chemistry, for his mentoring, immense knowledge, support and patients for these six years. As supervisor, Takahashi sensei always motivate me to focus to my research. I have learned a lot valuable lessons and experience from him. I am very grateful to Dr. Hideyuki Matsuura, for his advices on my doctor course research. I would also like to thank Dr. Setsuko Komatsu and Dr. Yohei Nanjo, National Institute of Crop Science, for proteome analysis. I also like to thank Dr. Abe Tatsuya, for his effort on my research. I would also like to express my thanks to all members, whoever already graduate or yet, in Laboratory of Natural Products Chemistry, for their help in many ways to make me feel home in laboratory. I really appreciate any effort they made.

To my lovely parents Mr. Mingqin Luo and Mrs. Guiju Liu, and also my super cute younger sister Jing Luo that I have been blessed with, thanks for always be with me and support me spiritually through my life and their unconditional love during my ups and downs. To thanks to all my beloved friends, who always support me and bring me pleasure and make me happy to go through the tough time in Japan and for listening and patients and tolerance they have to me over past six years.

Finally, I want to thanks to China Scholarship Council for the financial support during my doctor course.

Chapter 7 Lists of abbreviations

μM	:	micromolar concentration
12,13-EOT	:	12,13(<i>S</i>)-epoxyoctadeca-9,11,15-trienoic acid
ABA	:	abscisic acid
ABI5	:	ABA INSENSITIVE 5
AOC	:	allene oxide cyclase
AOS	:	allene oxide synthase
<i>aos</i>	:	PpAOS mutant
ATP	:	adenosine triphosphate
ATPase	:	ATP synthase
cDNA	:	complimentary DNA
DLD	:	dihydrolipoamide dehydrogenase
DNA	:	deoxyribonucleic acid
EFE	:	ethylene forming enzyme
GA	:	gibberellins
GAPDH	:	glyceraldehyde-3-phosphate dehydrogenase
GLD	:	glutamate dehydrogenase.
GO	:	Gene Ontology
GST	:	glutathione S-transferase
HSPs	:	heat shock proteins
Ile	:	isoleucine
IPTG	:	isopropyl β -D-1-thiogalactopyranoside
JA	:	jasmonic acid
KEGG	:	Kyoto Encyclopedia of Genes and Genomes
LOX	:	13-lipoxygenase
MDH	:	malate dehydrogenase
MeJA	:	methyl jasmonate
OEC	:	oxygen-evolving complex
OEE2	:	oxygen-evolving enhancer protein 2
OPDA	:	12-oxo-phytodienoic acid
OPR	:	12-oxo-phytodienoic acid reductase

ORGs	: OPDA-specific response genes
<i>P. patens</i>	: <i>Physcomitrella patens</i>
PEP	: phosphoenolpyruvate
PEPC	: phosphoenolpyruvate carboxykinase
PGM	: phosphoglucomutase
PyK	: pyruvate kinase
rbcL	: ribulose biphosphate carboxylase
redox	: reduction–oxidation reaction
RES	: reactive electrophile species
RNA	: ribonucleic acid
RT-PCR	: reverse transcription-polymerase chain reaction
SA	: salicylic acid
SAR	: systemic acquired resistance
SD	: standard deviation
Semi-qPCR	: semi-quantitative polymerase chain reaction
SOD	: superoxide dismutase
STRING	: Search Tool or the Retrieval of Interacting Genes
TCA	: tricarboxylic acid cycle
UPLC/MS-MS	: ultra-performance liquid chromatography - tandem mass spectrometry
Vsp	: vegetative storage protein acid
WT	: wild type

Chapter 8 References

- Abe T, 2011. ヒメツリガネゴケにおける 12-オキソファイトジエン酸の機能解析.
- Akiyama K, Matsuzaki K, Hayashi H, 2005. Plant sesquiterpenes induce hyphal branching in arbuscular mycorrhizal fungi. *Nature* **435**, 824-827.
- Anterola A, Gobel C, Hornung E, Sellhorn G, Feussner I, Grimes H, 2009. *Physcomitrella patens* has lipoxygenases for both eicosanoid and octadecanoid pathways. *Phytochemistry* **70**, 40-52.
- Ashburner M, Ball CA, Blake JA, *et al.*, 2000. Gene ontology: tool for the unification of biology. the gene ontology consortium. *Nat Genet* **25**, 25-29.
- Ashton NW, Cove DJ, 1977. The isolation and preliminary characterisation of auxotrophic and analogue resistant mutants of the moss, *Physcomitrella patens*. *Molecular and General Genetics MGG* **154**, 87-95.
- Balbi V, Devoto A, 2008. Jasmonate signalling network in *Arabidopsis thaliana*: crucial regulatory nodes and new physiological scenarios. *New Phytol* **177**, 301-318.
- Bandara PK, Takahashi K, Sato M, Matsuura H, Nabeta K, 2009. Cloning and functional analysis of an allene oxide synthase in *Physcomitrella patens*. *Biosci Biotechnol Biochem* **73**, 2356-2359.
- Benkova E, Michniewicz M, Sauer M, *et al.*, 2003. Local, efflux-dependent auxin gradients as a common module for plant organ formation. *Cell* **115**, 591-602.
- Bevan M, Bancroft I, Bent E, *et al.*, 1998. Analysis of 1.9 Mb of contiguous sequence from chromosome 4 of *Arabidopsis thaliana*. *Nature* **391**, 485-488.
- Binder RJ, 2014. Functions of heat shock proteins in pathways of the innate and adaptive immune system. *J Immunol* **193**, 5765-5771.

- Bottcher C, Pollmann S, 2009. Plant oxylipins: plant responses to 12-oxo-phytodienoic acid are governed by its specific structural and functional properties. *FEBS J* **276**, 4693-4704.
- Brosch M, Yu L, Hubbard T, Choudhary J, 2009. Accurate and sensitive peptide identification with mascot percolator. *J Proteome Res* **8**, 3176-3181.
- Calvin M, 1950. The path of carbon in photosynthesis. *Harvey Lect Series* **46**, 218-251.
- Campbell NaR, Jane B.; Urry, Lisa Andrea.; Cain, Michael L.; Wasserman, Steven Alexander.; Minorsky, Peter V.; Jackson, Robert Bradley, 2008. Biology. In.: Pearson Benjamin Cummings.
- Cheong JJ, Choi YD, 2003. Methyl jasmonate as a vital substance in plants. *Trends in Genetics* **19**, 409-413.
- Cove D, 2005. The moss *Physcomitrella patens*. *Annu Rev Genet* **39**, 339-358.
- Creelman RA, Mullet JE, 1995. Jasmonic acid distribution and action in plants: regulation during development and response to biotic and abiotic stress. *Proc Natl Acad Sci U S A* **92**, 4114-4119.
- Creelman RA, Mullet JE, 1997. Biosynthesis and action of jasmonates in plants. *Annu Rev Plant Physiol Plant Mol Biol* **48**, 355-381.
- Dave A, Graham IA, 2012. Oxylipin signaling: a distinct role for the jasmonic acid precursor *cis*-(+)-12-oxo-phytodienoic acid (*cis*-OPDA). *Front Plant Sci* **3**, 42.
- Dave A, Hernandez ML, He Z, *et al.*, 2011. 12-oxo-phytodienoic acid accumulation during seed development represses seed germination in *Arabidopsis*. *Plant Cell* **23**, 583-599.
- Delker C, Stenzel I, Hause B, Miersch O, Feussner I, Wasternack C, 2006. Jasmonate biosynthesis in *Arabidopsis thaliana*--enzymes, products, regulation. *Plant Biol (Stuttg)* **8**, 297-306.
- Dueckershoff K, Mueller S, Mueller MJ, Reinders J, 2008. Impact of cyclopentenone-oxylipins on the proteome of *Arabidopsis thaliana*. *Biochim Biophys Acta* **1784**, 1975-1985.

- Eckermann C, 2002. Stilbenecarboxylate biosynthesis: a new function in the family of chalcone synthase-related proteins. *Phytochemistry* **62**, 271-286.
- Farmer EE, Mueller MJ, 2013. ROS-mediated lipid peroxidation and RES-activated signaling. *Annu Rev Plant Biol* **64**, 429-450.
- Farmer EE, Ryan CA, 1990. Interplant communication: airborne methyl jasmonate induces synthesis of proteinase inhibitors in plant leaves. *Proc Natl Acad Sci U S A* **87**, 7713-7716.
- Farmer EE, Ryan CA, 1992. Octadecanoid precursors of jasmonic acid activate the synthesis of wound-inducible proteinase inhibitors. *Plant Cell* **4**, 129-134.
- Fleet CM, Sun TP, 2005. A DELLAcate balance: the role of gibberellin in plant morphogenesis. *Curr Opin Plant Biol* **8**, 77-85.
- Ge X, Zhang C, Wang Q, *et al.*, 2015. iTRAQ protein profile differential analysis between somatic globular and cotyledonary embryos reveals stress, hormone, and respiration involved in increasing plantlet regeneration of *Gossypium hirsutum* L. *J Proteome Res* **14**, 268-278.
- Hartl FU, Bracher A, Hayer-Hartl M, 2011. Molecular chaperones in protein folding and proteostasis. *Nature* **475**, 324-332.
- Hashimoto T, Takahashi K, Sato M, Bandara PKGSS, Nabeta K, 2011. Cloning and characterization of an allene oxide cyclase, PpAOC3, in *Physcomitrella patens*. *Plant Growth Regulation* **65**, 239-245.
- Hayat S, Ahmad A, 2007. *Salicylic acid: a plant hormone*. Springer Netherlands.
- Hedegaard J, Hauge M, Fage-Larsen J, *et al.*, 2000. Investigation of the translation-initiation factor IF2 gene, *infB*, as a tool to study the population structure of *Streptococcus agalactiae*. *Microbiology-Uk* **146**, 1661-1670.

- Hiss M, Laule O, Meskauskiene RM, *et al.*, 2014. Large-scale gene expression profiling data for the model moss *Physcomitrella patens* aid understanding of developmental progression, culture and stress conditions. *Plant J* **79**, 530-539.
- Huang H, Moller IM, Song SQ, 2012. Proteomics of desiccation tolerance during development and germination of maize embryos. *J Proteomics* **75**, 1247-1262.
- Jianghua S, Keke Y, Yu L, *et al.*, 2015. Phosphoenolpyruvate Carboxylase in *Arabidopsis* Leaves Plays a Crucial Role in Carbon and Nitrogen Metabolism. *Plant Physiol.*
- Kajiwara A, Abe T, Hashimoto T, Matsuura H, Takahashi K, 2012. Efficient synthesis of (+)-cis-12-oxo-phytodienoic acid by an in vitro enzymatic reaction. *Biosci Biotechnol Biochem* **76**, 2325-2328.
- Katsir L, Chung HS, Koo AJ, Howe GA, 2008. Jasmonate signaling: a conserved mechanism of hormone sensing. *Curr Opin Plant Biol* **11**, 428-435.
- Knight DJCaCD, 1993. The moss *Physcomitrella patens*, a model system with potential for the study of plant reproduction. *Plant Cell* **5**, 1483-1488.
- Kochhar A, Khurana JP, Tyagi AK, 1996. Nucleotide sequence of the psbP gene encoding precursor of 23-kDa polypeptide of oxygen-evolving complex in *Arabidopsis thaliana* and its expression in the wild-type and a constitutively photomorphogenic mutant. *DNA Res* **3**, 277-285.
- Komatsu S, Han C, Nanjo Y, *et al.*, 2013. Label-free quantitative proteomic analysis of abscisic acid effect in early-stage soybean under flooding. *J Proteome Res* **12**, 4769-6784.
- Kornberg RD, 1977. Structure of chromatin. *Annu Rev Biochem* **46**, 931-954.
- Kosova K, Vitamvas P, Prasil IT, Renaut J, 2011. Plant proteome changes under abiotic stress-- contribution of proteomics studies to understanding plant stress response. *J Proteomics* **74**, 1301-1322.

- Le Bail A, Scholz S, Kost B, 2013. Evaluation of reference genes for RT qPCR analyses of structure-specific and hormone regulated gene expression in *Physcomitrella patens* gametophytes. *PLoS One* **8**, e70998.
- Lin Z, Zhong S, Grierson D, 2009. Recent advances in ethylene research. *J Exp Bot* **60**, 3311-3336.
- Luo W, Nanjo Y, Komatsu S, Matsuura H, Takahashi K, 2016. Proteomics of *Physcomitrella patens* protonemata subjected to treatment with 12-oxo-phytodienoic acid. *Biosci Biotechnol Biochem* **80**, 2357-2364.
- Malinova I, Kunz HH, Alseekh S, *et al.*, 2014. Reduction of the cytosolic phosphoglucomutase in *Arabidopsis* reveals impact on plant growth, seed and root development, and carbohydrate partitioning. *PLoS One* **9**, e112468.
- Marino-Ramirez L, Jordan IK, Landsman D, 2006. Multiple independent evolutionary solutions to core histone gene regulation. *Genome Biology* **7**, R122.
- Marion-Poll ENaA, 2005. Abscisic acid biosynthesis and catabolism. *Annu. Rev. Plant Biol.* **56**, 165-185.
- Martinez-Cortes T, Pomar F, Merino F, Novo-Uzal E, 2014. A proteomic approach to *Physcomitrella patens* rhizoid exudates. *J Plant Physiol* **171**, 1671-1678.
- Matsuura H, Ohmori F, Kobayashi M, Sakurai A, Yoshihara T, 2000. Qualitative and quantitative analysis of endogenous jasmonoids in potato plant (*Solanum tuberosum* L.). *Biosci Biotechnol Biochem* **64**, 2380-2387.
- Minami A, Nagao M, Arakawa K, Fujikawa S, Takezawa D, 2003. Abscisic acid-induced freezing tolerance in the moss *Physcomitrella patens* is accompanied by increased expression of stress-related genes. *J Plant Physiol* **160**, 475-483.
- Misra N, Saxena P, 2009. Effect of salicylic acid on proline metabolism in lentil grown under salinity stress. *Plant Science* **177**, 181-189.

- Morishita R, Kawagoshi A, Sawasaki T, *et al.*, 1999. Ribonuclease activity of rat liver perchloric acid-soluble protein, a potent inhibitor of protein synthesis. *J Biol Chem* **274**, 20688-20692.
- Nanjo Y, Skultety L, Uvackova L, Klubicova K, Hajduch M, Komatsu S, 2012. Mass spectrometry-based analysis of proteomic changes in the root tips of flooded soybean seedlings. *J Proteome Res* **11**, 372-385.
- Nishiyama T, Hiwatashi Y, Sakakibara I, Kato M, Hasebe M, 2000. Tagged mutagenesis and gene-trap in the moss, *Physcomitrella patens* by shuttle mutagenesis. *DNA Res* **7**, 9-17.
- Olsen JV, De Godoy LM, Li G, *et al.*, 2005. Parts per million mass accuracy on an orbitrap mass spectrometer via lock mass injection into a C-trap. *Molecular & Cellular Proteomics* **4**, 2010-2021.
- Peebles CA, Shanks JV, San KY, 2009. The role of the octadecanoid pathway in the production of terpenoid indole alkaloids in *Catharanthus roseus* hairy roots under normal and UV-B stress conditions. *Biotechnol Bioeng* **103**, 1248-1254.
- Ponce De Leon I, Schmelz EA, Gaggero C, Castro A, Alvarez A, Montesano M, 2012. *Physcomitrella patens* activates reinforcement of the cell wall, programmed cell death and accumulation of evolutionary conserved defence signals, such as salicylic acid and 12-oxo-phytodienoic acid, but not jasmonic acid, upon *Botrytis cinerea* infection. *Mol Plant Pathol* **13**, 960-974.
- Pratiwi P, Tanaka G, Takahashi T, *et al.*, 2017. Identification of jasmonic acid and jasmonoyl-isoleucine, and characterization of AOS, AOC, OPR and JAR1 in the model lycophyte *Selaginella moellendorffii*. *Plant Cell Physiol* **58**, 789-801.
- Prigge MJ, Bezanilla M, 2010. Evolutionary crossroads in developmental biology: *Physcomitrella patens*. *Development* **137**, 3535-3543.

- Rensing SA, Lang D, Zimmer AD, *et al.*, 2008. The *Physcomitrella* genome reveals evolutionary insights into the conquest of land by plants. *Science* **319**, 64-69.
- Roberts AW, Roberts EM, Haigler CH, 2012. Moss cell walls: structure and biosynthesis. *Front Plant Sci* **3**, 166.
- Romano AH, Conway T, 1996. Evolution of carbohydrate metabolic pathways. *Res Microbiol* **147**, 448-455.
- Romeo JT, Downum KR, Verpoorte R, 1998. *Phytochemical signals and plant-microbe interactions*. Springer US; Plenum Press, New York.
- Schaefer DG, Zryd JP, 1997. Efficient gene targeting in the moss *Physcomitrella patens*. *Plant J* **11**, 1195-1206.
- Schaefer DG, Zryd JP, 2001. The moss *Physcomitrella patens*, now and then. *Plant Physiol* **127**, 1430-1438.
- Schaller A, Stintzi A, 2009. Enzymes in jasmonate biosynthesis - structure, function, regulation. *Phytochemistry* **70**, 1532-1538.
- Scholz J, Brodhun F, Hornung E, *et al.*, 2012. Biosynthesis of allene oxides in *Physcomitrella patens*. *BMC Plant Biol* **12**, 228.
- Seo M, Koshihara T, 2002. Complex regulation of ABA biosynthesis in plants. *Trends Plant Sci* **7**, 41-48.
- Stumpe M, Gobel C, Faltin B, *et al.*, 2010. The moss *Physcomitrella patens* contains cyclopentenones but no jasmonates: mutations in allene oxide cyclase lead to reduced fertility and altered sporophyte morphology. *New Phytol* **188**, 740-749.
- Szklarczyk D, Franceschini A, Kuhn M, *et al.*, 2011. The STRING database in 2011: functional interaction networks of proteins, globally integrated and scored. *Nucleic Acids Res* **39**, D561-D568.

- Szklarczyk D, Morris JH, Cook H, *et al.*, 2017. The STRING database in 2017: quality-controlled protein-protein association networks, made broadly accessible. *Nucleic Acids Res* **45**, D362-D368.
- Taki N, Sasaki-Sekimoto Y, Obayashi T, *et al.*, 2005. 12-oxo-phytodienoic acid triggers expression of a distinct set of genes and plays a role in wound-induced gene expression in *Arabidopsis*. *Plant Physiol* **139**, 1268-1283.
- Toshima E, Nanjo Y, Komatsu S, Abe T, Matsuura H, Takahashi K, 2014. Proteomic analysis of *Physcomitrella patens* treated with 12-oxo-phytodienoic acid, an important oxylipin in plants. *Biosci Biotechnol Biochem* **78**, 946-953.
- Tsan MF, Gao B, 2009. Heat shock proteins and immune system. *J Leukoc Biol* **85**, 905-910.
- Vitlin Gruber A, Nisemblat S, Azem A, Weiss C, 2013. The complexity of chloroplast chaperonins. *Trends Plant Sci* **18**, 688-694.
- Wang X, Komatsu S, 2017. Proteomic analysis of calcium effects on soybean root tip under flooding and drought stresses. *Plant Cell Physiol* **58**, 1405-1420.
- Wang X, Kuang T, He Y, 2010. Conservation between higher plants and the moss *Physcomitrella patens* in response to the phytohormone abscisic acid: a proteomics analysis. *BMC Plant Biol* **10**, 192.
- Wang X, Liu Y, Yang P, 2012. Proteomic studies of the abiotic stresses response in model moss - *Physcomitrella patens*. *Front Plant Sci* **3**, 258.
- Wang X, Yang P, Gao Q, *et al.*, 2008. Proteomic analysis of the response to high-salinity stress in *Physcomitrella patens*. *Planta* **228**, 167-177.
- Wang X, Yang P, Zhang X, *et al.*, 2009. Proteomic analysis of the cold stress response in the moss, *Physcomitrella patens*. *Proteomics* **9**, 4529-4538.

- Wasternack C, Hause B, 2013. Jasmonates: biosynthesis, perception, signal transduction and action in plant stress response, growth and development. An update to the 2007 review in *Annals of Botany. Ann Bot* **111**, 1021-1058.
- Weber H, Vick BA, Farmer EE, 1997. Dinor-oxo-phytodienoic acid: a new hexadecanoid signal in the jasmonate family. *Proc Natl Acad Sci U S A* **94**, 10473-10478.
- Wise MJ, Tunnacliffe A, 2004. POPP the question: what *do* LEA proteins do? *Trends Plant Sci* **9**, 13-17.
- Xiao L, Zhang L, Yang G, Zhu H, He Y, 2012. Transcriptome of protoplasts reprogrammed into stem cells in *Physcomitrella patens*. *PLoS One* **7**, e35961.
- Yamamoto Y, Ohshika J, Takahashi T, *et al.*, 2015. Functional analysis of allene oxide cyclase, MpAOC, in the liverwort *Marchantia polymorpha*. *Phytochemistry* **116**, 48-56.
- Yang SF, Hoffman NE, 1984. Ethylene biosynthesis and its regulation in higher-plants. *Annu Rev Plant Physiol Plant Mol Biol* **35**, 155-189.
- Yang Y, Yu Y, Bi C, Kang Z, 2016. Quantitative proteomics reveals the defense response of wheat against *Puccinia striiformis f. sp. tritici*. *Sci Rep* **6**, 34261.
- Zhang Y, Wen Z, Washburn MP, Florens L, 2009. Effect of dynamic exclusion duration on spectral count based quantitative proteomics. *Anal Chem* **81**, 6317-6326.
- Zhu JK, 2002. Salt and drought stress signal transduction in plants. *Annu Rev Plant Biol* **53**, 247-273.